Detached Retina: A Unique Diary & its Repair

James T. Fulton –April 30, 2019

Current Version https://neuronresearch.net/vision/pdf/Append ZF
Memorialized as DOI: 10.13140/RG.2.2.26535.39841 on 25 April

Abstract: A rare if not unique report by a patient knowledgeable in physiology and optics. Of comfort to fellow patients; invaluable to Ophthalmologists. It provides more information for the clinical and surgical community concerning the relationship between a successful surgery and the acuity realized by the patient. The author experienced a spontaneous detached retina in the left eye in February 2018 at the age of 82. It was a serous type detachment, believed to have occurred between the choroid and the retinal pigment epithelium, RPE. Over 85% of the vision was lost progressively over a period of 30 days prior to surgery. The limit of the scotoma varied during this time due to the sloshing of a fluid within the eye. Following surgery, the spatial performance of the peripheral retina returned to near normal. After one year, the foveola was still not able to support reading, at any level. By using the area adjacent to the foveola, reading at the level of 20/70 was possible, by reading individual letters only. Reading by this procedure was arduous. From a large perspective, the perceived image relating to the central field of view (out to about 4 degrees diameter about the point of fixation) was scaled down to about 85% of the image size in the right eye and displaced downward and to the right by about 3 degrees . This made coarse convergence of the two eyes problematical. Within the smaller 1.2 degree field supported by the foveola, the left half of the visual field was further reduced to about 70% of the size of the right eye and badly distorted. This made fine convergence of the two eyes impossible. The role of the foveal pit formed in the inner limiting membrane, ILM, as a field lens is thoroughly documented.

Keywords: detached retina, scotoma, surgery, laser stitching, choroid, acuity, spatial distortion, field lens, telephoto, telescope metamorphosia, dysmetropsia

Table of Contents, List of Figures, and Index at end of paper.

REFERENCES TO SECTIONS beginning with a numeric indicate a Chapter in "Processes in Biological Vision" available on line at https://neuronresearch.net/vision/ by clicking on *Download Chapters* on the left navigation panel.

The **Diary** begins at Page 7 after some introductory material. It ends at page 59, followed by technical information.

F.1 Macular dystrophy involving mechanical failures of the posterior ocular

Before delving into the diary of a retinal detachment, it is necessary to address some technical background.

Most of the literature relating to macular dystrophy relates to the chemical failures resulting in significant loss of vision in the elderly, occasionally starting at 50 years old. However a large group of mechanical failures related to the retina of the eye also fall under this broad name.

As noted by Wilkinson in a 2009 review, there is considerable confusion in the academic community when discussing these mechanical failures[1].

A class of macular dystrophies, also common in the aged population involves mechanical failures among the varied structures at the posterior pole of each ocular. These failures frequently involve mechanical separation between distinct layers of the complex structures involving the choroid, RPE, retina & vitreous cortex (containing the vitreous humor). They may also involve membranes only encountered in a small percentage of the population.

[1]Wilkinson, C. (2009) Mysteries regarding the surgically reattached retina. Trans Am Ophthalmology Soc. vol 107, page 55 *In my file as Wilkinson09pg55.pdf*

Figure F.1.1-1 describes the major classes of macular dystrophy, where macula is used in the very broadest sense to mean retina. The chemical dystrophies occur, and appear to the ophthalmologist, in a variety of forms. Whole books have been dedicated to these forms and their frequently progressive character.

There are three recognized types of mechanically detached retina. The mechanical dystrophies each have individual primary characteristic. The ILM/vitreous dystrophies, often called traction detachments are centered on the foveal pit. Gass[2] and other atlases of ocular surgical procedures often illustrate a variety of such failures in primarily cartoon form. He has not provided lengthy discussions in the atlas but he may have discussed the individual illustrations in his many other papers[3]. Recently many of these forms have come to be described using the term Epiretinal membranes, ERM, overlaying the ILM (**Section F.1.1-2**). The other types of mechanical dystrophies will be addressed below.

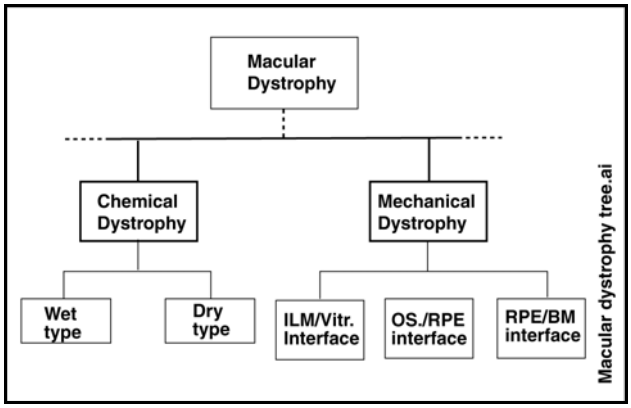

Figure F.1.1-1 Macular dystrophy tree describing the two main chemical types and three main mechanical types.

Figure F.1.1-2 is reproduced from Section 4.5, "The complete Photoreceptor-IPM-RPE Complex." The discussion found there are extensive and will not be repeated here. However, the relative position of the various elements of the retina are important in the following discussions. The retina is frequently compared to a piece of copy paper in thickness. Until the arrival of optical coherence tomography, OCT, as a way of imaging the cross section of a retina was not possible *in-vivo*. Only histological examination post mortem was possible.

> The commonly assumed etiology of a detached retina, based primarily on a very few cases of post-mortem histology, is that a tear occurs in the bulk retina that allows vitreous humor from the ocular to penetrate the bulk of the neural tissue and gain access to the inter-photoreceptor matrix as shown at lower left. By building up pressure in this matrix, it causes a separation between the root of the outer segments of the photoreceptors, PC, and the retinal pigment epithelium, RPE, layer. Exactly where this tear occurs relative to the outer segments of the PC is not well documented.

As a result, the highly successful techniques of retinal re-attachment available today have the surgeon treating the retina as a single layer of retinal material to be re-attached to the residue of the retina remaining attached to the choroid. The procedure calls for the removal of the fluid in the space between the two remnants, repositioning the retina and pushing it against the residue on the surface of the choroid and stitching the two pieces together, normally using an infra-red laser beam projected through the pupil of the lens system of the eye. The pushing action is usually aided by a gas bubble injected into the vitreous cortex after extraction of the vitreous humor.

> However, there are two other etiologies involving a detached retina as noted in the first figure, involving the RPE/BM interface and the upper right of this figure. In both of these, the complete retina is separated from the choroid. This can happen by the peeling away of the retina at its extreme edges (what is often labeled the serrated retina). First, the peeling can occur between the choroid and Bruch's membrane, BM. This type may involve a hemorrhage of the choroidal capillaries. Second, the peeling may occur between Bruch's membrane and the RPE layer. In this case, the build up of fluid forms a cyst.

There is an important difference between these types of failure. In the OS/RPE case the IPM is accessed by the oxygen and other oxidizers present in the vitreous humor. Oxidizers are enemies of the chromophores covering the discs of the OS. This condition quickly leads to the necrosis of the OS and must be surgically corrected within a few days to prevent long term blindness involving a significant area of the visual field. Without impinging on the IPM, the RPE/BM and BM/Choroid type of retinal detachments do not threaten the existence of operational OS. [The author went over 40 days with a detached retina without any significant loss of OS, as illustrated beginning in

---

[2]Gass, J. (1987) Stereoscopic atlas of macular diseases : diagnosis and treatment

[3]Johnson, R. & Gass, J. (1988) Idiopathic macular holes: Stages of formation, and implications for surgical intervention *Ophthalmo*l vol 95, pp 917-924

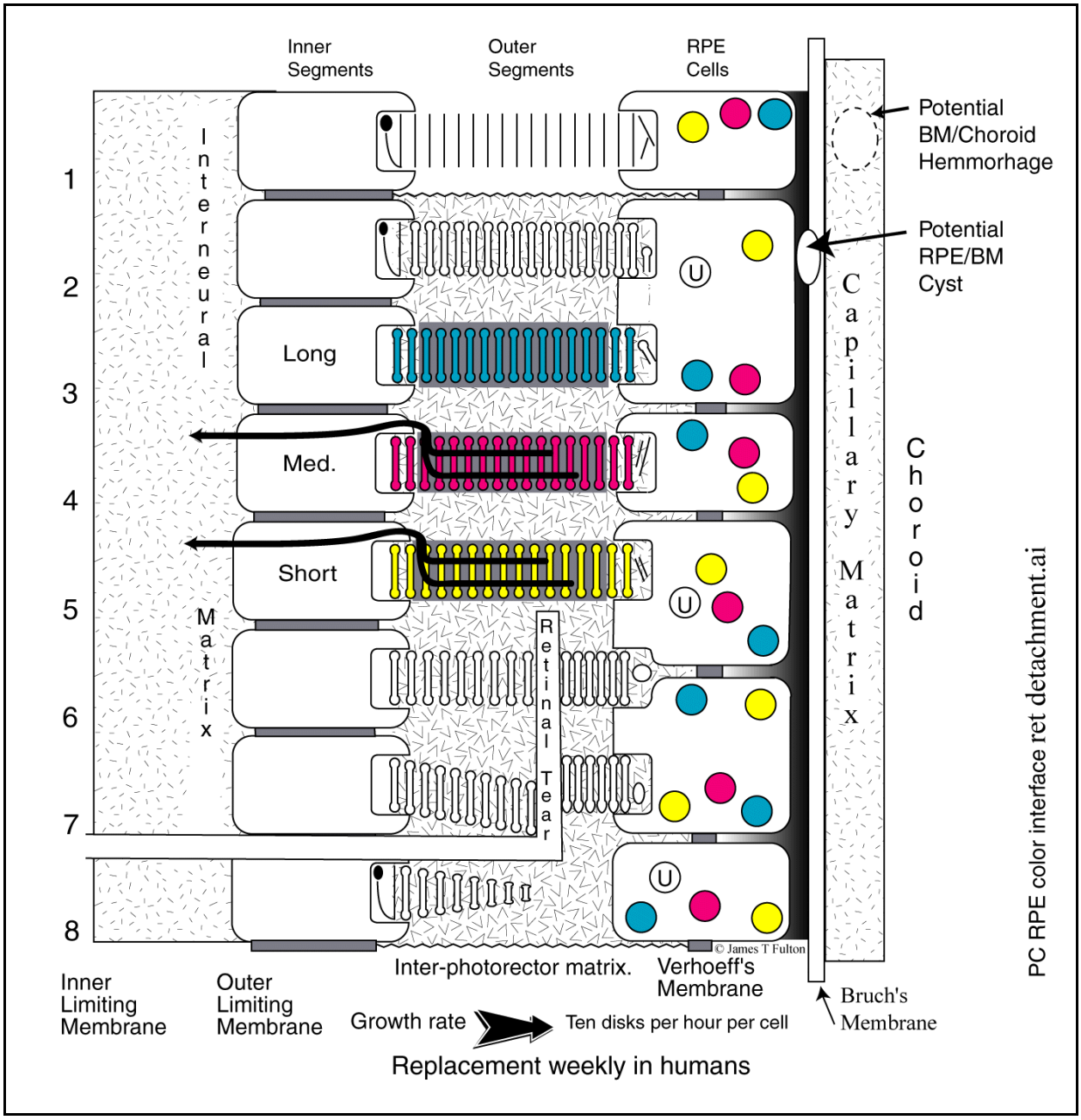

Figure F.1.1-2 The photoreceptor cell-IPM-RPE interface. To the left of the inner limiting membrane is the vitreous humor. The location of the Outer Limiting Membrane is shown as between the Inner Segments of the PCs. In the most common retinal detachment, the retinal tear shown extends into the vitreous humor. Alternate retinal detachments can occur between the choroid and Bruch's membrane or Bruch's membrane, BM, and the RPE cells as shown at upper right. See Text.

Section F.1.3.] A new method of imaging the living retina in cross section has recently appeared and been improving very rapidly. **Figure F.1.1-3**, also appearing as [**Figure 3.2.2-2**], shows an ultrahigh-resolution spectral

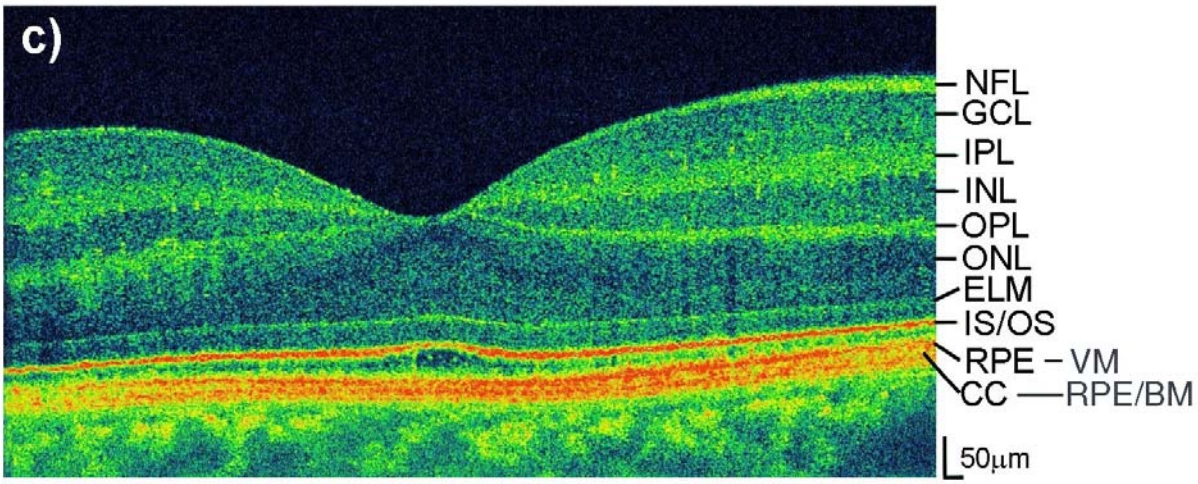

Figure F.1.1-3 Ultrahigh-resolution spectral OCT image of living human macula using 2nd & 3rd order numerical dispersion compensation. Nominal axial (vertical) resolution is 2.1 microns. Lateral resolution is poorer than 5 microns. Illumination was 144 nm wide FWHM centered on 850 nm. Alternate labels are shown as used by various investigators. Note asymmetric magnifications as indicated by the Plimsoll mark at lower right. VM = Verhoeff's "membrane." CC = choriocapillaris. BM = base membrane. From Wojtkowski et al., 2004.

OCT image of human macula from Wojtkowski et al[4]. Note, this ultra-high resolution image does not identify an inner limiting membrane on the surface of the NFL. This version employs false color imaging to highlight specific features. The technique employs Fourier domain optical coherence tomography (FDOCT) with numerical compensation for the dispersion of light within the biological tissue.The caption is quoted verbatem to capture the subtleties involved. Alam et al[5]. and Choi et al[6]. have provided similar examples of the FDOCT technique applied to the human retina. The term spectral domain optical SDOCT is also used to describe this technique. The technique views the retina through the pupil and measures the time delay (convertible to distance traveled by the light) associated with each axial layer of the retina. This new technique is the first to "resolve" Verhoeff's membrane in a living human retina. Verhoeff's membrane is actually a representation of the average response from a more complex layer containing a variety of individual elements, including terminal bars formed between adjacent RPE cells (**Figure F.1.1-2**). The representation represents the 1/3 of the RPE closest to the foveal pit. The remainder of the RPE and the closely associated Bruch's membrane (BM) are represented by the feature labeled either choriocapillaris (CC) or RPE/BM by different investigators. Note the longer outer segments directly below the pit of the foveola. This is typically found in healthy retina. No inner limiting membrane, ILM, is labeled in this figure. The ILM is usually shown as just above the NFL in this figure. The ILM is usually used as a benchmark because of its ease of recognition *conceptually*. However, there is some question of whether the inner limiting membrane is truly a membrane or just the surface of a liquid crystalline mass made up primarily of Müller cells. In this case, it may be the orderly arrangement of the "feet" of Müller cells that are considered a membrane (**Section 2.4.3.5**). Ultimately, the question is a histological one. Most academic literature does not address the precise cellular nature

[4]Wojtkowski, M. Srinivasan, V. Ko, T. et al. (2004) Ultrahigh-resolution, high-speed, Fourier domain optical coherence tomography and methods for dispersion compensation *Optics Express* vol 12(11), pp 2404-2422

[5]Alam, S. Zawadzki, R. Choi, S. et al. (2006) Clinical application of rapid serial Fourier-domain optical coherence tomography for macular imaging *Ophthalmology* vol 113, pp 1425-1431

[6]Choi, S. Zawadzki, R. Greiner, M. et al. (2008) Fourier-domain optical coherence tomography and adaptive optics reveal nerve fiber layer loss and photoreceptor changes in a patient with optic nerve drusen *J Neuroophthalmol* vol 28(2), pp 120-125

of the ILM. The RPE/BM dystrophies, often labeled serous retinal detachments because of their frequent involvement with the capillaries adjacent to the choroid are occasionally label exudative retinal detachments. They frequently occur near the posterior pole of the ocular and these are labeled central serous chorioretinopathy, CSV. They can also occur at the far periphery of the retina. The separations are frequently associated with the flashes of light at the edges of the retina as the beginning of the separation of the complete retina from the choroid. Whether these separations involve hemorrhage of the vascular system or merely allows vitreous humor to occupy the space between the RPE and Bruch's membrane must be determined on a case by case basis. In either case, no damage to the chromophores of vision is to be expected due to oxygen entering the IPM as discussed in the next paragraph. The retinal detachments of this type can last more than 40 days without significant permanent blindness.

The type of mechanical dystrophy written about most extensively, and presumably statistically most common, is the separation of the outer segments, OS, of the neural layer from the RPE, retinal pigmented epithelium. These involve the outer limiting membrane, OLM (a.k.a. external limiting membrane, ELM). Sometimes, this membrane is associated with the juncture of the inner segment, IS, of the photorecetors and the outer segment, OS.

Of the three, the OS/RPE retinal detachment is probably the most serious because of the damage to the chromophores of the OS (**Section 5.5.15.3**). The oxygen dissolved in the vitreous humor enters the inter-photoreceptor matrix, IPM, and damages the chromophores of the OS. The spatial area of damage can be large and result in permanent blindness in portions of the retina if not surgically repaired quickly.

There is a word frequently surfacing in discussions of retinal detachments. It is frequently used as a synonym for the the OS/RPE retinal detachment even though the name is not descriptive. The word is rhegmatogenous (reg-ma-TODGE-uh-nus) from the Greek for tear. In the case of the commonly described OS/RPE retinal detachment, the tear if present is a tear through the entire retina from the ILM to th IPM described above. This tear allows the vitreous humor access to the IPM. This tear through the neural layer is generally called a rhegmatogenous retinal detachment, RRD, among the surgical community. When associated with the RPE/BM retinal detachment, the tear is more easily related to a peeling back of the serrated peripheral retina from the choroid. No tearing of the neural tissue is involved. The noun for peel in Greek is floúda, pronounced as feelda according to Google Translate. The verb form is xefloúdizo, pronounced as sefloudiza as in (of a surface or object) lose parts of its outer layer or covering in small strips or pieces, "the walls are peeling."

The term rhegmatogenous appears to be falling into disuse in the more recent literature in favor of more definitive definitions based on *in-vivo* imagery.

These three different types of retinal detachment are described on the internet at WebMD.com in less precise language designed for the general public.:

It appears that the Author encountered the RPE/BM or BM/choroid type of retinal detachment following a period of flashing lights along the temporal serrated edge of the peripheral retina over an extended period of time estimated to exceed one year. as discussed later in this report. The presumed fluid building up between the choroid and the RPE is seen to vary over a period of weeks after initial failure.

Most of the academic and clinical literature is focused on the RRD type detachment. However, see Wilkinson's citation to Maruko below. *The term RRD seems to leave many visual perceptions of the patient unaccounted for.* If RRD is used to include the floúda type detachment, the damage to the OS is a binary uncontrolled parameter in the discussion.

F.1.1 Mechanical failure (traction) at the vitreous/neural tissue interface

The failures at the vitreous humor/ILM interface, not involving the bulk of the neural material and generally identified with the word "traction" are not of interest in this diary and analysis.

Medscape, in April 2019, announced a CME/CE Courses: Long-Term Natural History of Idiopathic Epiretinal Membranes With Good Visual Acuity. The thesis was, "Epiretinal membranes (ERMs) are a common retinal condition characterized by the growth of fibrocellular tissue on the inner surface of the retina. While ERMs may occur as a consequence of retinal vascular diseases, uveitis, trauma, or retinal tears or detachment, most are idiopathic (iERM) ."

One of these iERMs involves the potential presence of a hyaloid membrane generally overlaying the inner limiting membrane, ILM, of the neural portion of the retina. It is typically reabsorbed after morphogenesis of the ocular is complete.

F.1.2 Scotoma resulting from detached retina at the periphery encountered by the author

The condition to be described here does not correspond to the medical diseases known as "central serous chorioretinopathy[7]" or vitreous-retinal interface neuropathy involving a hole in the foveola[8], or a pseudo-hole in the foveola[9]. It does relate to other disorders of the vitreoretinal interface[10]. The 2007 paper by Varano & Tedeschi was followed by one by Maruko et al[11]. That paper cited Spaide et al[12] and Spaide[13]. The two Spaide papers contain a large volume of *pertinent data* and deserve a section in this work, as time allows. The optical coherent tomograpy, OCT, technology was advancing rapidly beginning in the early years of the 21st Century.

However, there is a significant difference between the widely available OCT from Heidelberg Engineering available in the typical ophthalmology clinic and the more advanced adaptive optics augmented optical coherent tomography, AO-OCT, instrument available in various research institutions. The more advanced systems can image individual photoreceptors of the central retina in order to establish both their orientation and physical position.

On 1 February, 2018 at 82 years of age, the author awoke to a loss of vision on the nasal side of the visual field of the left eye. Under a low level of incandescent light, the scotoma was quite opaque and exhibited a granular flickering of the edge of the scotoma. It was perceived as basically circular and extended into about 15-20 degrees of the point of fixation at the equator. The center of the scotoma appeared to be near the equator at about 42 degrees. The scotoma bridged the horizontal equator, and appeared to present a turning back toward the equator as it disappeared at its edge (near the 45 degree radial of the eye. It was by definition hemianopic in the language of perimetry. This term is related to the far-field character of the perceived image and is not related to the hemispherical form of the CNS. **Figure F.1.2-1** shows the estimated perimetry of the affected eye.

---

[7]Spitznas, M. (1986) Pathogenesis of central serous retinopathy: a new working hypothesis *Graefe's Arch Clin Exp Opthalmol* vol 224, pp 321-324

[8]Kroyer, K. Christensen, U. la Cour, M. & Larsen, M. (2009) Metamorphosia assessment before and after vitrectomy for macular hole *IOVS* vol 50(12), pp 5511-5515

[9]Varano, M. Scassa, C. Capaldo, N. et al. (2002) Development of macular pseudoholes *Retina*, vol 22(4), pp435-442

[10] Varano, M. & Tedeschi, M. (2007) Disorders of the vitreoretinal interface: Clinics *In* Midena, E. *ed.* Perimetry and the Fundus. Thorofare, NJ: Slack, Inc. Chapter 4.8

[11]Maruko, I. Iida, T. Sugano, Y. et al. (2011) Subfoveal choroidal thickness in fellow eyes of patients with central serous chorioretinopathy *J retinal & vitreous diseases* vol x(x). pp 1-6 *Initially issued online*

[12]Spaide, R. Koizumi, H & Pozzoni, M. (2008) Enhanced depth imaging spectral-domain optical coherence tomography *Am J Ophthalmology* vol 146, pp 496-500

[13]Spaide. R. (2009) Age-related choroidal atrophy *Am J Ophthalmology* vol 147, pp 801-810

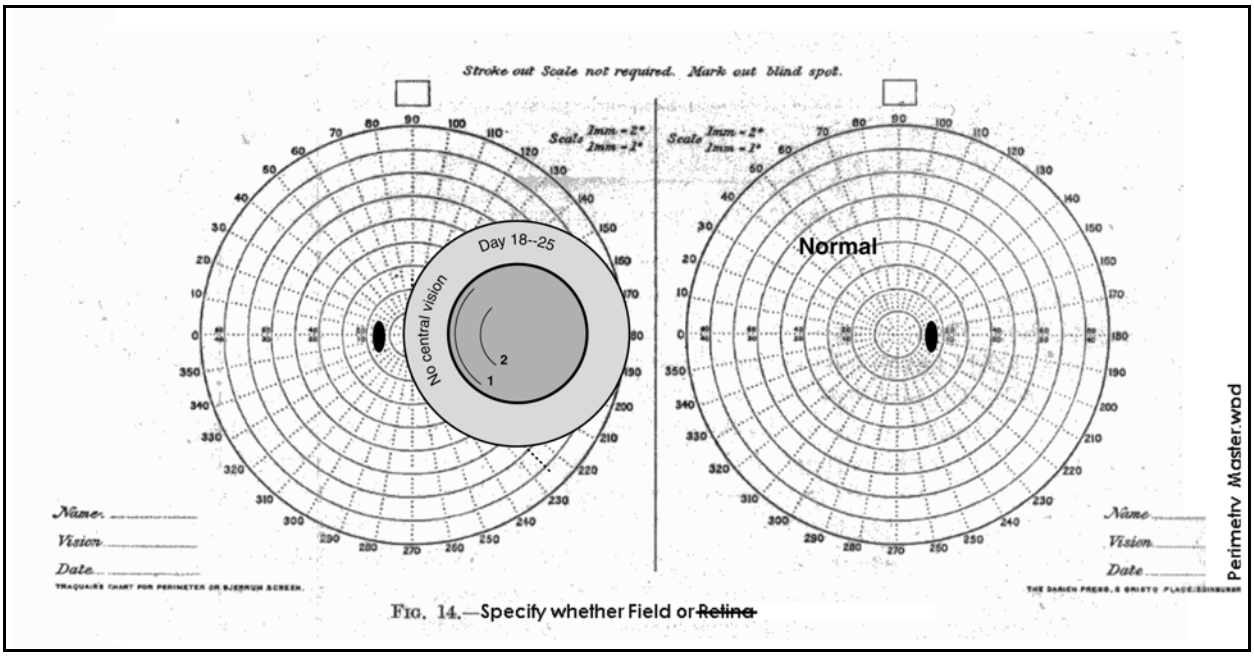

Figure F.1.2-1 Perimetry of an *acute onset*, short lifetime *unilateral hemianopic scotoma*. Following acute onset, it appeared to dissipate within two weeks as a significant optical artifact, except under mesotopic illumination. See text for an extensive analysis. The inner circular scotoma shown (coming within 15 degrees of the fixation point) was the author's estimate prior to clinical perimetry. The outer circle was the state of vision after 18 days. The loss of resolution associated with the foveola was significant, and stereovision was totally lost. See text.

The grid shown in the figure, although universally used, is of ancient origin (the tangent board) and does not properly represent any projection of the visual field of the human eye. It does not represent a polar projection of a spherical field or account for the wide angle optical system of the eye. Its only redeeming feature is its ease of recognition by the patient and optometrist. A secondary feature is that it can be used to represent both the field of view as seen by the patient and the retina as seen by the optometrist or other clinical personnel.

A more appropriate representation for physiological purposes would recognize the field actually acquired by the human visual system and recognize the broad optical field of the human optical system (**Appendix L, Standard Eye**).

As a result of these recognitions, the lower scale along the horizontal meridian is reasonable appropriate but overemphasizes the zero to 5 degree region. The upper scale does not do justice to the area of the field of view dedicated to the peripheral field. The upper scale should indicate the region between the 80 and 90 degree contours is nearly twice as wide as the region between the zero to 10 degree contours.

After recovering from the shock and novelty of the situation, an examination was arranged with my ophthalmologist. His examination with a slit lamp uncovered no unusual conditions; no excess blood near or in the neural layers of the retina, no edema, and no inflammation of the head of the optic nerve or elsewhere in the retina. He ordered a perimetry examination to more clearly delineate the condition as reported.

While awaiting the perimetry examination, more analysis of the condition was attempted. The condition was clearly a scotoma, as opposed to a *contraction* or area of *depressed acuity*. It was also *unilateral*. The scotoma was estimated to have a diameter of 52 degrees. It was optically very dense (on the order of 1 to 10% transmissive) in the mornings under mesotopic conditions becoming more transparent during the day and as time progressed (in terms of days) to between 30 and 50% transmissive. The scotoma exhibited no central nucleus of higher optical density. Under all illumination conditions the loss of acuity was deemed significant in this off-axis area. During the first week, it was observed that the area near the edge of the scotoma (location 1 to the scotoma edge, about 1.4 degree wide), exhibited a sparkling characteristic without any correlation with the heart beat. The individual sparkles had a

frequency of about 2-4 Hertz. After a period of minutes to an hour, this area exhibited a few striations of about 10 to 20 degrees of arc. A more interesting characteristic occured when the ocular was rotated quickly and stopped suddenly. As a result, the edge of the scotoma nearest the point of fixation exhibited a fluidic motion of about 1/4 degree. The motion above the horizontal meridian was not synchronous with the edge below the meridian. It may have been in counterphase to the upper portion. Upon closer study under daylight conditions (higher end of the photopic illumination range), it was possible to determine that the region suggested by the arc at location 2 also exhibited a fluidic motion.

While the scotoma exhibited a variation in transmissivity and a significant reduction in acuity, the performance was not compatible with any pulse signaling (stage 3 signal projection) involving the ganglion cells of the retina or later in the visual modality. The effects observed were compatible with a liquid filled (probably not liquid crystalline filled) pocket in the region between the choroid and the retinal pigmented epithelium (including Bruch's membrane). Such a pocket could deprive the analog circuits (stage 1 signal generating and stage 2 signal processing circuits) of the retina with electrostenolytic energy. Such deprivation could reduce the amplitude of the signals encoded by the stage 3 ganglion neurons that could encode a lower level of scene brightness without significantly reducing the amplitude of the action potential pulse streams. Whether the fluid consisted of whole blood or just plasma could not be determined by this analysis.

A review of several atlases did not provide scotomas with the location or shape of that observed in this case. They also did not provide any time lines as short as that observed. After ten days, the scotoma was largely unobservable under daylight conditions, except for a potentially continuing loss of acuity. This loss could be due to the pocket of fluid continuing to push the relevant portion of the retina out of the plane of best focus.. The scotoma had retreated to a diameter of about 20 degrees centered about 60 degrees from the point of fixation. It was essentially out of the useful region of the retina for normal vision (even when only employing the left eye. By blinking, the scotoma could be momentarily returned to its full extent and somewhat less transparency for only a second or two.

The choroid induced scotoma varied significantly in its perceptual appearance during its variation with time. Initially, and particularly upon awaking, it appears totally black, except for the above mentioned fringe. During this *first interval*, the pressure on the retina, and particularly the stage 3 encoding neurons, causes these ganglion neurons to completely shut down and not generate and propagate any action potential streams to the CNS. As time progresses during the day, the blackness of the scotoma gives way to a neutral gray for an interval measured in hours. During this *second interval*, a restoration of the ganglion cells operations is observed along with a continuing interference with either the stage 1 signal generation or stage 2 signal processing resulting in a neutral amplitude signal being passed to the stage 3 encoding ganglion cells ***or*** significant pressure still able to push the area of the retina in front of the fluid pocket out of the focal plane of the stage 0 opitcal system. The result of the latter action is a neutral gray blob representing the scotoma due to the light rays not furnishing an image on the stage 1 photoreceptors. As the pressure reduces further during the day, effectively defining a *third interval*, the distortion of the retina is reduced to the point that the scotoma becomes semi-transparent (about an optical density, D ~0.3, and an image is formed within the diameter of the scotoma by the optics. However, it remains seriously out of focus within the boundary of the scotoma. The image is not in focus sufficiently to provide significant vision.

By day 14, the scotoma was no longer of concern to me. During most of the day, it was merely a nuisance obscuring my perception of my nose while my right eye was closed. With the right eye open, the bilateral field of vision appeared effectively normal. No medical treatment had been used during this period of acute disease, nor was any of the subjects normal medications for other conditions changed.

On day 16, the situation changed dramatically. The scotoma appeared to expand about the center point, reaching within about 5 degrees of the fixation point and extending above and below the 45 degree diagonals in the above image. The effect was highly sensitive to the light intensity of the scene. At daylight levels, it remained a low density filter with significant defocusing of the scene content. At interior residence light levels, it appeared solid black. When semi-transparent, the scotoma continued to exhibit the characteristics of a low-viscosity fluid enclosed in a pocket.

Only computer-aided tomography of the retina, performed in a timely manner, could confirm the above analysis (diagnosis?).

The change in the appearance of the scotoma during this transient experience is suggestive of the significant variation in the appearance of scotomas reported by other patients to medical practitioners.

> Another phenomenon occurred during the above scotoma and has not yet been investigated fully. During the first interval, when the scotoma was totally black, a large luminescent blob floated from the bottom of the scotoma to the top in less than 2 seconds sporadically (more than two minutes separating the events, that

made it difficult to be attentive to it). The blob was about 1/5th to 1/8th of the height of the scotoma and extended from the meridional edge to at least the central vertical of the scotoma. The best hypothesis at this time would suggest the blob was due to a "wave" in the fluid within the pocket formed between the choroid and the RPE. This wave reduced the pressure sufficiently that the stage 3 ganglion cells were able to temporarily return to generating action potential streams indicating to the CNS that the light level was being reported but virtually no scene detail was being reported (as in the second interval).

[Following surgery and a period of recovery, the luminescent blob was subsequently recognized as going in the opposite direction, from top to bottom.]

On day 18, the scotoma expanded during the night and upon awakening, its solid edge reached the point of fixation and extended beyond the 50 degree upper radial. It was now slightly half of a heart in shape (as in a child's valentine heart). The upper edge curved back toward the horizon (see overlay in above picture). This expansion precluded any ability to read via the left eye and destroyed my stereo-based depth perception.

The outer edge of the scotoma may have reached the edge of the visual field and satisfied the term-of-art, known as "breaking through."

Upon retiring, and closing the eyes in a room at scotopic light levels, the area of the scotoma contained a sparse array of scintillating (twinkling) points of white light. The perceptions did not twinkle in synchronism. The points were random in location and appeared to be separated by 3 to 5 degrees. This pattern had been noticed one or two nights earlier and extended to day 25+.

This condition is not related to multiple evanescent white dot syndrome, MEWSD, involving stationary white spots on the retina observable by the ophthalmologist.

On day 20, the situation remained the same as day 18. A closer examination of the initial condition upon awakening was made.

On awakening in a darkened room, and before opening my eyes, the scotoma is not recognizable. Upon opening the left eye under scotopic light conditions, the scotoma is jet black and the edge is striated along the circumference. Within about 15 seconds, the edge becomes feathered and the striations are no longer visible. Upon closing the eye, the scotoma is now white against a neutral gray field and the striations are quite visible. The edge becomes feathered after about 15 seconds and the striations are obscured. This cycle beginning with an initial striated edge can be repeated cyclically.

As days 18 through 20 progressed, the scotoma becomes more transparent as the light level approaches full daylight. At full daylight, the scotoma has a density of about 50% (D ~0.3) but the resolution remains at a negligible level. Looking back into a lighted room, the scotoma takes on an average brightness approximately that of the larger objects in the field.

On day 24, while in bright daylight, with pupil reduced in diameter, it was possible to "see" people walking in a parking lot at ranges of 20-50 feet without any optical aids. There was no sign of any variation in the opacity of the scotoma with eccentricity. There was also no significant detail resolvable regarding these characters.

The ability to see through the entire scotoma at this time depended upon the light level. Without, any glasses, hockey players on a white rink were little more than stick characters.

On day 25, while in bright daylight, with pupil reduced in diameter, it was possible to resolve the fronds of a palm tree about 500 feet away upon fixation by using a lens of +3.5 diopters. Without the lens the fronds could not be resolved. Only the one lens was available. With some computation, these parameters could be used to compute the nominal height of the foveola compared to its normal position (see next two paragraphs). The normal uncorrected visual acuity of the eye before the appearance of the scotoma was at least 20/25 and can be considered 20/20 in this calculation.

On day 26, the improvement in vision through the scotoma was significant. A 3 degree vertical by 6 degree horizontal window opened up around the fixation point (sporadically, probably dependent on the light level). However, this introduced a drawback. Currently, the perception of the left eye involves some curvature of objects near the foveola as well as a change in magnification of objects in the external field. The scaling is to approximately 2/3 of the size of the right eye image. The perceived point of fixation is also displaced 3–4 degrees to the lower right along a radial 45 degrees below the horizontal meridian. **Figure F.1.2-2** illustrates the situation using a different perimetry scale. With specific intent, it is possible for the right eye to become dominant and the composite image with both eyes open to ignore the image provided by the left eye.

Varano & Tedeschi note, “Different studies document the preferential location of the pseudofovea in order to preserve lower left visual field. According to the authors’ observations, the new area of fixation in most cases is located superior and to the left of the anatomic fovea, immediately close to the dense scotoma.”

The distortion of straight lines shown in the figure, which was also accompanied by a tilt of the entire visual field of about 10 degrees (or a rotation of the field about the point of fixation of about 10 degrees) appears to be due to the physical optics involved in the displacement of the foveola itself by the displacement of the inner limiting membrane. It is difficult to distinguish between these two situations due to the conditions illustrated in the next figure. The distortions may or may not involve the term, spatial metamorphism or spatial metamorphopsia (page 174). The definition of this term in Wikipedia takes many forms and may not be adequate;

> “*Metamorphopsia* is a type of distorted vision in which a grid of straight lines appears wavy and parts of the grid may appear blank.”

The system had difficulty merging the images from the two eyes. As a result, working at the computer became difficult. Introducing an available 1.5 diopter lens in observations of the far field improved the acuity of the left eye marginally. A 3.5 diopter lens was also available. Depending on the specific time, the 3.5 diopter lens provides better acuity than the 1.5 diopter lens. The image seems to exhibit more fluidity than it did earlier. Both suggest the fluid presumably pushing the RPE out of position, is now under less pressure than previously.

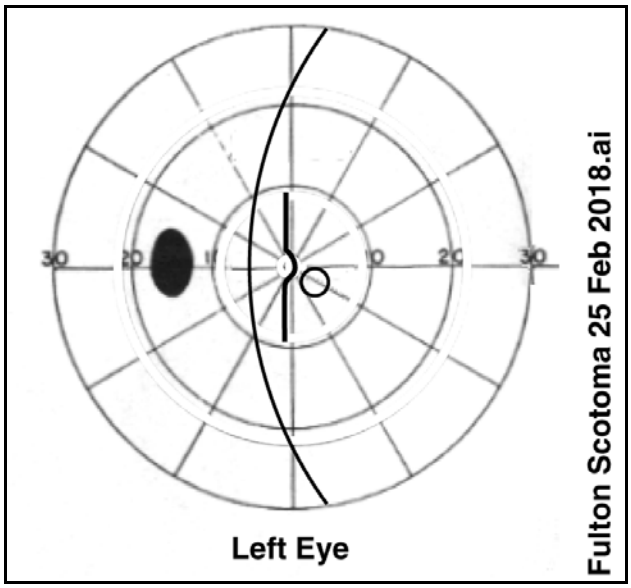

Figure F.1.2-2 Fulton scotoma beginning 25 Feb 2018. Note the expanded scale. The scotoma edge follows the large circular segment and is generally semitransparent in daylight. The foveola is displaced from its normal position by 3-4 degrees along a 45 degree diagonal. A vertical element in the scene at the position of the previous (anatomic) foveola exhibits a curvature as shown at the horizontal meridian.

Day 27 saw changes in the performance of the left eye. It became possible to perceive images across the entire field of view under daylight conditions. However, the majority of the image tended to be rotated approximately 10 degrees clockwise and the image was still of very low acuity. It still exhibited distortions as indicated in the above figure but vertical lines appear rotated along with the majority of the image field. The scotoma had expanded to cross the vertical meridian in the lower quadrant of the field. While the scotoma remained highly fluid, this change would not be related to gravity since the area affected was in the upper portion of the retina .

Day 29 saw the scotoma extend into the lower left field reaching the 45 degree diagonal in that quadrant. The scotoma also began to encroach on the upper left field to a point projecting vertically from the 5 degree point on the horizontal meridian. The photoreceptors remainded functional in these areas but were considerably hindered by the fluid in the chamber causing the scotoma. This fluid continued to slosh around on sudden rotational movement of the ocular. The performance of the eye continuted to vary significantly on light intensity. The curvature of vertical lines to the left of the dislocated point seems to have been ameliorated. The condition continued through day 30.

Day 32 saw the scotoma extend into the left lower quadrant dramatically. **Figure F.1.2-3** illustrates the change from day 25 Feb 2018. The upper field of the scotoma has extended to a vertical position straddling the blind spot. It is generally stationary but highly subject to illumination level. The upper field exhibits considerable structure generally centered on the displaced fixation point. This structure will be discussed further in later paragraphs. The darker gray area is in fact totally opaque under most illumination conditions and extends to within 5-10 degrees of the ora serrata of the retina. The volume between the inner limiting membrane associated with the neural layers of the retina and the neural layers themselves is filled with a low viscosity serum from the blood with a viscosity similar to that of water. When the ocular is rotated rapidly in the vertical direction, upon stopping; this fluid sloshes with a frequency of about one Hertz. The sloshing is highly damped and only sloshes for one observable cycle.

The perception through the left eye has changed modestly from 25 February. Vertical lines in the upper gray field of view are not exhibiting a curvature around the original point of fixation but the present point of fixation is still displaced along a 45 degree diagonal and the external scene is still perceived as rotated or tilted about 15 degrees. The acuity in this area is slightly at the moving finger stage in the absence of an external lens. A lens of 3.5 D considerably improves the acuity of the eye but it remains far below 20/20 with that correction.

Days 35 & 36 saw marginal regression of the upper field scotoma nasally and a somewhat lower level of the fluid forming the lower scotoma to the extent that the author was surprised to see his toothbrush at the point of left eye fixation upon awakening. The acuity was not significantly improved. The point of fixation of the left eye remained displaced as illustrated.

Day 38 saw a period of three hours in late afternoon when the fluid level of the lower scotoma dropped below the displaced foveola by about 5 degrees relative to the vertical meridian. The size of objects in the far field were about 50-60% of their size in the right eye and the point of fixation remained about 5 degrees from the normal fixation point along the 45 degree radial as shown in the previous figure. The distinctive tilt in the image varied with distance from the vertical meridian. Close to the meridian, it was approximately 5 degrees sloping down to the right. Vertical structures remained warped to different degrees depending on where they were to the left of the displaced fixation point. The 3.5 D lens provided significant acuity improvement, but acuity was at best 20/100. The crenelation, introduced in the following material introduced in the Gass material and discussed in Varano & Tedeschi, has been quite obvious during the last week. The dark arcs are about 1-1.5 degrees apart and radiating from the displaced fixation point. The fluid level is quite sensitive to blinking. The level will fall about five degrees along the vertical meridian and then return to its nominal level within a second or, at most, two seconds after blinking. There is no observable change in visual performance synchronous with the heart beat!

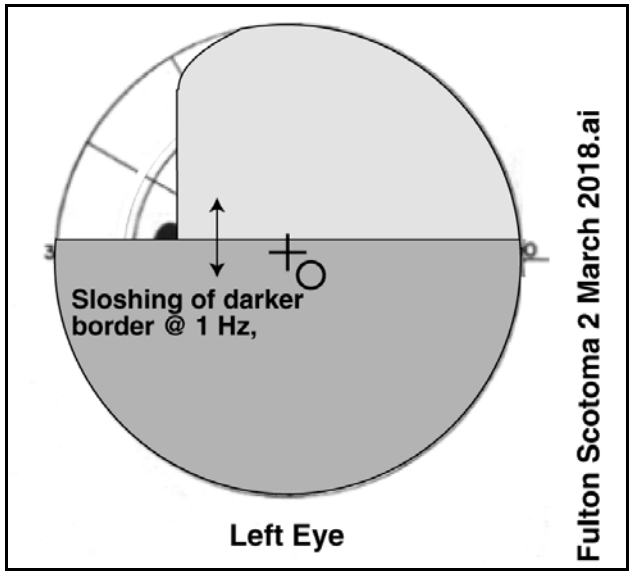

Figure F.1.2-3 Fulton scotoma, 2 March 2018. Note the same scale as in previous figure central 30 degree diameter centered on original fixation point, the cross. The current fixation point is at the center of the foveola, the small circle. The upper area, light gray, has expanded beyond the vertical meridian to straddle the blind spot. This area exhibits the cellophane and crumpled cellophane described by Varano & Tedeschi. See text. The fluid within the darker area sloshes upon sudden vertical ocular movements, See text,

The above described situation appears compatible with **Figure F.1.2-4** from the website of the American Society of Retinal Specialists (Chicago). It appears to show a right eye with a significant tear at upper right leading to a partial detachment at lower right;' the opposite of the author's situation, with damage to the temporal side of the left retina. In this image, the foveola would be to the right of the optic nerve head and about 50% of the way to the edge of the detachment. As in this image, one of the stretch marks may have directly involved the foveola.

Figure F.1.2-4 Vitreous fluid flows through a retinal tear (at upper right) to cause a partial retinal detachment involving the macula. The optic nerve and nasal retina, or portion of the retina closest to the nose, are normal and uninvolved. Vitrectomy surgery is indicated to restore vision. Image courtesy of the ©ASRS Retina Image Bank, contributed by Brandon Busbee, MD. Image 2939.

In the author's case, the retina remained fully functional except for eventual loss of imaging capability, as described above and suggested by the gross displacement of the temporal retina in the initial OCT scan. Based on my amateur research, this was a serous detachment between the choroid and the RPE. The "tear" referred to in the caption, may have occurred at the perimeter of the retina rather than an internal tear. The laser stitching, used in the repair, was along the edge of the retina. No large scale permanent damage to the photoreceptors of the retina was encountered based on the visual performance encountered one year following re-attachment surgery.

However, the discoloration of the separated portion, may suggest a separation between the RPE and the outer segments of the photoreceptor layer. This type of separation is generally associated with more damage to the outer segments than encountered in the author's case. On days 39–41, no significant change in the performance of the left

eye was observed. The Herbert Eye Institute at the University of California–Irvine was contacted. Within a matter of hours after reviewing their initial tests, they diagnosed a detached retina requiring prompt surgical intervention. They arranged for the surgery to occur four days later (day 46). The surgery involved the pars plana and the puncture of three holes in the white of the eye readily accessible by the surgery. A gas bubble was employed to accelerate healing. Physical recovery was uneventful.

F.1.3 Lab work detailing the Detachment of the author's retina & repair surgery

Detachment of the retina can occur under several distinctly different conditions. The detachment can occur for the entire retina, including the RPE from the choroid. It can originate from conditions within the choroid/RPE space. Alternately, it can occur due to conditions within the vitreous/retina space. It can involve sudden traumatic force applied to the eye or to less significant force applied over an extended period, particularly in the elderly.

Simple trauma can result in detachment of all or part of the retina from its normal association with the RPE. This detachment may appear as a simple tear or a more significant dislocation. Section 4.5 illustrates the overall photoreceptor-IPM-RPE complex and how tearing can occur.

Anderson, et. al. have provided significant laboratory information related to retinal detachment and re-attachment in cats[14]. Their data, although dated, stresses the importance of rapid repair of such damage. Due to the sensitivity of the chromophores of vision to attack by oxygen, it is suggested their use of air to aid in retinal repositioning relative to the RPE is unwise. The use of dry nitrogen or other unreactive gas would be preferred. In the author's case, the gas was perfluoropropane, C_3F_8, and the injected fluid appears to have been saline solution.

It has become common to surgically repair damage due to retinal detachment in human subjects. If the detachment involves the OS/RPE interface, the repair should be done as soon as possible. The residual problems for such a failure are discussed briefly in Anderson, et. al. and they provide additional references.

F.1.3.1 Sudden detachment in an 82 year old without trauma

This author sustained a detachment during his sleep or upon awakening that involved the temporal portion of the retina of the left eye, resulting in the loss of vision in the right visual field of that eye. It initially consisted of a 20 degree circular field with a center at about 40 degrees from the point of fixation very near the horizontal meridian. It grew within a day or two to about a 40 degree diameter. Within a week, it had expanded to include most of the right hemi-field and nearly all of the lower hemi-field. A visit to the first ophthalmologist at the 40 degree diameter stage resulted in a recommendation to observe the condition for the next six months. A visit to a second ophthalmologist after a total of forty days resulted in surgery within four days to suppress any further loss of visual function.

The subject had cataract surgery in both eyes during the prior 10 to 15 year period. Thus, the eye had an accommodation range of less than 0.25 diopters.

Figure F.1.3-1 shows the OCT scan obtained at the forty day point by the surgeon at the Herbert eye Institute of the University of California-Irvine. The detachment is obvious. Chapter 4.8, by Varano & Tedeschi in Midano describes the potential situations that may arise and the detailed labeling of the tissue involved. The condition in this case has traditionally been identified as a posterior vitreous detachment, PVD. This type of detachment can be further described by the types of epiretinal membranes involved, **Section F.1.5.2**.

On further analysis by the author (and patient), there appears to be a difference of opinion between the surgeon and the author as to whether the figure describes a tear resulting in what is called a posterior vitreous detachment, PVD, or a retinal detachment between the RPE and the barrier membrane, BM, or between the BM and the choroid). The surgeon may have been using the term, rhegmatogenous, implying a tear, as a synonym for a vitreous retinal detachment. The question remains undecided, however,

- the patients observations would suggest the serous detachment because of no loss of outer segments was encountered during the first 40 days from initial detachment.

- There appears to be no sign of outer segment, OS, detachment from the RPE (a vitreous detachment) in the OCT image involving either the foveola or the temporal portion of the retina along the horizontal meridian.

- The ripples in the BM on the temporal side of the foveola are significant. Unfortunately, the abbreviation

[14]Anderson, D. Guerin, C. Erickson, P. Stern, W. & Fisher, S. (1986) Morphological recovery in the reattached retina. Invest. Ophthal. & Visual Sci. *Am J Ophthalmol* Vol. 27, pp 168-183

BM, is used variously in the literature, barrier membrane, base membrane or Bruch's membrane. It is also occasionally lumped into the BM/RPE layer. In this case, the ripples were present prior to surgery.

•*Note the inversion of the ILM pit into a prominence due to the fluid pressure developed between the choroid and the BM.* This will be discussed later in conjunction with the dysmetropsia still present after 6 months (**Section F.1.7.1**).

• The major void associated with the retina/choroid complex appears to a novice in surgical preparation to be between the choroid and the BM not between the BM and the photoreceptor neurons.

• The surgeon confirmed there was no significant tear in the face of the retina only multiple small tears at the serrated edge of the retina.

Wojtkowski et al., 2004 provides the most explicit definition of the RPE/Choroid complex. in **Figure 18.8.3-29** of **Section 18.8.3.5.3**. They illustrate the VM = Verhoeff's "membrane." on the PC side of the RPE and the BM = base membrane and CC = choriocapillaris on the choroid side of the RPE. Verhoeff' membrane is shown in quotation because it may in fact be a cribiform membrane or merely a grouping of Müller cells filling the space between RPE cells.

On careful examination of the left frames, there appear to be several circular features grouped around the original point of fixation. These may play a role in the overall detachment or post surgical recovery.

Wong[15] has discussed the ripples noted along the lower edge of the detachment using the term displacement or translocation of parts of the retina. His focus was on folds as a result of surgery. "Patients with macular folds may complain of metamorphopsia, diplopia, and/or blurred vision." These are not exclusive symptoms of retinal detachment. He did note, "As demonstrated in this study and others, macular folds tend to resolve spontaneously because of the elasticity and/or "memory" of the retina." "Although the retinal folds spontaneously regress and the outcome was good in the majority of cases, a displacement fold may require further surgical intervention rather than conservative management." "However, the optimal treatment for displacement folds requires further research."

[15]Wong, R.(2012) Longitudinal Study of Macular Folds by Spectral-Domain Optical Coherence Tomography *Am J Ophthalmol* vol 153, pp 88-92

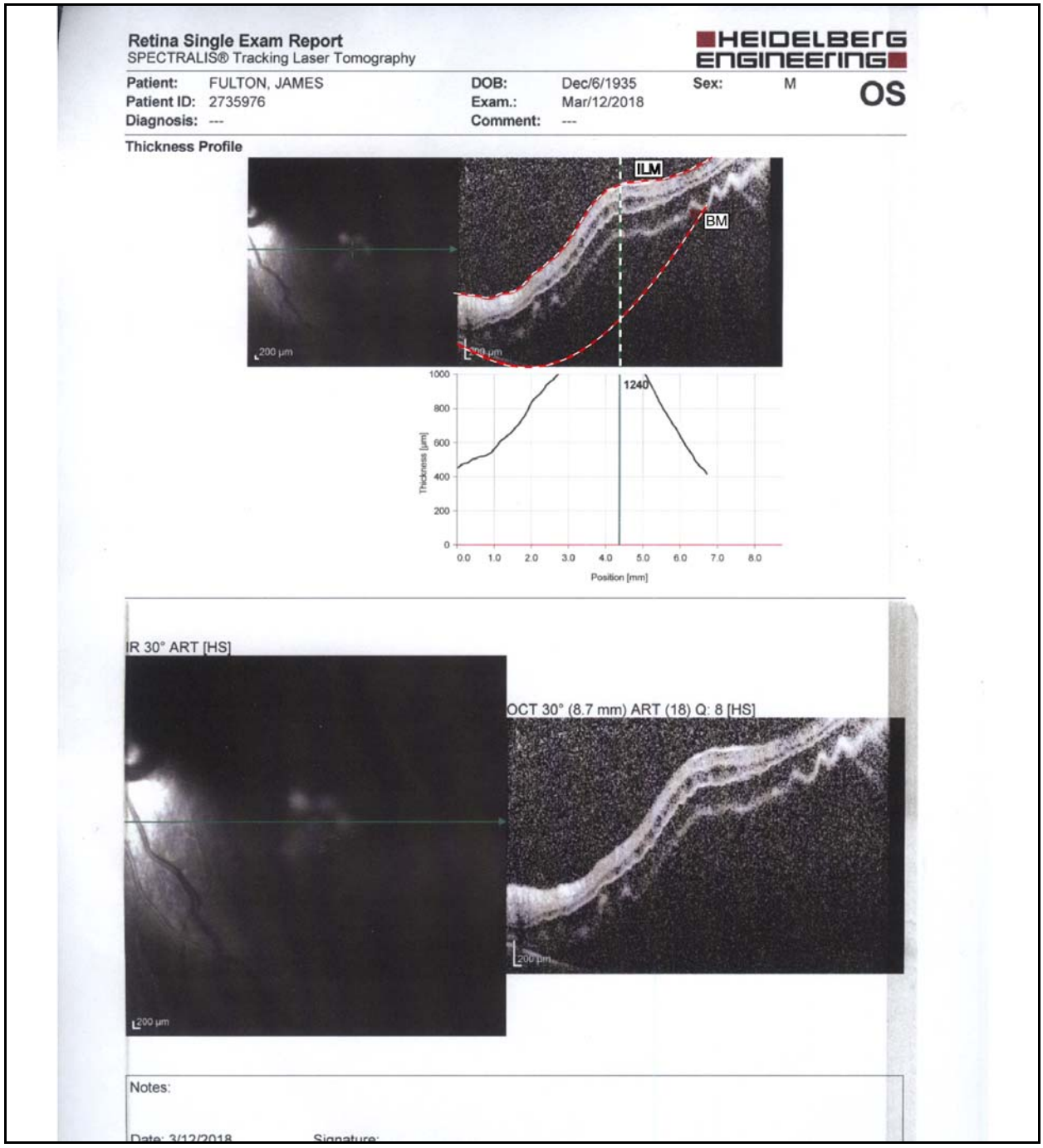

Figure F.1.3-1 OCT scan of authors detached retina after forty days. Note red lines marked ILM and BM. Note green vertical line through inverted foveal pit in upper right graph. Note ripples along lower edge of retina in frames on right associated with translocation of the foveola. The barrier membrane, BM, appears fractured in this frame but there is no sign that the OS/RPE interface was disturbed. The numeric, 1240, is the thickness between the two red lines, the BM line was apparently estimated by the Heidelberg software. See text.

F.1.3.1.1 Interpreting the BM representation in OCT of 3/12/2018

The BM in the above simple OCT scan can be interpreted as missing, interrupted or merely transparent. The OCT

technique relies upon very marginal reflections from each surface within the retina/sclera complex. Reflection coefficients of less than one percent can be important in interpreting the OCT image.

The expected reflection at the BM can be understood better using a higher performance OCT device of higher resolution than that used here.

Looking first at **Figure F.1.1-3** and then **Figure F.1.1-2** provides a better understanding of the BM region. The key is to recognize the BM actually represents the RPE/Bruch's membrane complex and that this area is indeed a complex from several perspectives. As shown in the first figure, the reflection related to the RPE are resolved into two components in the best OCT images, the RPE/OS interface and the RPE/Bruch's membrane interface. These two interfaces are more reflective (hyper-reflective in the range of a few percent at most) because of the critically important chemical processing occurring at these locations. The chemical processes can be surmised from **Figure F.1.1-2**. The RPE are the principle site of chromophore creation and application within the eye. Within the RPE/Bruch interface, the proto-chromophores arrive at the RPE surface from the blood stream as described in **Section 7.1**. **Section 7.1.2** describes the chemistry at both faces of the RPE. **Section 7.1.3** illustrates the operating cycle of the normal RPE. This includes how the RPE accommodate the four chromophores of animal vision and distributes the appropriate chromophore to the appropriate OS.

- - - -

Figure F.1.3-2 presents a graphic combining a variety of functions and the critical spatial distances between them. The purpose is to define the reason for the bright lines defined by the IN•OCT panel discussed in **Section F.2.4** for a typical on-visual-axis human OCT image. Only one dimension is shown in the figure, the distance between the defining points of the Inter-photoreceptor matrix, IPM. The range is considerable as observed in practice for healthy eyes. This variation among the layers of the retina is discussed in **Section F.2.1** based on the recent work of Yiu et al employing six Rhesus macaque monkeys in each of two groups. As noted in **Section F.2.1**, this number of animals is insufficient to provide statistical values based on the data of their Fig. 3.

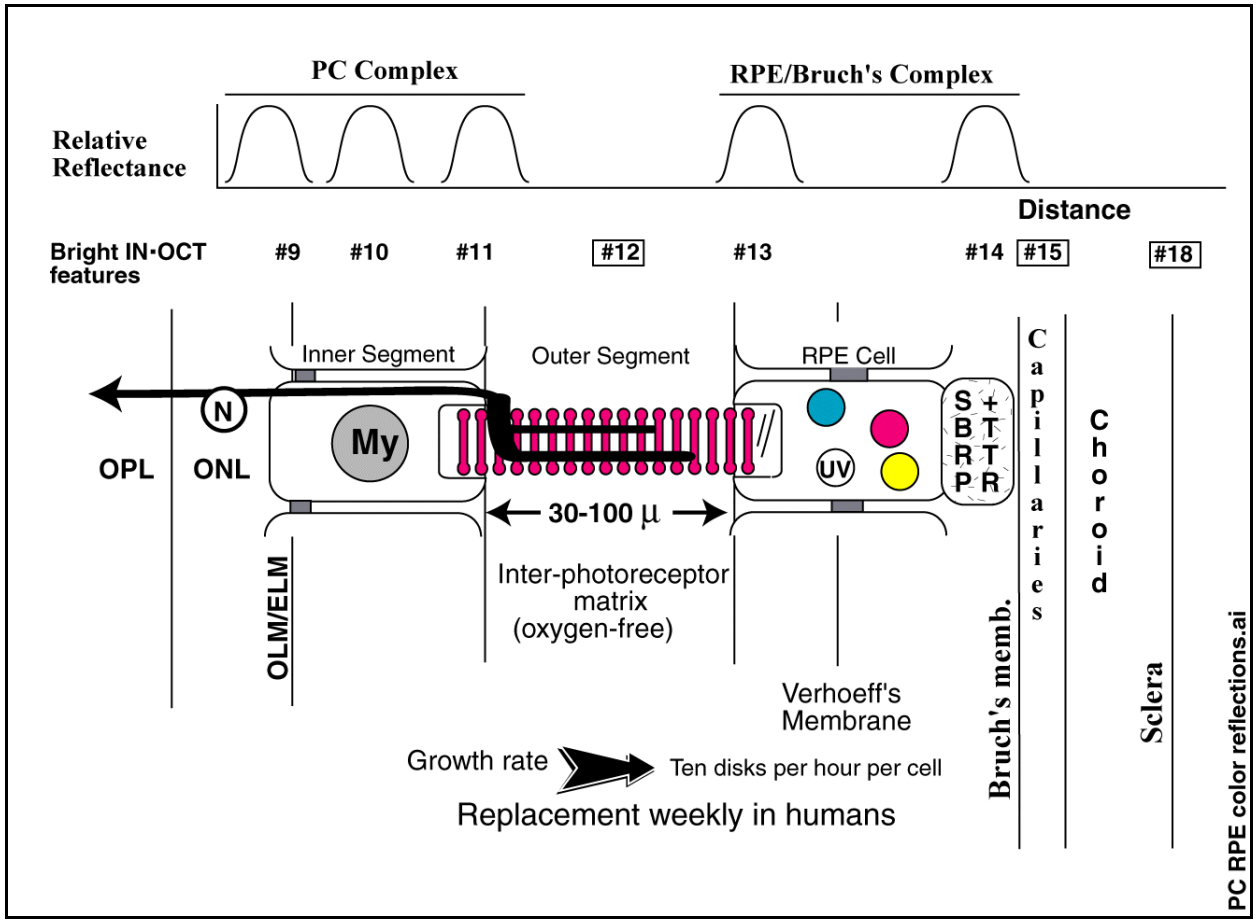

Figure F.1.3-2 Composite of functions occurring within the PC & RPE/Bruch's complexes in relation to an OCT scan. The distances are not to scale. The relative reflectances have all been normalized and shown of equal width. My; myoid of the inner segment, a controversial name; also described as the ellipsoid or paraboloid by different investigators over time. The shape of the myoid is not one of its characteristics. See text.

The specific features illustrated are,

#7	Hyporeflective area	Outer Plexiform Layer; pedicels of the PC and neurites of stage 2 neurons
#8.1	Hyporeflective area	Henle Layer; Axons PC neurons
#8.2	Hyporeflective area	Outer Nuclear Layer; Nuclei of PC neurons
#9	ELM/OLM	
#10	Myoid of Inner Segment	
#11	Ellipsoid of IS/OS junct.	Actually the secretory zone of the IS creating discs & their coating with a chromophore
#12	Hyporeflective area	OS segment between #11& #13
#13	Interdigitation Zone	Actually the combined chromophore extrusion and phago-disc regions.
#14	RPE/Bruch's Zone	Actually the chromogen delivery zone of the RPE.
#15	Hyporeflective Zone	Choroid capillaries
#16		
#17		
#18	Choroid/Sclera junction	

The label, zone, in the above table indicates the IN•OCT panel was not able to define the precise origin or function of the cause of a specific hyper-reflective line.

Layers and Zones 8.1, 8.2, 12, 15, 16, 17 & 18 are all hyporeflective. The major bright lines are 9, 10, 11, 13, 14. The commonly easiest bright line to identify is #14. This is the keystone line for analyzing the medical condition of a retina.

#9, the external limiting membrane is a hyper-reflective line due to the presence of the face and content of the IS as much as to the membrane. A membrane alone is typically not recorded well in OCT because of its low specific volume and relatively smooth (therefore, specular) surface.

#10, is the bright line due to the significant reflectance of the coarse surface and high index of refraction of the myoid compared to surrounding portions of the IS.

#11, is the bright line due to the secretion of the opsin forming the discs and the high concentration of unstructured chromophoric material in the "ellipsoid." The name ellipsoid has no histological significance. Jonnal et al[16]. identified this line. "By quantifying cellular morphology on each of the 9593 cones, we found that band 2 has a thickness of 4.7 μm, corresponding to an object thickness of 3.5 μm or less, and that it lies approximately equidistant from the ELM and [OS/RPE Interface]. These findings are consistent with the interpretation that band 2 arises from the junction between IS and OS, but *inconsistent* with the recent hypothesis that the band arises from the IS ellipsoid.

> There seems to be some confusion between the myoid and ellipsoid in these author' terminology. They and Spaide[17] were in a significant debate over terminology in the rapidly advancing ability to identify and measure the length of axial features in the retina using AO-SDOCT techniques. There is a significant problem in their debate; they have not identified the materials within the IS/OS interface they are observing by reflection. The material consists of the bulk chromophore, one of the four Rhodonines of human vision (**Chapter 5**), that is being used to coat the discs of the OS. Their debate even involved the archaic question of rods versus cones, without providing any evidence of the spectral performance of any of their outer segments. *Their discussion was based only on OCT evidence versus histological evidence.*

#13, is the bright line in the interdigitated region shared by the terminal ends of the OS and two distinct parts of the RPE cells; the first is the macrophage capability and the second is the chromophore secretion capability of the RPE. Both of these functions deal with concentrations of opsin and the chromophores just as in the ellipsoid region. These concentrations of unstructured material can lead to significant hyper-reflectivity in OCT imaging.

#14, is the bright line due to the repackaging and reformatting of chromogen material as it is delivered to the RPE cells from the capillaries. The delivery process is a bit involved but the retinol-based material is delivered to the area of Bruch's membrane in a corked bottle consisting a transport protein, serum retinol binding protein, SRBP, with a hollow cavity in its interior, and a cork consisting of a protein, transthyretin, TTR (**Section 7.1.2.1.3**). In the process of unloading the retinal-based material, the material is converted into one of four types of chromogen that is then stored within the RPE cells in granules When called upon, each chromogen material type is converted to an active chromophore and secreted as discussed in connection with bright line #13.

These descriptions of the location and function generating the hyper-reflective lines are all provided in greater detail in **Section 7.1** of this work.

> **Note:** The reflections defined above cannot be associated with a conventional histological feature, such as a lemma of a cell. These features represent the center of reflection from a distributed set of reflections, just as a center of gravity does. There is no requirement that any material object exist at the center of gravity of a ship, airplane or other object. Note also, if a single reflection from a single flat surface were the cause of a bright line, the source of the reflection would be indicated by the centroid of the distributions shown in the relative reflection graph.
>
> **Note also:** The chromophores of vision are very sensitive molecules with very energy small band gaps in the language of quantum chemists (typically less than 2.0 electron volts). These molecules are frequently destroyed or dissolved during the preparation of histological slides of retinal material. Thus comparing an in-vivo OCT scan with a in-vitro histological sample from a different eye may not be rational.

F.1.3.2 The repair surgery

On 6 April, Dr Mutil Mehta performed the surgery, on an ASAP basis, after his formal examination on 3 April 2018.

---

[16]Jonnal, R. Kocaoglu, O. Zawadzki, R. et al. (2015) Author's Reply: Outer Retinal Bands; Letters to the Editor *IOVS* vol56, pp 2507-2510 doi:10.1167/iovs.15-16756

[17]Spaide, R. (2015) Critique: Outer retinal bands. *IOVS* vol 56, pp 2505–2506

The initial diagnosis by Dr Mehta was, Cystoid macular edema, retinal detachment and vitreous hemorrhage.

The surgery involved "removal of the viscous gel (Vitrectomy), re-attachment of the retina using laser coagulation (photocoagulation) along the temporal edge near the horizontal meridian, and introduction of a gas bubble (perfluoropropane, C_3F_8) to encourage return of the retina to its original position within microns of the choroid (Pneumatic retinopexy)." According to *Web*MD, "The bubble helps to flatten the retina until a seal forms between the retina and the wall (choroid) of the eye. This was estimated by the ophthalmologist to take about 1 to 3 weeks. The eye slowly absorbs the gas bubble." Some of the epiretinal tissue may be peeled away during this surgery. No epiretinal material was found during surgery. To heal optimally, "You must keep your head in a certain position for most of the day and night for about 1 to 3 weeks after the surgery." This maintains the gas bubble adjacent to the damaged area. This is not practical if the break is on the bottom of the eyeball. You would have to keep your head upside down." *Web*MD is considerably less than precise concerning the outcome of retinal re-attachment surgery. The results can vary widely but are virtually always considered successful by the patient. Achieving 20/25 visual acuity is not uncommon after successful surgery, but it may take more than a year.

The surgery involved three penetrations of the ocular at the recommended points of the surgical manuals as of 2017.

> "Typically, the dilated eye is entered through the pars plana, a "safe zone" in the white part of the eye or sclera; hence this procedure is called a pars plana vitrectomy. (ASRS, same page)"

Two of the penetrations were positioned at 45° from the sagittal plane of the eye and at points about 60° from the center of the pupil. The third penetration was in the lower temporal quadrant at an angle of about 45° from the sagittal plane. It was also at about 45° from the center of the pupil.

After clearing foreign material from the area between the displaced retina and the surface closest to the choroid, the retina was repositioned and tacked into place with about five pulses from an external laser positioned to fire through the pupil at locations along the temporal edge of the retina. This action reattached the retina at multiple points but left the intervening retinal area only approximately positioned. Significant parts of the intervening retinal area was apparently not in the focal plane of the optical system. It was anticipated that these areas would reattach themselves to the tissue still attached to the choroid as part of the healing process. As the re-attachment progressed, the retina would become nominally spherical and in the focal plane of the optical system.

At the completion of the re-attachment procedure, the ocular was filled with a perfluoropropane, C_3F_8, gas bubble to aid the re-attachment process over a period of multiple weeks. By looking straight down, it was possible to observe the dissipation of the gas bubble over time. After about 100 days, the bubble only occupied the pit of the retina. After about 120 days, it disappeared completely. **SectionF.1.3.4** provides details related to this process.

The retinal map following surgery appeared as in the caricature of **Figure F.1.3-3**. Combining, • the progression of the scotoma in Figures F.1.2-1 thru F.1.2-4 in Section F.1.2, • the graphic from Busbee in **Section F.1.2** (and ignoring the tear), • the OCT scan of **Figure 1.2-5** in **Section 1.2.1** and • the retinal map of the repaired retina,

some conclusions can be drawn concerning the retinal detachment of the author.

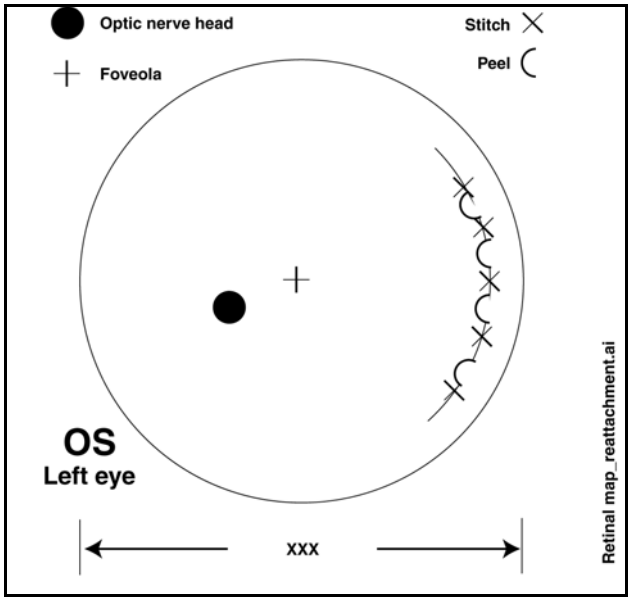

Figure F.1.3-3 Retinal map caricature showing multiple tears/peelings and stitch locations following surgery. See text.

F.1.3.3 Determination of the type of retinal detachment

It is appropriate to diagnose the type of detached retina that occurred based on the initial perceptual evidence, the initial OCT scans and the surgical repairs made during surgery as described by the post surgery documentation. 1. The foveola was displaced prior to surgery by the ballooning of the retina due to the accumulation of fluid over a period of at least a week during the 40+ days between acute damage and repair surgery..

2. As confirmed by the surgeon, there was no single major tear in the neural tissue. There were multiple small tears (peelings) near the temporal periphery of the retina.

3. The fluid build up was between the choroid and Bruch's membrane initially until the membrane was

shattered, allowing fluid to enter the space between Bruch's membrane and the RPE layer.

4. There was no build up of fluid in the IPM, between the OS and the RPE.

5. There was likely to be a fold or stretch mark passing right through the foveola, ala the Busbee photograph. Thus, ***the conclusion is drawn that the retinal detachment was of the serous type, with major fluid build up between the choroid and Bruch's membrane. This is confirmed by the lack of fluid build up in the IPM and no significant OS damage after 40+ days prior to repair surgery***.

F.1.3.4 Followup on the retinal detachment surgery–diary for 1st 6 months

The fact that the visual system employs what is known as an "immersed optical system" becomes immediately obvious when the vitreous humor (index of refraction, n = 1.336) is replaced with a mixture of water (n = 1.336) and a gas bubble (n = 1.000(32)) of variable thickness. The optical system is thrown completely out of focus, even as the foveola is returned to near nominal position. Of apparently equal significance is the meniscus between the gas bubble and the saline water introduced into the ocular. At least in the situation under discussion, the meniscus introduces a cylindrical optical element that appears to occupy a location almost directly in front of the foveola. Furthermore this meniscus is subject to sloshing due to the movements of the eye and the body. The result is a highly distorted out of focus visual image presented to the CNS by the left eye. The fact the foveola is not centered on the optical axis also introduces a spatial distortion further complicating any potential for the two eyes to converge.

After one week, it is possible to confirm the acuity of the retina and left eye has improved beyond the counting finger stage, but it remains far from adequately focused, and only small portions of the far field can be resolved due to the sloshing of the gas bubble meniscus and its introduction of a cylindrical optical element of unstable character.

By day 57 (day 11 after surgery), the acuity of the left eye had begun to approach usefulness. The amount of cylindrical distortion was reduced and the size of the gas bubble had been marginally reduced (based on looking straight down and exploring the edge of the now circular image of the gas bubble circumscribing the point of fixation at an eccentricity of about 75-80 degrees). In the absence of the high degree of cylindrical distortion and sloshing of the gas bubble/saline solution, broad objects of a given color within the field of view were observed in their appropriate color.

> When looking straight down, an unexpected phenomenon was observed. On each heart beat, a brief window opened in a difficult to describe and variable area of the field of view. This area exhibited a much higher acuity for a brief period of probably less than one second. It appears that the presence in the optical path of the bubble/saline solution mixture was damping the normal tremor associated with the eye. During the heart beat, the microsaccades of the eye was enhanced, replacing the normal ocular muscle-based microsaccades, and raising the acuity within the window.

On day 57, the point of fixation of the left eye was approximately 5 degrees eccentric along a diagonal at 45 degrees in the upper right quadrant compared to the right eye as a reference. There is some evidence the two eyes were seeking to retrain for convergence, but the potential was limited by the significant smearing of light due to the various out of focus conditions and the recurrent image motion in the left eye due to pressure induced image artifacts related to the heart beat. The location of the fixation point appears to vary significantly during the day depending on the optical path through the gas bubble and saline solution mixture. It appears that the shape of the gas bubble may have been determined by the surgeon's repair activity; how much of the vitreous humor was actually removed relative to the axis of fixation. Chapter 13 of Michels et al. show a variety of situations available to the surgeon[18].

On day 60, significant improvement in the acuity, and image quality associated with the visual field was noted. However, the improvement was incremental from day 57. The gas bubble shrank a noticeable amount as observed when looking straight down.

On day 62 (post surgery day 16), the surgeon reviewed the situation. His technician was unable to take OCT scans through the pupil because of the presence of the meniscus. The surgeon noted the small hemorrhage remaining at the bottom of the retina but did not show significant concern. He indicated it probably accounted for the current clouding of the ocular fluid. The gas bubble was down to 35% of the original size and he estimated the meniscus would cease to be in the optical path within one to two weeks. Upon questioning, he indicated the fluid introduced into the ocular as the gas was absorbed entered from the anterior of the ocular and it would remain a liquid for the foreseeable future. With adequate illumination, the author was able to observe a fine hair on one finger without

[18]Michels, R. Wilkinson, C. & Rice, T. (1990) Retinal Detachment. St louis, MO: Mosby Chapter 13

glasses but at a distance of only an inch or two from the eye. The surgeon scheduled the next observation in four weeks and indicated the desire to keep the head in normal vertical position during the day.

On day 66 (post surgery day 20) there was significant improvement in the performance of the left eye. The gas bubble had shrunk to the point, its bottom edge was no longer intersecting the line of fixation (by about 10 degrees) Upon arising before dawn, a significant number of street lights that were between 3 and 15 miles away could be seen. Many of the optical distortions mentioned above have become less significant. The magnification is still only about 2/3 of that in the right eye and there remains about 5 degrees of rotation due to the prism phenomenon. The two eyes are attempting to converge but it is apparent that the right eye is being treated as dominant and the perceived image from the left eye is routinely being suppressed. The performance of the left eye remains very sensitive to the light level but it was functional throughout most of the day.

On day 67, the left eye was able to read the time on a large luminescent font alarm clock upon awaking in a dark room. The gas bubble continued to shrink marginally. The image outside the bubble became good enough to drive using only the left eye in an emergency. It no longer encountered the sloshing of the gas bubble/saline interface. However, the imagery was scaled to about 60–75% of the right eye and there remained distortion in the foveola that resulted in prosopagnosia at the level of the retina. The image perceived by the left eye still exhibited a variety of local optical distortions, including one in the horizontal meridian through the point of fixation. The two eyes were now able to converge but the right eye achieved dominance. By de-converging, the point of fixation of the left eyw was about 5-10 degrees to the right and slightly down along a 15-20 degree radial from the right eye.

On day 68 (post surgery day 22), the gas bubble appears to continue to shrink. There is on the order of 25 degrees in the clear on the temporal border at the horizontal meridian. The bubble/saline interface is currently at least 15-20 degrees below the line of fixation when gazing horizontally. Sloshing no longer impacts the field more than a few degrees above the bubble/saline interface. Convergence of the two eyes became automatic even though the left field remained at about 80% of the scale of the right eye. Hence the perceived image was dominated by the right eye. The reduced image suffers from some optical pin cushion distortion. The left eye prosopagnosia remained with a local region of distortion remaining spanning the horizontal meridian through the point of fixation. The distorted area was about 0.6 degrees high and about 0.9 degrees wide. The distorted area, and waviness in the left and right borders, move up and down with the point of fixation. The stage 4 saliency map appears to remain spatially uniform and is updated properly by the right eye. It is the spatial geometry of the retina, and/or optical path through the pupil, that is distorted at this time.

On day 70, after performing a test using an Amsler Grid, it was possible to confirm the inability to see the central black dot when fixated on it with the left eye. It was necessary to fixate 5 squares above or below the spot to actually sense the dot. Similarly, it was necessary to fixate seven squares to the left or right to actually sense the dot. When fixated on the dots location, the grid exhibited a puckered appearance in the area of the foveola. Two or three other puckered locations were observed fleetingly at the corners of a box teb squares on a side. Depending on the light level, the pin cushion effect and the shrinkage of the image occasionally disappears **or** is ignored by the brain giving dominance to the right eye. The two eyes are converging more and more frequently, or the brain is primarily depending on the right eye. Following coarse convergence, diplopia is typically perceived with the image from the left eye at about 0.4 degrees eccentricity and ten degrees below horizontal nasally compared to the right eye. Frequently, the right eye will be accepted as dominant because the image sizes do not match adequately to achieve precision convergence. This condition was encountered pre-surgery as well. Wong[19] discusses this condition using the term displacement, and occasional translocation.

There is every indication that the two eyes are converging resultng in some degree of depth perception.

On day 74 (post surgery day 28) the left eye still exhibits a variety of optical distortions but the general image quality is now approaching usefulness. The image magnification is now approaching that of the right eye for areas below the horizontal meridian. However, there are clear signs of an off-center cylindrical lens problem distorting the size of objects in the upper hemifield of view. It is now possible to recognize lines of scrolling type on a TV news channel. However, the type presented to the foveola remains highly distorted and unreadable. When driving, it is virtually impossible to perceive a stop sign on the right side of the road until you are within about 20 feet of it. Then the hexagonal shape of the sign becomes obvious but the lettering on the sign remains unreadable. Progress is being made. The gas bubble extends over 75 degrees of the visual field and continues to shrink incrementally. Rough estimates say it has shrunk to 20-25% of its original size but will remain significant for another 2-3 weeks. The sloshing and distortion problems due to the meniscus have largely ceased.

On day 77 (post surgery day 31) the distortion in the left eye is significantly reduced. The gas bubble is now well

---

[19]Wong, R. (2012) Longitudinal Study of Macular Folds by Spectral-Domain Optical Coherence Tomography *Am J Ophthalmol* vol.153(1), pp 88-92

below the fixation point (30-40 degrees) but reflections from specular light sources, like sunlight, and their reflection are generating significant artifacts from bouncing off of the bubble. Bubble now at 48 degrees diameter when looking straight down. It continues to shrink incrementally every day. When driving, the bubble no longer obscures the dashboard although it does obscure the center of the steering wheel. Convergence is now definitely occurring, and appears to be occurring on an area basis within the LGN. The fronds on the palm tree at 200 yards from my office window are now resolvable. Early in the morning, Catalina Island at 26 miles was observable, even at the low contrast level. Text is generally resolvable on my TV except for the foveola surrounding the point of fixation. Imagery projected upon the foveola (1.2 degree or 350 microns diameter) is still not recognizable or resolvable. The remaining distortion is primarily associated with the horizontal meridian passing through the fixation point.

An OCT scan would show whether the retina is forming a pit for the foveola or whether on-axis acuity of the left eye will be a long term problem.

On day 81 (day 35 post surgery), the precision convergence system via the Precision Optical Servomechanism began operating, at least while watching a hockey game (with large amounts of white space among a limited number of objects imaged on the foveola at one time). There was still observable spatial distortion when looking at an extended set of venetian blinds (multiple locations of local puckering and some cylindrical distortion in vertical locations away from the horizontal meridian).

> Later the same day, it was noticed that the precision convergence system was operating when viewing talking heads on the TV. The convergence system was concentrating on the moving lips in particular (even though the scale of the image recorded by the left eye was only about 80% of the scale of the right eye. But by concentrating on the moving lips, the images were converged. This phenomenon would suggest the tremor associated with the eyes did not play a significant role in the operation of the precision convergence system.
>
> It may be that the combination of the moving lips in the scene, and the intrinsic motions associated with tremor, provided an enhanced contrast component that was advantageous in performing the precision convergence task.
>
> The foveola remained unusable for imaging. When fixating on a prominent object, such as a car, that fit into the dimensions of the foveola and was surrounded by a complex foliage background, the prominent object disappeared and the perceived image was filled in. The result was just the way the blind spot is perceived as filled in unless a specific effort is employed to highlight it.

On day 84 (day 38 post surgery), the gas bubble was 54 degrees in diameter when looking straight down. It was no longer a hindrance when looking at objects on the horizon. However, it was still a problem when looking below the horizon to read. It still generated a large amount of scattered light within the ocular, from any object in the near field below the horizon. The gas bubble, when looking straight down caused best focus to appear at about 4–6 inches from the eye.

On day 92 (day 45 post surgery), the gas bubble continues to shrink but at a decreasing rate. While driving, it is now below the center of the steering wheel. The two eyes appear to be achieving coarse convergence; however, the foveola of the left eye is not supporting fine convergence. The left foveola still presents a highly distorted representation of the central 1.2 degree diameter field. The horizontal meridian passing through the fixation point of left eye continues to suggest a “wrinkle” or crease due to previous folding. There is also a suggestion of a remaining cylindrical optical error. Heads on talking heads on TV still appear shorter and much narrower than appropriate.

On day 98 (day 51 post surgery), the gas bubble was now at about 40 degrees in diameter when looking straight down. When looking horizontally, the bubble was very low along the vertical meridian and not readily noticable when driving except for light being scatter by the bubble interface within the ocular. The spatial geometry of the image being captured by the left eye was much improved. However, the perceived image remained about 75-80% as high as that of the right eye. In width the lower field was approaching normal scale compared to the right eye except right along the horizontal meridian passing through the point of fixation. Faces in that region remained about 50% as wide as they should be. While large letters and words could now be recognized by the left eye, the foveola remained unusable for reading and stop signs could not be recognized when fixated upon at more than 50 feet. The size difference between the images generated by each eye continued to cause a problem between the two eyes attempting to converge properly. If one eye was closed, the other eye would be relied upon as the dominant eye even after the other eye was opened. This reliance on the dominant eye could continue for a period of many seconds. Closing the dominant eye would cause the open eye to become “dominant,” even after the other eye was opened. With effort the two images could both be viewed. Under this condition, the two images were normally displaced. If a “talking head” was near the point of fixation, the visual servomechanism involved would attempt to merge the two mouths and leave the eyes in a non-convergent condition because of the difference in scale involved. The scale problem led to a tiring condition where the left eye was kept closed to relieve the strain.

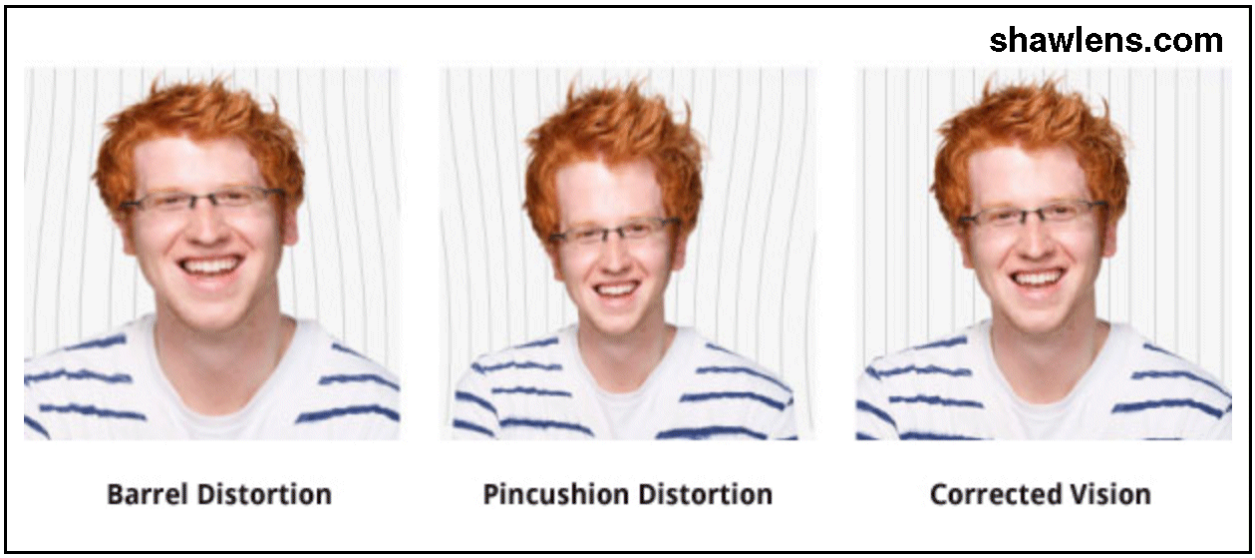

Figure F.1.3-4 Pincushion distortion. Note extended forehead and reduced mouth size in this "talking head." The width at the shoulders is near normal. In the author's case the total height of the pincushion distortion is only about 75-80% of the pereived image of the right eye. Either the mouth or nose is generally not perceived at all depending on the point of fixation. Whichever is perceived, it is usually perceived at 50% of the size of that perceived by the right eye. From Shawlens.com.

On day 102 (day 55 after surgery), the gas bubble was observable by the patient as a 26 degree diameter cone when looking straight down. The bubble is no longer visible when looking at the horizon. The fine convergence servomechanism remained inoperative because of the failure of the left foveola to resolve objects adequately. The overall perception relating to the left eye alone continues to involve significant pin-cushion distortion on a highly variable time scale measured in minutes or possibly somewhat less, **Figure F.1.3-4 Figure F.1.3-5** illustrates the problem of aniseikonia, as labeled by the Shaw Lens Company, very accurately as perceived by the author without any optical correction.

On day 104 (57 days post surgery), I awoke to a set of four gas bubble

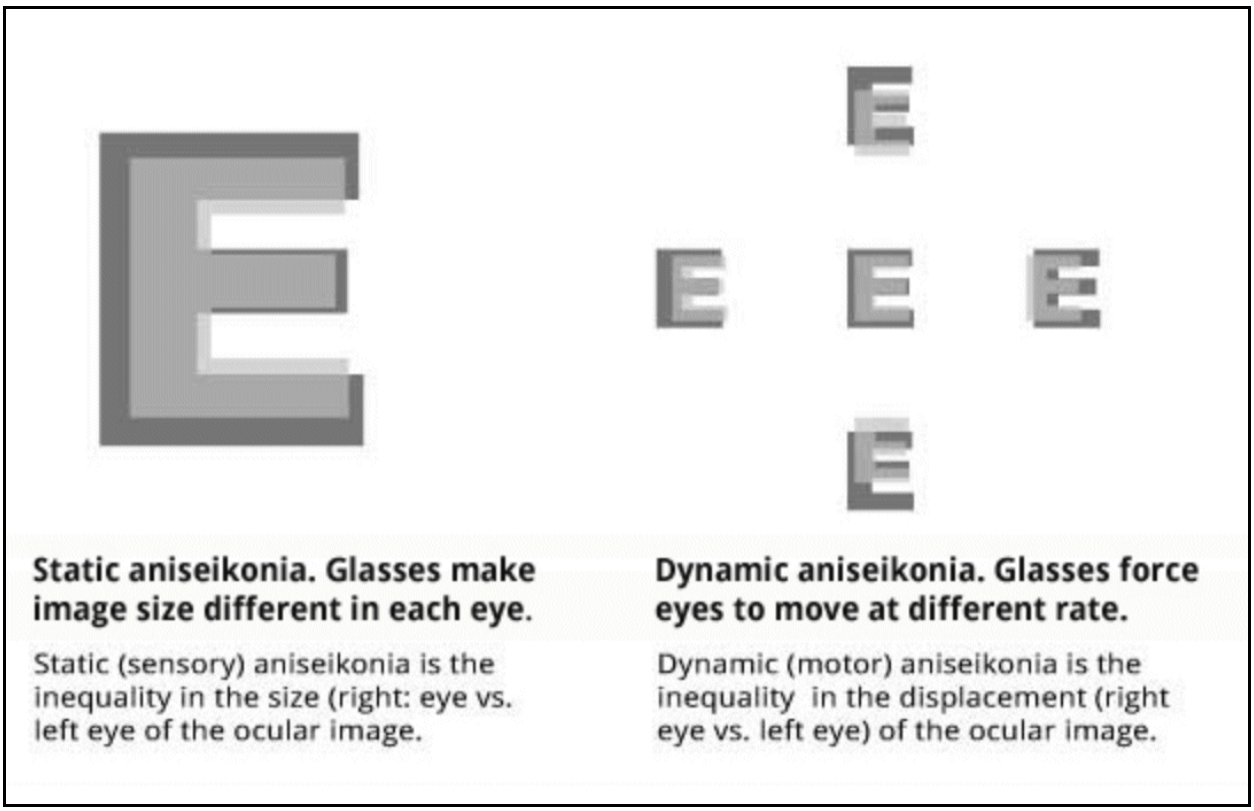

Figure F.1.3-5 Aniseikonia from Shaw Lens Co. The wording is theirs. In the author's case, the condition is encountered without glasses. The gray image is generally displaced to the lower right by about 2 degrees when at the point of fixation.

s resembling a fractile with a major bubble (remaining at a 26 degree field when looking straight down) and three progressively smaller gas bubbles in the 2 degree in diameter or smaller range. The bubbles were all transparent and the main bubble caused to optics of the eye to be optimized for at least 4 feet viewing distance. The bubbles ran around the edge of the main bubble when the eye was redirected. The gas bubbles made no effort to recombine into one suggesting the surface tension of the fluids within the eye was low. Six hours later, there were still two small and one large gas bubbles present. The spatial distortion of the perceived scene occasionally became very small. At other times it continued to display significant pincushion.

A medical examination on this day showed an acuity of 20/150 for the left eye by varying the fixation point to optimize the visibility of each character. The ophthalmologist first stated the gas bubble had disappeared. However, on pointing out the bubble was still visible on looking straight down (cone angle of about 26 degrees), he re-examined the left eye and announced the gas bubble was now 5% of its initial volume. The fringe gas bubbles were not discussed. He estimated the gas-bubble would be gone in a week depending on the subjects activity level. **Figure F.1.3-6** shows the composite of a fundascope for each eye at the top of the graphic and two variants of the OCT for the left eye at the bottom of the graphic (in color in the online version). The fundascope image at upper right of the graphic includes the range of foveola heights that remain the controlling factor in the acuity of the left (OS) foveola. The range was about 80 microns within a one millimeter diameter on that date. The shape of the "pit" above the foveola appears asymmetrical with a less sloping left edge (note yellow area of the region within the one millimeter circle). This slope can effect the optical performance of the foveola. The average measurement would be more useful if it only averaged the values within the diameter of the foveola (nominally 0.35 mm diameter). Based on the color scale provided, the variation in the condition reported by the OCT is shown in the two frames at the bottom of the graphic. Compare with the images in **Section 18.8.3.6.** There appears to be some discussion concerning what layers are labeled what in the images of that section. The diagnosis indicated some remaining fluid between the photoreceptor cells and the RPE and some fluid within the layers of the photoreceptor cells at the edges of the foveola.

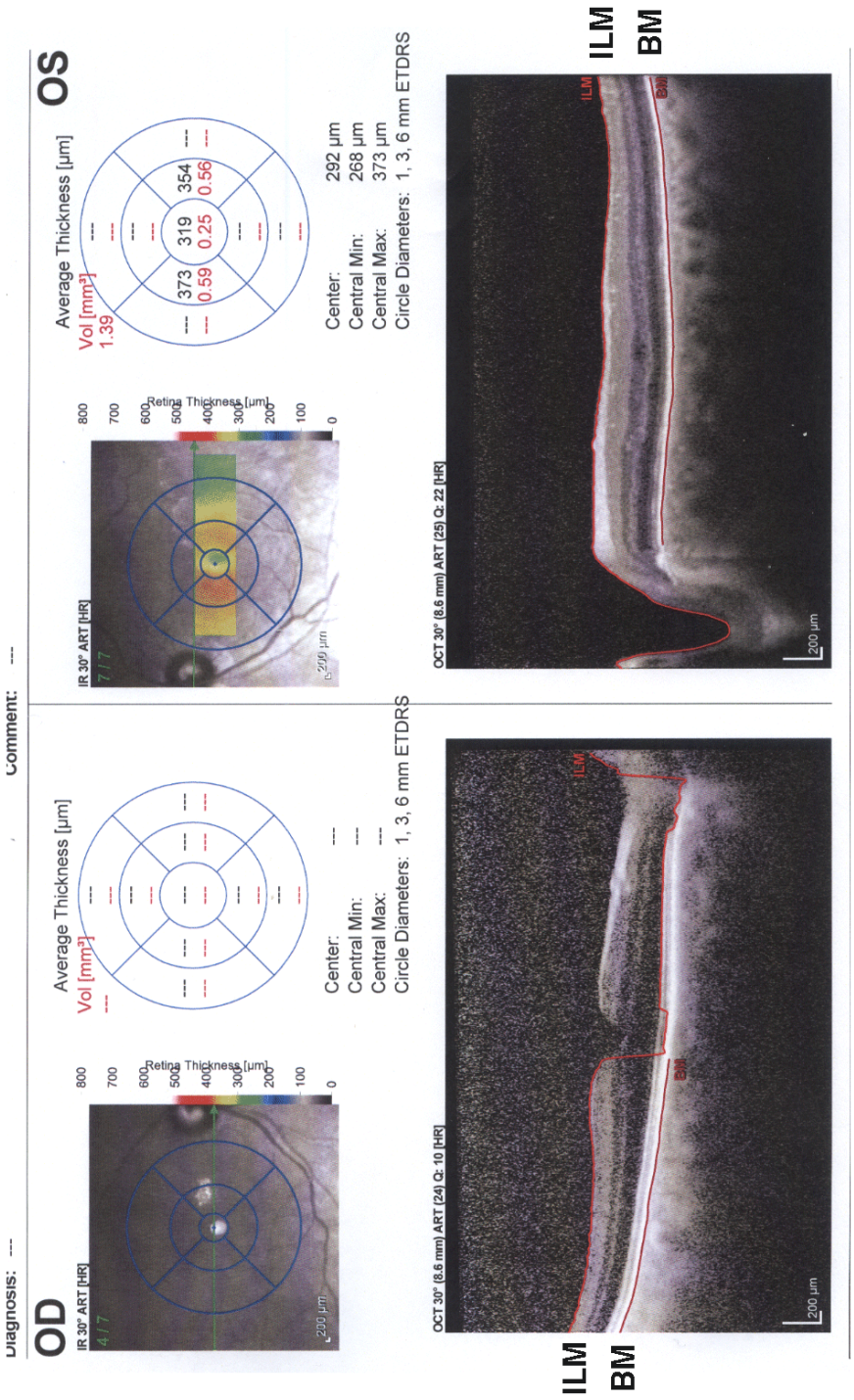

Figure F.1.3-6 Volume and linear transverse OCT scans of 14 May 2018 for Fulton. The two fundascope frames are at the same scale. The green region within the 1 mm circle is approximately the diameter of the expected foveola. The lower right frame is the OCT scan for the foveola of the left eye. The upper right frame shows the OCT scan for the blind spot for the same eye. The scale bars are the same at 200 microns. The red lines are machine drawn with labels and are somewhat ambiguous. Note the ripples at the right of the foveola; a feature typically associated with the RPE layer. See text.

In the frame for the OCT scan of the foveola, the line labeled interior limiting membrane, ILM, appears to jump from the ILM on the left to the RPE layer and then back to the outer face of the outer segment of the photoreceptor array before reaching the rippled area on the right. After, passing this area, it jumps back to the true ILM location. The line labeled the BM, Bruche's membrane, appears to be correct as far it extends in the OCT scan of the foveola region. The OCT frame of the Optic nerve and blind spot appears to be properly labeled throughout.

The group of gas bubbles re-coalesced into one bubble by day 107. On awaking on day 108, a second small bubble reappeared.

By pointing the left eye in an apparently chaotic manner, it was possible to trap the smaller bubble in an area of depression versus the average curvature of the retina. This location was presumed to be the end of the optic nerve. When in this position, the small bubble was un-perceivable. When returning the left eye to observing straight down, the small bubble would suddenly reappear from the temporal portion of the visual field moving at high speed back to a position adjacent to the large bubble, with their two edges in contact.

On day 109, the major bubble now obscures a cone of 18 degree full angle when looking straight down. No smaller bubbles were observed when awakening. The bubble is no longer of concern when looking toward the horizon. As of day 109, the eyes are performing coarse convergence well. The fine convergence is now performing well for about one-half the time, when the pincushion in the left eye goes below 3% distortion. When the pincushion distortion is low, the acuity of the left eye is approaching that of the right eye in about one-half of the normal field of view of the foveola (nominally 1.2 degrees full diameter).

On day 112 (day 65 after surgery) the bubble was 14 degrees in diameter when looking straight down. It is no longer visible while looking at the horizon. Driving is such a horizon–observing activity. It is the chaotic motion of the bubble that is such a nuisance in descending stairs or stepping over a curb. The bubble still provides a compressible fluid in the ocular that may contribute, in conjunction with the ocular muscles, to the geometric distortion of the perceived scene that remains a dynamic process.

On day 114, the bubble was 6.6 degrees in diameter (roughly five times the diameter of a typical foveola). The bubble was circular but spatially unstable at this time, with a chaotic motion of about four degrees center-to-center. This motion when looking straight down suggested the geometry of the inner surface of the retina contained multiple indentations that provided "multiple minimums" of about 4 degrees diameter for the bubble to settle into.

On day 116, the bubble was 3.2 degrees in diameter when looking straight down. Its shape was that of a moon three days after full. The right-lower quadrant of the visual field was affected and suggested the bubble was now smaller in diameter than the maximum diameter of the pit of the retna. The bubble was invisible when looking horizontally. It was much less distracting when walking because its position remained stable. Under low (indoor) light conditions when the bubble was nearly transparent except for the outer ring, it could be ignored because of the lack of performance of the foveola.

On awakening on day 117 (day 70 after surgery) the bubble had totally disappeared. No amount of shaking the head could bring it into view. The primary problem remaining was in the reduction in scale of the perceived image from the left eye. The foveola remained essentially non-useful at an acuity estimated at 20/100.

On day 120 the vertical degree of pincushioning was very small and the vertical shapes of talking heads on TV was approaching normal. The horizontal degree of pincushioning was still of concern, with talking heads being compressed horizontally to about 80% of normal. The system was still attempting to achieve convergence. Occasionally, faces would look like they had sharpened features due to the addition of a differentiated copy of the face. The leading cause of the improvement in metamorphosia appears to be a greater conformance of the ocular, and the retina, to their expanded volume and the rigidization of the sclera due to the pressure within the ocular in the absence of a more compressible gas bubble. More study is required to confirm this hypothesis.

The 2008 and 2009 papers of Spaide (**Section F.1.2**) suggest the choroid may have been mis-shapened by the surgical intervention and that the horizontal metamorphosia may await the healing of the surgical openings in the choroid. The healing would be commensurate with additional structural strength in the choroid and the concurrent rigidization.

The foveola remained non-functional. On the night before, the full Moon (0.518 degrees in diameter) rose at about 8:00 local time. Being slightly under the nominal size of the foveola (1.2 degrees in diameter), it was possible to position the full circular Moon within the foveola. When placed in the right hemisphere, it was observed as a full circular Moon. When placed in the left hemisphere it was unresolvable as to shape. When moved along the vertical meridian, the left hemisphere of the Moon remained largely unresolvable while the right hemisphere was largely

resolvable as a circular object.

On day 125, the convergence capability was improving and competition between the eyes for dominance was significant. In observing a wall of narrow horizontal Venetian blinds, the amount of scattered puckering in the field of the left eye was considerably reduced but not yet un-noticeable. This was suggestive of the healing of the holes in the ocular made during surgery. The healing of these holes was commensurate with the ability of the ocular to reinstate its normal shape and thereby achieve the necessary shape and rigidity of the ocular to support a normal mapping and image magnification in the left eye.

> The above observations caused a review of any re-education or reprogramming of engines of the brain to accomplish any relearning within the visual modality. Any remapping has at least two elements; the large scale remapping which may be accomplished by merely readjusting the placement of the retina relative to the image, produced by the stage 0 optics, to match the condition in the partner eye, and the rerouting of any neural paths on a neuron-by-neuron, or at least a fascicule-by-fascicule basis.
>
> The rerouting of any individual, or group of neurons, is unlikely due to the multiple paths involved. There is no obvious mechanism or place for rerouting alont the fovea/ LGN pathways. Similarly, there is no obvious location for rerouting along the LGN/ occipital lobe pathway. However, some of the perceived imagery in the later stages of healing, involving a competition to present imagery at two different magnifications at one time, might be compatible with some rerouting. This situation might suggest a degree of rerouting via the capabilities with the TRN. However, the fovea/LGN, and the functionally similar foveola/PGN, pathways are not normally via the TRN.

It appears the precision relocation of the retina by structural tensioning remains more likely than by any mechanism involving individual neurons.

On day 127 (80 days after surgery) the two eyes are attempting to converge routinely. However, the convergence process has to date remained unsuccessful because of the difference in the scale between the two eyes. The vertical scales vary by a ratio of 80:100. The horizontal scale is more difficult to define. The gross scale is roughly 80:100 but the region near the horizontal meridian through the point of fixation remains furhter compressed to the point the area of fixation (1.2 degrees in the normal eye) is essentially obliterated and is treated as a blind spot.

> The above condition makes driving a challenge. In the author's case, the left)damaged) eye has always been dominant. In the current situation, the left eye does not see stop signs at greater than 100 feet away. Similarly, cars directly ahead disappear at distances greater than 200 ft as they become smaller than 1.2 degrees in angular subtense. In the current situation, the brain tends to rely upon the most recent image from either eye. Therefore it behooves me to close the left eye briefly to insure the imagery from the right eye is used as the dominant image when in traffic. Within ten seconds the brain will rely upon the dominant eye if I do not take this action.

On day 133 (86 days after surgery), an Amsler Grid was marked up to show the remaining metamorphopsia in the visual field of the left eye. This procedure and the resulting perceptions will be discusses in **Section F.1.4.2**. It is presented in **Figure F.1.3-7** .

- - - -

There does not appear to be any synchronization between the above activities but there may be a subconscious search going on the establish which state causes the best coordinated operation between the two eyes.

In attempts to converge the two eyes, the importance of motion within the image projected on the foveola again became obvious. When looking at talking heads on the TV screen, the eyes would converge on the moving mouths and leave the eyes totally out of convergence due to the scale factor difference. Frequently, the brain would then assign a dominant role to the right eye.

Because both coarse and precision convergence involve area correlation mechanisms, the complexity of the relevant portions of the image fields presented to both eyes is highly relevant to the results obtained by these mechanisms.

- - - - -

On day 145, a follow-up visit with Dr Mehta was held. At that time, the acuity of the left eye was 20/70. This was probably the result of looking to the right of the target by about 2 degrees, suggesting this value conformed to the acuity of the peripheral retina adjacent to the foveola (**Figure 2.4.8-4** in **Section 2.4.8.2**). The foveola has improved but is still unusable for reading and objects image on the foveola still tend to disappear. License frames on an automobile directly in front of my car are now discernible but not readable. The OCT of the foveola and surroundings are approaching normal. The pit is considerably more symmetrical and Dr Mehta noted only a small amount of edema to the left of the pit and at the RPE/choroid interface. The pin cushion is better on average but still

changes at intervals on the order of 10-15 seconds. Where I tend to think of this change as related to the ocular muscles causing a reshaping of the ocular, the doctor attributed this problem to changes in blood flow. On day 149, the foveola was working very much better with regard to specifically red light from a phosphor used on my alarm clock. I was able to read all three characters and the two dots flashing between the hours and minutes without any difficulty. Each character was a bit larger than 1.2 degrees in diameter. There was no area of distortion between, or related to, any of the individual characters.

During the first three weeks of the month of August, 2018 (from post-surgery day 114 through the third week, day 135), the two eyes were in a very competitive mode attempting to achieve coarse convergence. The signal level generated by the area integration process was not good. During the fourth week (beginning with post-surgery day 136, the geometric fidelity of the left eye continued to improve although a scale factor of around 80% for the upper half of the field still existed. The eyes began to converge reasonably satisfactorily for about 50% of the day.

Also during the fourth week of August, the geometric spatial fidelity improved to the point that the left eye could recognize, but not read, a license plate frame on the car immediately in front of my car at a stop light (~ 10 feet away). The frame appeared to be about one-half its normal size. If I looked about 2 degrees to the right, the peripheral fovea recorded the license plate at about 80% of normal size in both vertical and horizontal dimensions.

On 26 August (post surgery 138), a full moon was observed with the left eye. It largely filled the foveola. When filling the foveola, the left half of the moon was reproduced reasonably well (acuity remained low) but the right half was not observable.

When watching television, the eyes converged considerably better than previously. Having both eyes open improved the reading performance of the right eye (probably due to the scanning pattern of the visual system).

The acuity of the left eye now suffered primarily from the scale factor and the failure of the temporal half of the foveola to operate properly.

On day 139 post surgery, I was surprised at the ability of the left eye to image the very fine filigree in some Cirrus clouds, although tracking small airplanes at distances of 4-5 miles was still difficult and transient.

On 20 September (post surgery 163) the geometric (spatial) quality of the damaged eye over the full field is approaching normal, there is little remaining spatial distortion relative to the peripheral field. **Section F.1.4.2** will provide a detailed description of this performance level.

On the other hand, the distortion of the central 1.2 ° centered on the point of fixation, associated with the foveola, remains significantly distorted. Isolated objects within this field are largely ignored by the brain. The brain largely ignores the signals from the foveola, much like it replaces the lack of useful information from the blind spot with a low resolution average of the light intensity from the immediately surrounding region.

The rate of foveola improvement is slow but noticeable over each subsequent 7-day period.

By 1 December, 2018 (post surgery 235), the geometry of the upper half of the field, including the fovea, had improved considerably but the scale was still at about 80% of that in the lower field. Faces in the upper field were still too small, but they were approaching a roundness with all details of a face being recognized. Acuity was reported as 20/85 by Dr Mehta's technician but this was only achieved by taking a long time to move the eye marginally side to side and use the photoreceptors outside of the foveola.

Driving a car is now back to normal with both eyes working together. However, the scale mismatch is still present between the two upper fields. This is generally not observed while driving. The left foveola is at the point where it can recognize the first and last characters of a license plate at 15 feet. The characters between these two characters appear as a jumble of lines and are not recognizable. The left eye can read prominent text on the TV but there is still significant geometrical distortion in the upper field of view that seems to be a function of blood pressure. Distortion appears less in the morning. The scale problem remains significant. Phone numbers can be read with difficulty by scanning the foveola to read only 2-3 characters at a time of 7.

The process of healing remains slow. The recent improvement does not appear to be "learning" related but a continuing flattening of the retina against the choroid. The OCT (without adaptive optical enhancement) looks quite normal. The fluid between the outer segments and the RPE was effectively removed by an injection by Dr. Mehta around 10 November. An AO-OCT would probably show a continued jumble of outer segments relatable to those shown in **Section 18.8.3**. The reduction in the jumbled aspect does not appear to the rate of outer segment disk replacement. It may depend on new photoreceptor growth and phagocytosis, or narcosis, of the old outer segments (and associated photoreceptor cells).

F.1.3.4.1 The dimensions of the gas bubble

The dimensions of the gas bubble can be appreciated by looking straight down with the affected eye. By using the optical schematic of Appendix L, The Standard Eye, the dimensions and potential shape of the gas bubble is easily approximated. **Figure F.1.3-7** displays this rotated and annotated wide full field schematic. The complete optical system without a gas bubble is a, Broad spectral band, immersed, anamorphic, afocal, 4-element with field corrector & collimator With the gas bubble acting as an additional lens due to its low index of refraction in an immersed system, the overall description of the optical system is quite complicated.

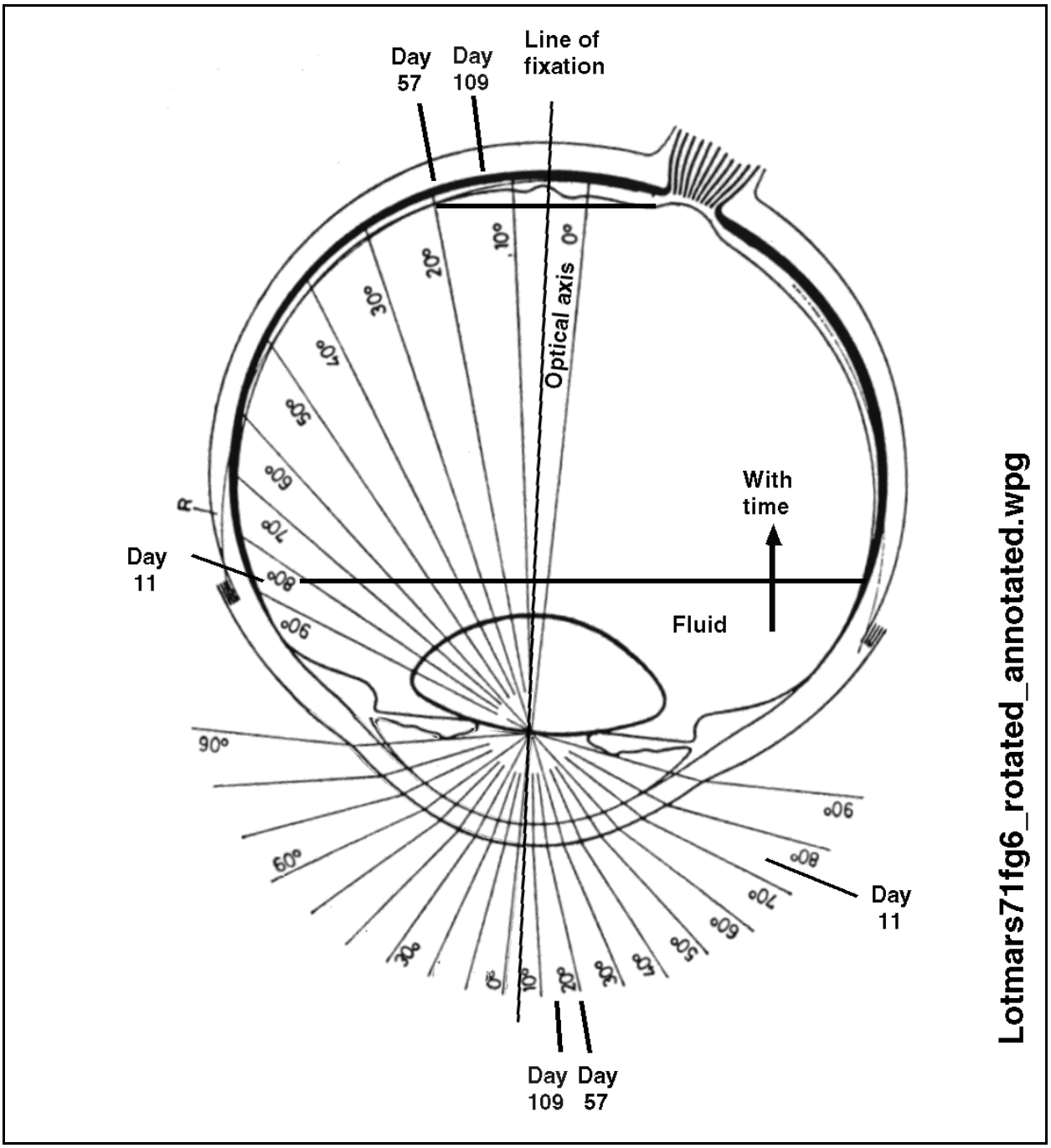

Figure F.1.3-7 Gas bubble dimensions with time as observed looking straight down. All days are "post surgery." See text.

At day 0, post surgery, the surgeon nominally filled the ocular with gas. By day 11, the gas had been absorbed by the hydraulic system of the eye to the level shown by the lower horizontal line. The large volume of gas above the line constitutes a large and significant gas lens within an immersed optical system The defocus due to this lens is appreciable. By day 57, the amount of gas absorbed was considerable. As a result, the remaining gas lens occupied only about 5% of the volume of the vitreous chamber. The resulting gas lens within an immersed optical system was less significant and can be considered a field lens or a field corrector lens. It may affect the focal condition of the foveola but will have a minor effect on the peripheral retina.

> The large gas bubble during the first days following surgery caused the optical system to operate as a non–immersion system (a gas on each side of the main optical group). As a result, the magnification of the image projected onto the retina should have been about 66% of the size of the image projected on the right retina according to Snell's Law. This is very close to the nominal size of the distortion estimated early in the recovery process.

At about 20 days post surgery, the gas bubble caused significant distortion of the visual field when looking toward the horizon. The meniscus of the gas bubble was at the level of both the foveola and the center of the pupil. It was also subject to significant sloshing about when walking or due to any other activity.

The detailed shape of the gas bubble "corrector lens" played no significant role in the geometric fidelity of the perceived field at the 57 day point.

When looking horizontally, the gas bubble at 57 days took a position near the top of the eye, near the serrated part of the peripheral retina (Ora serrata). As a result, it was nearly out of the useful field of view. It affected only the extreme lower portion of the field of view, primarily when walking and looking down at a greater than 45 degree angle.

The gas bubble continues to decrease in cone angle when looking downward as of day 106. At that time, the Ophthalmologist estimated it would become negligible within 1 to 2 weeks, even when looking downward.

The gas bubble did in fact disappear at about day 120 after spending about a week in an unstable position defined by the irregularities in the curvature of the retina. The bubble would oscillate between these positions when the subject looked straight down.

F.1.3.5 Patient's partial evaluation of the surgical solution to detached retina

The overall surgical experience was highly successful, compared to being essentially blind in one eye. By the end of six months, the spatial distortion in the peripheral field of view was nearly negligible. It was adequate to allow the eyes to perform coarse convergence. This was adequate for routine activities other than reading at close range from books etc. The distortion related to the foveola, central 1.2° diameter disk of the retina centered on the point of fixation, remained significant and prevented fine convergence. It also prevented effective reading of printed characters within the diameter of the disk. The distortion of the foveola was due both to positioning errors relative to the point of best optical focus, and orientation of the photoreceptors (Stiles-Crawford Effect). These two parameters cannot be evaluated with the current clinical OCT apparatus. They can be evaluated with the newer adaptive optics augmentation to the baseline OCT; AO-OCT, SDOCT or AOSLO. Genead et al[20]. have presented a comparison of the capability of the SDOCT and AOSLO machines.

> ***Genead has demonstrated that both the SDOCT and the AOSLO machines are capable of resolving the individual photoreceptors near the point of fixation, at least to examine the necrosis of, or shearing over of, any photoreceptors.*** Their figures 3a and 3b obtained with the AOSLO machine are particularly relevant. Figure 3a shows a shaded area that may relate to an area of OS damage. Figure 3b shows damage to only scattered individual photoreceptors.

It is anticipated that the performance of the foveola (due to continually improving positioning of the photoreceptors of the foveola at the bottom of the "pit" in the nominal retina) will continue to improve although the process can be related to an exponential mathematical function. Improvement becomes slower as the end point is approached because the differential force driving the process, the error in position and orientation both, approaches zero. By the one year anniversary of detachment, visual acuity in the left eye is expected to exceed, 20/200 uncorrected. Whether any significant correction will be possible at that point depends on the remaining disorientation of groups of the

---

[20]Genead, M. Fishman, G. Rha, J. et al. (2011) Photoreceptor Structure and Function in Patients with Congenital Achromatopsia IOVS Papers in Press. Published as Manuscript *iovs*.11-7762 In journal as vol 52(10), pp 7298-7308

photoreceptors.

> At the one year point, a small area (~0.3 degrees diameter) to the right of the point of fixation is not responding to light. It is being interpreted within the brain as if it were a small blind spot reminiscent of the ocular nerve head. ***This failure of part of the foveola to respond makes a conventional Snellen acuity representation largely meaningless***.

F.1.4 Spatial distortion (metamorphosia) of the perceived scene after surgical repair

Textbooks and atlases on surgical repair of retinal diseases focus on the physical elements of the diseases with little said about the visual performance of the system following surgery. In the author's case, the retinal detachment along the temporal wall of the left ocular was repaired using the gas bubble approach (pneumatic retinopexy). The result was physically satisfactory from day one. However, the visual performance of the ocular was significantly less satisfactory initially. This was due to the distortions introduced into the optical path between the lens and the repaired retina in this immersed optical system as described above. The replacement of the vitreous humor along this path by a combination of a gas bubble and a saline solution with the viscosity of water introduced many optical distortions. These consisted of ;

1. significant defocus due to the change in the index of refraction along this optical path.
2. significant defocus due to the introduction of an additional optical element due to the curvature of the bubble/saline interface.
3. significant metamorphopsia (change in scale, or magnification) due to the spherical optical element described in 2.
4. significant displacement of the point of fixation in the visual field due to the cylindrical component of the optical element described in 2. This cylindrical element was formed at the gas/saline interface and could change continuously.
5. a significant displacement of the point of fixation in the visual field due to the prism component of the optical element described in 2. This prism element was also formed at the gas/saline interface and could change continuously.
6. a significant distortion of the field of view associated with the additional optical power, cylinder and prism that was continuously introduced by the highly mobile meniscus between the gas bubble and the saline solution.

Beginning about day 53, one week after surgery (on the 46th day after detachment), the performance of the visual system began to resolve the above problems, but in a largely uncontrolled manner. As noted above, about day 57, the gas bubble began to shrink noticeably, but only incrementally, on a daily basis. By day 58, it was possible to perceive the entire perimeter of the gas bubble when looking straight down and slightly to the right (to compensate for the off axis location of the foveola and its point of fixation (**Section 2.2.2.2**). It was also possible to confirm that the gas bubble appeared in the lower hemifield of vision as the head was raised to look forward. The saline solution occupied the upper hemifield, with the meniscus almost precisely passing through the line of fixation. The result was significant on-going distortion in the horizontal meridian passing through the line of fixation until the gas bubble shrank further or the saline solution was replaced by a gel of new vitreous humor.

By day 60, the visual acuity of the left eye had improved to the point (still probably less than 20/200 in the left eye) where the two eyes began attempting convergence, overlaying the fixation points of the two eyes to improve visual acuity and support stereo-vision (depth perception). These attempts were generally unsuccessful due to the sloshing of the meniscus and the continual change in the optical power, metamorphosia (associated with cylinder) and prism effects. The visual acuity above and below the horizontal meridian through the fixation point did continue to improve incrementally but was highly sensitive to the light level in the visual field. The region occupied by the meniscus continued to be greatly disturbed by the sloshing due to the pulse of the cardiovascular system. It was impossible to use the upper or lower hemifield perceived by the left eye when walking due to the sloshing of the gas/saline interface. This sloshing significantly changed the position of the optical rays entering the left eye and interfered with the natural tremor of the eye required to achieve satisfactory acuity.

Figure F.1.4-1 describes the kinds of long term geometric (spatial) distortions that are relevant to retinal detachment. The community has divided these into two categories; metamorphosia (changes from rectilinear perception), and dysmetropsia (changes in perceptual scale compared to the fellow eye). The following material will relate to metamorphosia. Dysmetropsia will be addressed in **Section F.1.6**. At this time repair surgery is focused on returning the retina to its original position in a large scale sense. It makes little effort to replace the foveola precisely. When dealing with a complex liquid crystalline with the thickness of a piece of wet paper, it is difficult to avoid stretching the retina wherever surgical tools contact it.

F.1.4.1 Biological description of pincushion distortion

Figure F.1.4-2 can be used to recognize the differences involved in the conventional definition of barrel distortion (left) and pincushion distortion (center) versus that needed in biological optics right. The conventional description of these distortions is based on cylindrically symmetrical optics and a flat focal plane. The rotationally symmetrical representations at left and at center are courtesy of Edmund Scientific, Co. The definitions are based on a 45 degree diagonal as shown. In biology, the optical system is not necessarily rotationally symmetrical and the curvature of the retina is significant. As a result, pincushion distortion needs to be defined differently based on the author's recent experience. The distortion can be best defined with reference to the horizontal and vertical axes

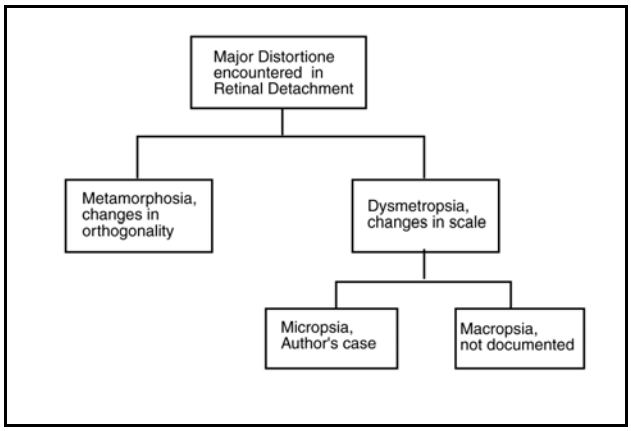

Figure F.1.4-1 Principle spatial distortions following surgical repair of a retinal detachment. Macropsia, although defined by one investigator was not found and is not documented here or in the literature. See text.

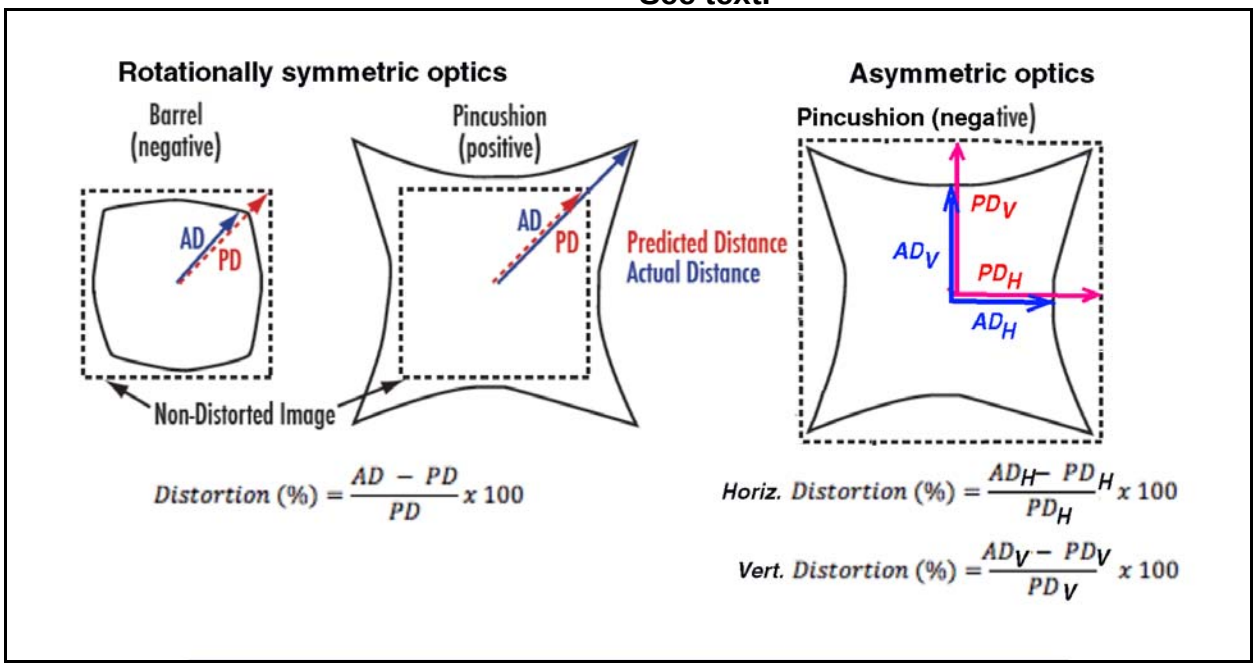

Figure F.1.4-2 Pincushion parameters for rotational symmetric and asymmetric cases. The two cases on the left are used in man-made optics. The asymmetric case on the right requires the use of a horizontal and vertical component. See text.

The dashed non-distorted box of the asymmetric effect on the right is established by comparing the left and right eyes of the author alternately. Horizontal distortion has been more prominent in his left eye in the author's case. The distortion will be discussed in combination with other distortions below. Because of the curvature of the biological focal plane, the distortion appears to be a function of the eccentricity where measured. The non-rotational situation encountered by the author at about day 100 following his detached retina is very interesting. Not only is the degree of pincushioning different between the horizontal and vertical components, the upper and lower distortions are not necessarily equal, each first order component can be accompanied by higher order components. The first order components can also be a function of time, with periods lasting from on the order of a few seconds to tens of seconds. At day 106, during the interval when to vertical distortion falls below the nominally –3% distortion, the two eyes appear to be converging adequately, at least for one talking head (over a 1.2 degree field surrounding

the point of fixation) of multiple talking heads portrayed simultaneously. The degree of distortion is not necessarily a linear function of the distance above the horizontal meridian. It appear there is more distortion near the vertical and horizontal meridians passing through the point of fixation. This effect may relate to the continuing poor performance of the foveola of the left eye at day 106.

The Amsler Grid can be used effectively to measure the field of view while recognizing the corners of the grid are typically moved in for the asymmetrical case. The first order distortion can be estimated by asking the subject to estimate the bowing of the horizontal and/or vertical borders relative the the corners of the perceived grid.

Any second order distortion can then be estimated by asking the subject to indicate any other distortions in the perceived square. In the authors case, there is a persistent compression of the imagery in the left eye along the horizontal meridian passing through the point of fixation. This compression is in both directions and essentially makes the region of the left foveola appear smaller than normal, to the point of disappearing. As of day 100 (day 53 after surgery), the visual modality treated this reduced perception of the small region surrounding the point of fixation as a second blind spot and ignores any input from this region. As of day 110, this small area is dynamic. It is ignored when the vertical distortion calculated as defined above goes to zero percent. When the vertical distortion exceeds a few percent, the representation of the foveola disappears and the brain treats it as a second blind spot.

F.1.4.2 Astable spatial distortion outside of the fovea and beyond the retina

On day 133 (86 days after surgery, 1 July, 2018), an Amsler Grid was marked up to show the remaining metamorphopsia in the visual field of the left eye. Metamorphopsia is limited to the geometric distortions and excludes the scale of the imagery, dysmetropsia. Dysmetropsia is addressed in **Section F.1.6**. The metamorphosia on this date is illustrated in **Figure F.1.4-3** .

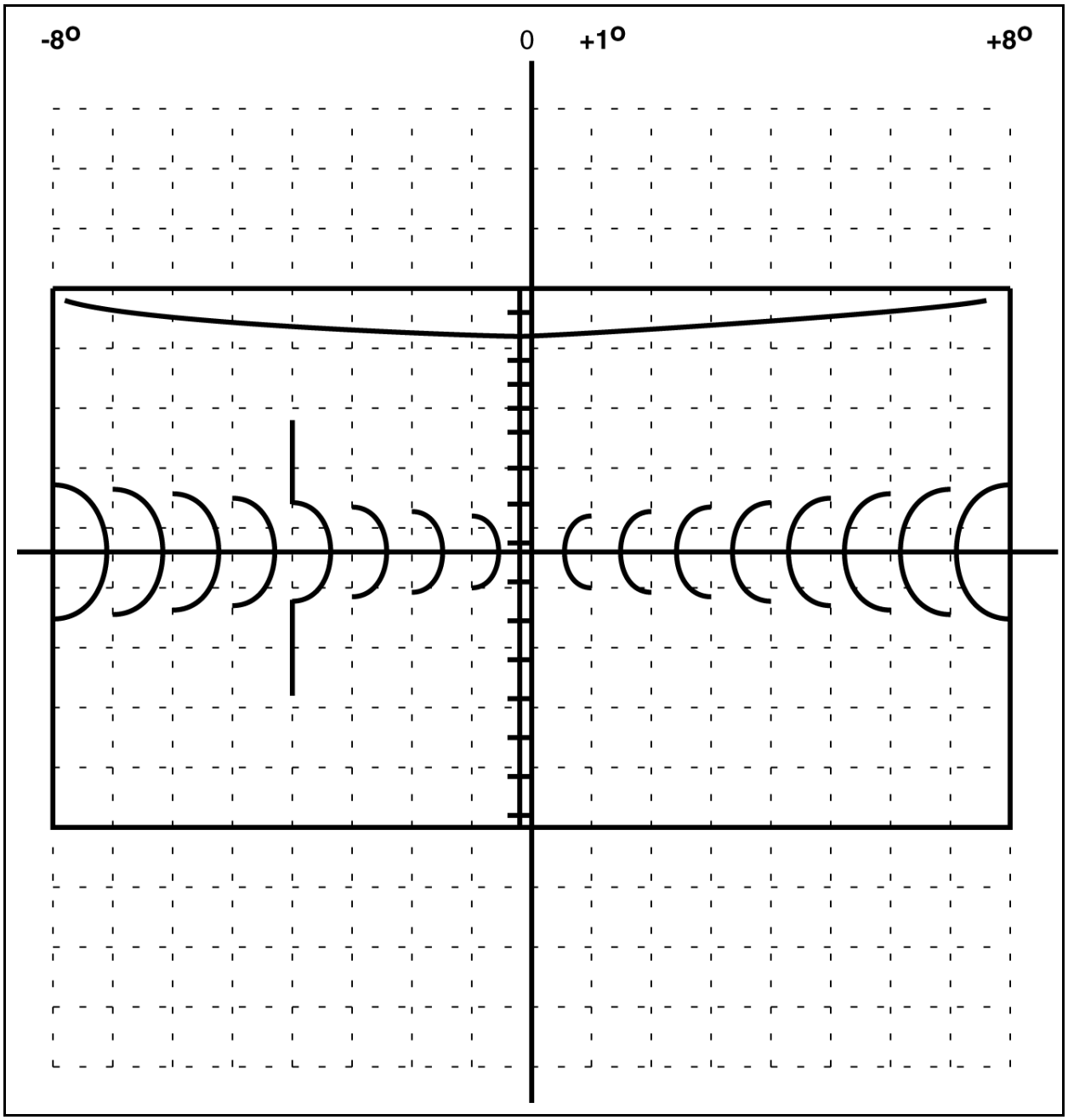

Figure F.1.4-3 Amsler Grid at day 86 after surgery. The rectangular box overlaying the Amsler Grid represents a 55 inch HD TV extending horizontally a total of 16 degrees. The dashed boxes of the Amsler Grid are nominally one degree on a side. Curved arcs are shown as worst case at this date in recovery. The curved parts of each vertical meridian shown can become reduced to a radius of about one-quarter degree in vertical extent during intervals as described in the text. See text for detail discussion.

The highlights of this figure are many. The most important point to make is the dynamics of the perceived field. Several elements of the scene can vary every few second as outlined in the following discussion.

= The amount of bending in the top edge of the box, pincushioning (defined in next subsection) is still highly

variable along the top edge and can change in tens of seconds, typically during the blink of the eye. =The amount of curvature along each of the vertical meridians (one example shown explicitly) can vary within one second. The rapidity is such that a particular curve can appear to be boiling.

=The vertical extent of the curvatures in each vertical meridian can vary such that sometimes all of the curvatures have a height of nominally the height of the foveola, about 1 degree.

=The horizontal extent of the curvatures, cause the position of the foveola to be highly compressed horizontally, to the point of disappearing as a functional element of the visual modality.

=Compare the curvatures documented at this time with that initially documented before surgery in **Figure F.1-3**. The curvature in that figure appears to relate to the shift of the fixation point of the left eye to the right and downward along a diagonal.

= The scale of the upper hemisphere of the perceived grid is nominally 80% of the scale of the lower hemisphere and compared to the scale of the right eye in both hemispheres. Note the different pitch of the indices on the meridian next to the vertical meridian.

=The top edge of the TV screen frequently shows a variation in pincushion (vertical distortion) from about 0.0% to about -10% that may vary over intervals of less than 10 minutes (**Section F.1.3.3**). On 20 September (post surgery 163) a set of papers by Baldwin et al. were located describing the relative sizes of disks located at different parts of the visual field (**Section 19.5.1** in **PBV**). A US patent #9,684,946 B2 by the Baldwin team (Perrell & Burleigh) includes multiple drawings relative to the healing process after a detached retina. They can be used for discussions with the ophthalmologist/surgeon. By comparing the vision of the damaged eye with the good eye, the status of the healing can be evaluated. At post surgery day 163, the geometric quality of the damaged eye over the full field is approaching normal, there is little remaining spatial distortion relative to the peripheral field, **Figure F.1.4-4** . The correlation mechanism involved in the distortions of this figure are discussed below. Reviewing this subject on April 22, 2019, the temporal field appears essentially distortion free and the arcs associated with the nasal field have become negligible except for the vertical line at about 0.6 degrees.

F.1.4.3 Explaining the astable aspect of the merging along the horizontal meridian

The astable characteristic of the distortion along the horizontal meridian suggests it is not driven by a mechanical mechanism. Looking at the remainder of the neural system of the visual modality suggests where the astability occurs.

Figure F.1.4-5 is presented for reference, to be considered before displaying the likely solution to the astable image characteristics in the previous section. There is data to show that the neurons in each quadrant and the central foveo near the vertical and horizontal meridians and the arcs of the small circle are shared. These neurons are connected to the ganglions on each side of each demarcation line. The overlap region is typically two degrees wide along each demarcation line.

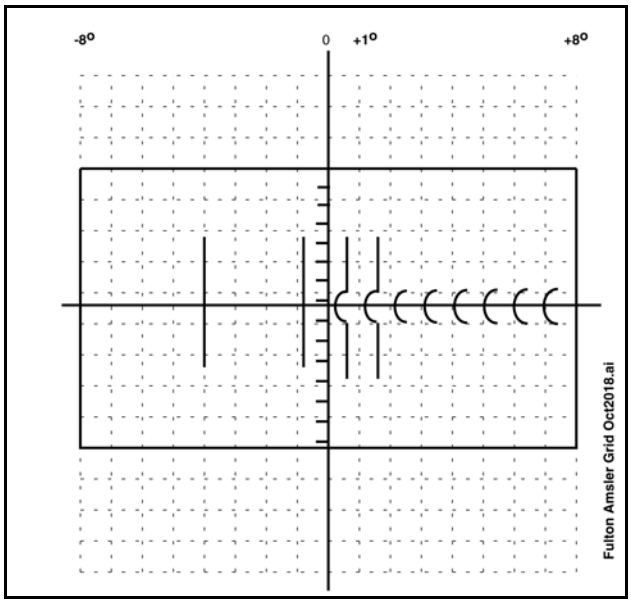

Figure F.1.4-4 The observed field against an Amsler Grid, Oct. 2018. The remaining distortion is largely along the temporal side of the retina near the equator. The region immediately adjacent to the vertical axis appears highly compressed. The peripheral field all around the point of fixation is nearly orthonormal. However, the field of the left eye remains at a scale of about 80% of that of the right eye.

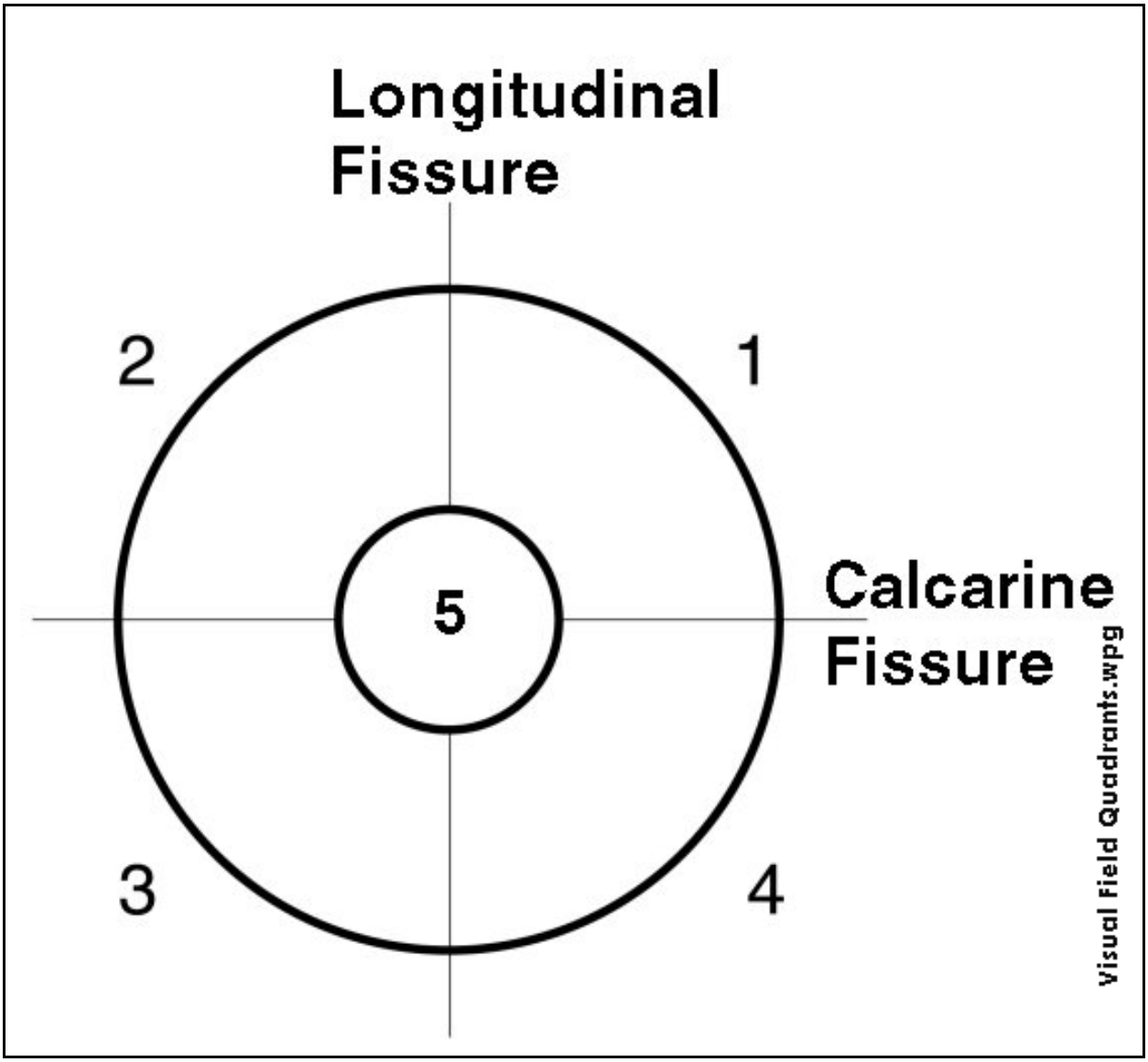

Figure F.1.4-5 Visual field processing within the neural circuitry of the visual modality. The brain processes the visual signals from the retina on a quadrant by quadrant basis, except for the foveola (5) which is handled separately. The quadrants are separated in the occipital lobe, the visual cortex, by the longitudinal and calcerine fissures. The large circle defines the nominal fovea at 8.46 degrees in diameter.

The sharing described above is a key feature of how the image data from each eye is processed within the visual modality of the brain.

Figure F.1.4-6 shows the organization of the neural circuitry serving the visual modality. This figure can be used to desribe a variety of disease conditions in human vision and will not be discussed in detail here.

The image data projected onto the retina of each eye is encoded by the photoreceptor cells, PC, which are in fact neurons, PN's. The resulting neural signals are further spatially encoded into groups of neural signals before the signal groups are encoded further into pulse signals for projection to the higher information extraction engines of the brain. As noted above, neurons along the vertical and horizontal meridians and those along the arcs of the smaller circle share their signals with spatial encoding ganglion neurons on both side of the demarcation lines. This encoding feature is used after additional information extraction to reassemble the imagery information into a single "saliency map" presenting a neural interpretation of the external visual environment to the cognitive engines of the prefrontal cortex.

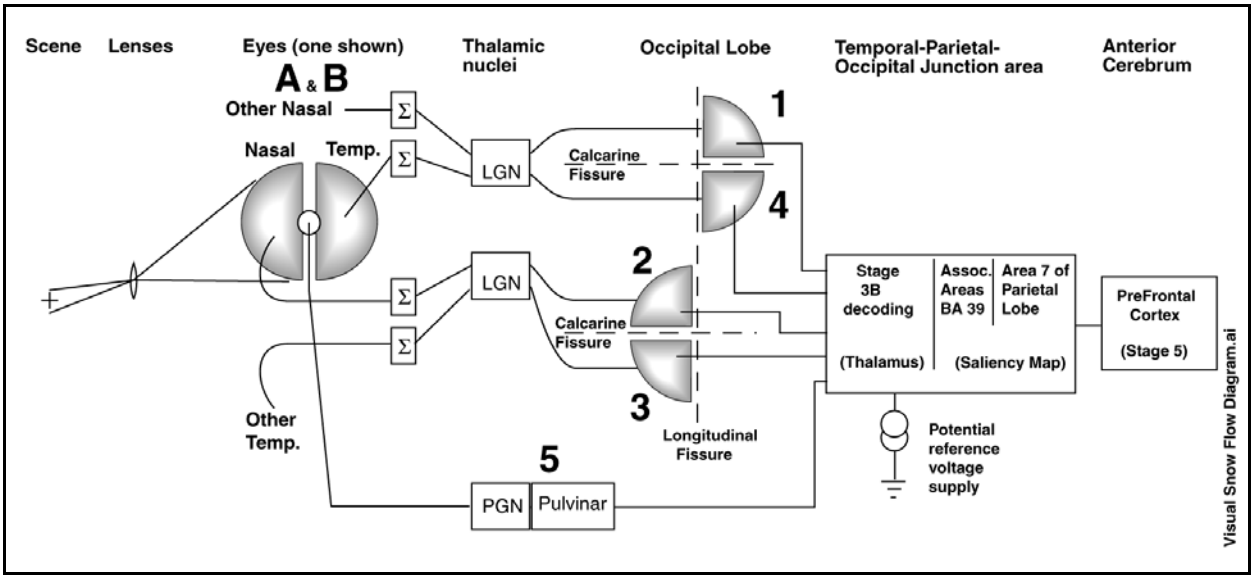

Figure F.1.4-6 Visual modality signal flow diagram, annotated. The left and right hemispheres of each eye are processed separately in order to process stereo vision. The coarse stereo capability is processed in the LGN. The fine stereo vision is processed in the PGN/pulvinar. All of the data associated with the numeric area come together in the thalamus and/or the association areas noted. See text.

A fundamental capability and critical mechanism of the visual modality is that of image comparison. It brain is adept at comparing one "image" of data with a second "image" whether the image is of visual information, sound information, taste information, etc. Image comparison is a key neural function. The comparisons are generally performed in a multi-dimensional correlator. In the case of the foveola, the area corrlator is known to consist of a nominal 23,000 photocells (a nominally circular region with a diameter of 175 PC's). The correlator used in preparing the saliency map is considerably larger because it combines the information from multiple sensory modalities. In the case of vision, the correlator also incorporates stereo information.

In the case of multiple quadrant of the visual field, correlators are used to reassemble a master neural image of the visual field by correlating the spatially relevant neural signals doubly encoded along the demarcation lines. By comparing the two "images" of the same visual information, the individual quadrant maps can be recombined.

When the correlators of the brain fail to combine the multi-quadrant information properly, it is considered a psychosis. In the worst case, the patient perceives what look mildly like medieval fortification. Fortifications is one of the labels used to describe these psychoses.

In the case of retinal detachments, any stretching of the retina laterally and differentially along one of the defined demarcation line can interfere with the correlation function defined above. This appears to be the cause of the astabel distortions in **Figure F.1.4-2** and differentially in **Figure F.1.4-3**. Based on the progression healing between these two images, it is likely that metamorphopsia will disappear from the author's vision within another few months.

The astable aspect of the metamorphopsia is due to the contrast between the two images presented to the correlators used in image reassembly. The distortion is hardly noticeable in complex scenes of moderate contrast. Howeve, in

high contrast scenes involving a sharp edge and extending across the demarcation line, the sharp edge is displaced as presented in the two images and the correlator provides an erroneous output that varies with time and ocular pointing.

> The situation within the correlator is similar to the displacement of fences and highways following an earthquake along the San Andreas Fault in Central California. The correlator is attempting to report a straight line that is no longer straight.

F.1.4.4 Potential re-mapping of Petzval surface on to retina ADD

Ophthalmology texts and the author's ophthalmologist frequently describe a remapping of the position of the visual field by the brain in the interval following surgical re-attachment of the retina to the choroid. This is a complex subject because of the number of degrees of freedom involved.

For a partial re-attachment *not involving the optic nerve*, an analogy can be made to temporarily rolling back a wall-to-wall carpet while avoiding disturbing the area around the fireplace with its more complex spatial geometry. When the carpet is rolled back into its original position and tensioned with a carpet stretcher, the vast majority o the carpet is restore to its original position with a high degree of precision. The degree of precision required in rolling back the retina is much less than the dimensions of a photoreceptor cell, except in the area of the foveola. This is because of the summation of signals from many adjacent cells at the level of the ganglion cells of the retina.

Only in the area of the foveola are individual photoreceptors cells served by uniquely individual ganglion cells. In the area of the foveola, it is only the relative location of the photoreceptors that is critically important. Thus the replacement of the foveola in its precise location is important, but primarily for purposes of stage 4 intelligence extraction. For a mis-positioning of the entire foveola of one eye, the precision optical servomechanism can adjust to converge the two eyes based on the new location of the errant foveola. This may involve a remapping of the precision convergence lookup table. This is a relatively small table resulting from an area-wise correlation process. It is normally subject to remapping on a long term basis to accommodating aging, etc.

> The experience of the author/subject is that both the coarse and fine convergence mechanisms involve area correlators. When operating under disturbed conditions of photoreceptors within the foveola, the correlation functions may be broader than optimal and may even incorporate multiple peaks. A broader peak may lead to a lesser ability to maintain convergence under some conditions. Multiple peaks could lead to conditions where the eyes move between optimal and sub-optimal convergence conditions, possibly following a complicated time line.

There appears to be no need to remap the field of view of the visual modality, in its entirety, if a reference point such as the point of attachment of the optic nerve, is maintained. Only the precision converge lookup table associated with the foveola/PGN/pulvinar pathways of the two eyes need be re-written (**Section 7.3**). It may be necessary to also rewrite the 3D lookup table associated with stereo-vision, the mechanisms of accommodation and estimations of depths-of-field associated with objects in the field (**Section 7.4**).

F.1.5 Evaluation of the detached retina experience at 1 year point After one year, the peripheral retina of the left eye is operating satisfactorily. Looking at a tiled surface, the spatial geometry outside of the foveola (1.2 degree diameter) is sufficiently improved that no laser stitch marks are no longer apparent.

F.1.5.1 Perception at the one-year point–patient's evaluation of the surgical solution to detached retina

The performance of the foveola remains largely useless. The performance of the foveola is light level sensitive. 1. A full moon appears to be a defocused half moon. Only the left half is visible.
2. The first and last characters of an automobile license plate are readable at 12 feet, but the middle five characters appear like a bunch of straws as in the children's game, pickup-sticks.
3. Faces on a TV remain significantly distorted, with the right half usually compressed horizontally. The left eye of a talking head is usually displaced downward about one half the diameter of the eye.
4. The scale of the foveal image of the left eye remains at about 80% of the size of the right eye. It appears the periphery of the left eye exhibits the same scale at the right eye. When driving, it is necessary to concentrate on the image from the right eye to estimate distances to cars ahead of mine.
5. Color performance of the left foveola appears to match the right eye in all chromatic aspects.
6. A 1/4 inch diameter low contrast spot at 4 feet (0.298 degree diameter), and centered on the point of fixation, disappears completely when presented against a uniform background, just like the blind spot related to the optic nerve but smaller. A high contrast spot of the same diameter disappears at greater than 6 feet (0.2 degrees). These actions and other data suggest a scotoma of semicircular character to the right of the fixation point in the exterior scene.

F.1.5.2 Perception of spatial distortion related to the foveal pit at the one-year point

The peripheral retina has recovered quite substantially from the stitching performed during retinal re-attachment. The remaining problems can be summarized as,

- A significant reduction in image size within a few degrees of the point of fixation compared to the right eye (**Section 2.4.1.2**).
- A significant reduction in the nasal half of the foveola image perceived by the visual modality.
- A dislocation in the nasal half of the foveola image perceived by the visual modality.

These distortions appear to be directly related to the deformation of the field lens defined in **Section F.1.5.3**. The reduction in image size can also be associated with this lens. Since this is a field lens, a change in the curvature of only a portion of the lens can also be responsible for a change in focal length for a zone of the field presented to the photoreceptors. A change in the local slope of the lens surface can also result in a prism-like action displacing the presented image in any direction relative to the rest of the image presented to the photoreceptors.

Since the lens is formed entirely from the Inner Limiting Membrane, ILM, the lens is very susceptible to minimal pressure from the column of material between the ILM and the choroid caricaturized in figure in **Section F.1.5.6**. Excess material is seen to the right of center in these OCT images. A cyst or excessive fluid in the choroid/RPE area can easily cause both the prismatic and curvature distortion.

Following surgery for a detached retina in the left eye of an otherwise matched pair of eyes, the field lens discussed above showed significant distortion. This could have been to the original detachment and possible folding of the retina along a line passing through the foveola or due to the stitching of the retina back in position. The result was a reduction in image magnification on the temporal side of the foveola to 85% of nominal and a reduction iin image magnification on the nasal side of 72% of nominal. The perception produced by the nasal portion of the field lens was of an additional displacement of the image vertically of about one-quarter degree.

Figure F.1.5-1 shows an attempt to describe the perception available at one year. There are two obvious problems. The perceived overall image of the central 3 degrees of the fovea is only about 85% of the size of the periphery retina of that eye versus *the complete field of the right eye.* In addition, the temporal field of the left foveola is further reduced in size. The mouth is perceived as continuous by the left eye. This results in the left eye of the emoticon being lower than expected in relation to the right eye of the emoticon . The implication is that the lens element at the neural/viscous medium boundary (usually described as a field lens) is probably misshaped. This is likely to be due to excess fluid between the RPE and the photoreceptor outer segments (sometimes described as cystoid macular edema).

Another implication is that the previously identified poor performance of the temporal retina of the left eye has improved considerably from 3-4 months ago (when looking at the full moon (a low light level), this part of the disk was missing. It now appears to be working much better and improved from the 80% size noted earlier to the 85% size shown in the figure. If true, it can be expected that the nasal portion of the retina may also continue to enlarge over the next 2-3 months.

The vitreous humor pressure reached 24 mm of mercury, compared to a normal 17 mm of mercury in the right eye. I was prescribed a NAIS medication (eye drops, 2x/day) for the next six weeks to treat any associated inflammation. A re-examination occurred on 6 March. The medication was continued as a precaution until the next examination scheduled for 16 April. The medication was dropped at that time as the pressure was then 21 mm Hg.

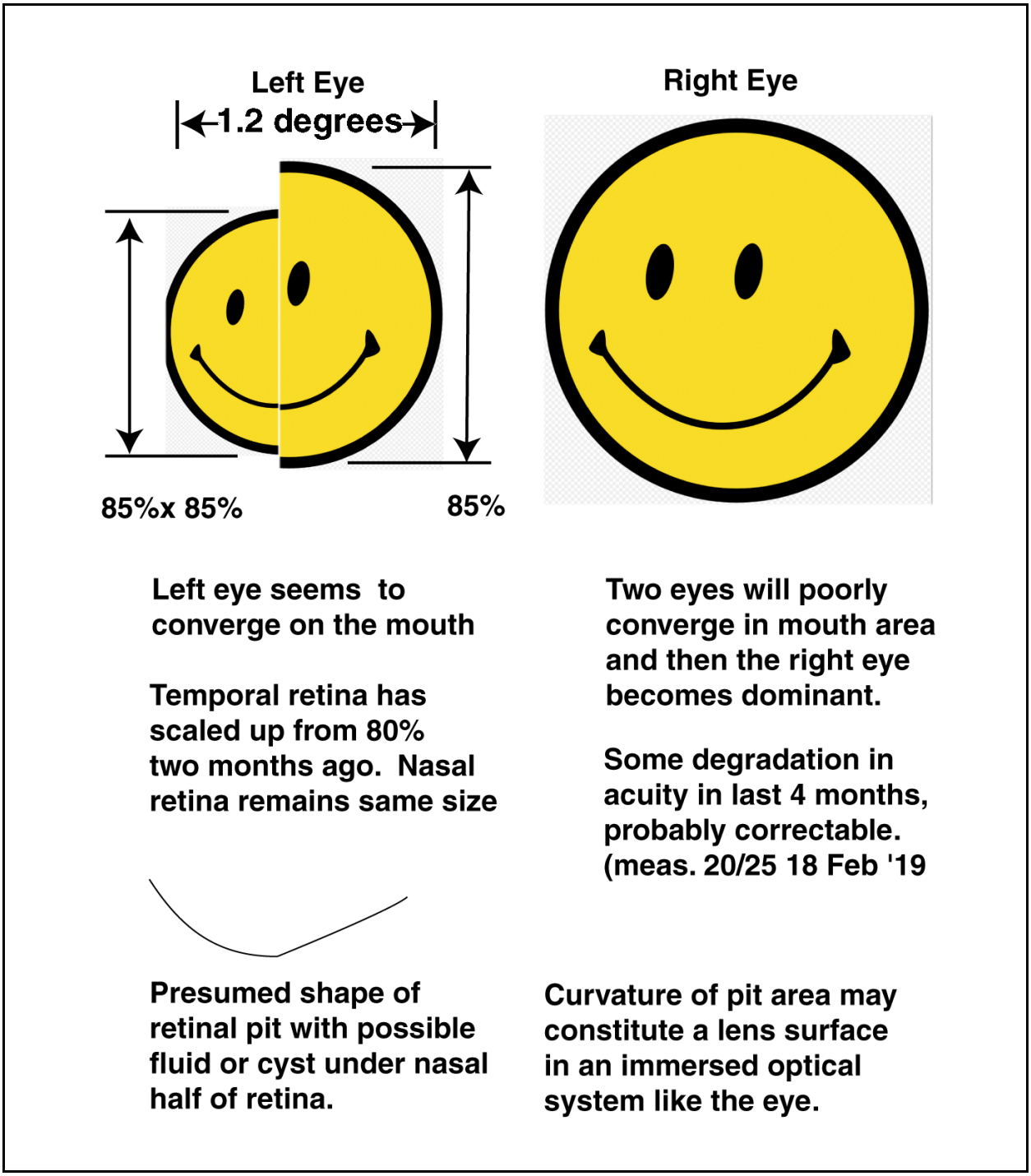

Figure F.1.5-1 Perceived spatial performance of foveola at one year point. Distortion appeared to extend to ~3° eccentricity. See text. Surgery occurred 40 days after the initial hemorrhage.

The fovea of the left eye, significantly beyond the 1.2° foveola, appears to be operating normally with little or no

spatial distortion relative to the right eye. Coarse convergence is operating properly, but fine convergence is problematical based on the difference in scale between the two halves of the perceived field by the left eye within the 1.2° foveola. There remains some patchiness in the acuity throughout the fovea of the left eye when arising in the morning (looking up at a "popcorn plaster" ceiling) but it is not observable later when observing complex scenes.

On 2 April, 2019, the large scale spatial performance of the left fovea appeared to be approaching normal. The pin cushion distortion when looking at a large flat screen TV appeared minimal in the toroid between a three degree and a five degree radius of the point of fixation. Within the three degree radius, the distortion remains. Coarse convergence appears more rapid than earlier but the visual system must rely on the right eye for reliable vision.

The foveola remained displaced along the previously identified –45 degree radial but at only 1 degree compared to the original, pre-surgery, value of 3-4 degrees. The fine convergence capability of the system is now working normally but any stereographic capability is still questionable.

By April 20, 2019, the perception of talking heads by the left eye is nearly symmetrical, after being squeezed horizontally earlier. The scale is still reduced to nominally 85% of the right eye. And, the distortion within the foveola is still as shown in the following figure.

Acuity impairment associated with the foveola

The dominant limitations on acuity, in addition to the scale changes indicated above, appear to relate to the disorganization of the normally regular array of outer segments of the photoreceptors within the foveola. This disorganization appears to result in the closely placed outer segments pointing in randomized directions (at least exceeding the Stiles-Crawford acceptance cone (**Section 17.3.7**). This randomization of the location of the entrance aperture of the outer segments (adjacent to the inner segment, **Section 2.4.6.1**) destroys the ability of the pulvinar to interpret the information delivered to it (**Section 19.8.4.2.1**). With the alignment of photoreceptors exceeding the Stiles-Crawford acceptance cone, a diminution of signal level within the neural system might also be expected. The author does experience a reduction in signal amplitude within the field of view associated with the foveola when observing a uniformly illuminated surface under some illumination conditions.

The mis-orientation of the apertures of the outer segments of the photoreceptor array can be caused by, or a residue of earlier pressure, forcing the RPE/outer segments to be compressed. Such compression of the outer segments may even cause their columnar form of the outer segments to become bent. This bending could cause the Stiles-Crawford acceptance cones to be misdirected.

On 28 March, 2019, while turning on a Windows® computer, I noted the small revolving series of dots. At a distance of about 30 inches the pattern was about ½ inch in diameter. **Figure F.1.5-2** reflects the pattern observed by each eye. The pattern seems to match the above figure. The pattern at the top of the series of dashes is unstable, suggesting a continued mis-pointing of individual photoreceptors due to a distortion in the outer segments of the photoreceptors.

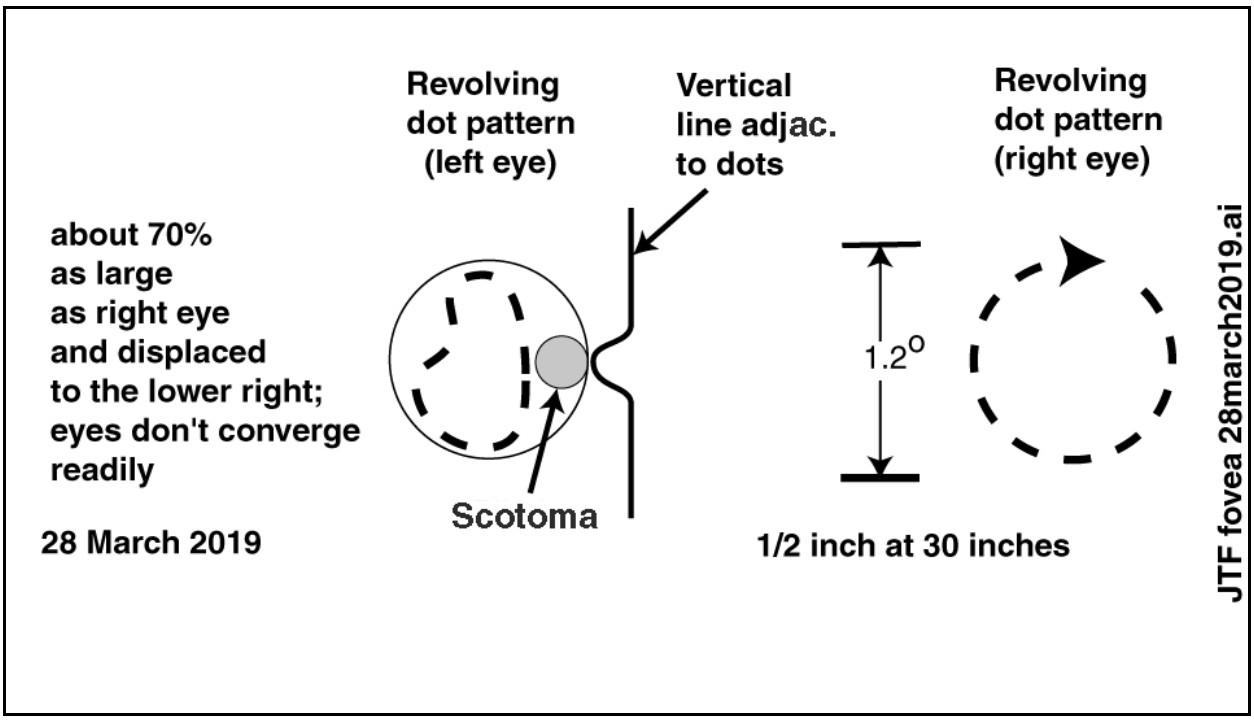

Figure F.1.5-2 Perceived distortion in a rotating pattern of dots by foveola. Only about three trailing dots are observed at one time. The period of one rotation is about 8 seconds. The vertical line has been added to the left eye perception. The dimple emphasizes the indentation introduced into the perceived circular pattern. The overall effect was to generate a scotoma that was sensitive to the intensity of the stimulus. The indentation at upper left of the left eye appears to be due to the deformation of the lower right wall of the foveal pit. See text.

At room light levels, the scotoma appeared similar to the conventional blind spot at the entrance of the optic nerve into the retina. A small high contrast disk on an otherwise uniform field would disappear when imaged on the scotoma. At higher (mid day outdoor) light levels, the first and last characters of an automobile license plate are readable at about 12 feet, but the middle five characters appear like a bunch of straws as in the children's game, pickup-sticks. The dimple in a vertical line near the1.2° circle only appears in the perception of the left eye. It suggests some of the photoreceptors associated with the nasal side of the perceived scotoma may be bent over toward the nasal side of the field in order to capture the light from the straight line and represent it as a dimple.

The poor arrangement of a small number of photoreceptors within the foveola is potentially related to a "stretch mark" or fold artifact passing through the foveola. Such marks or folds are suggested by the detachment illustrated by Dr. Busbee in **Section F.1.2**.

A high definition SDOCT scan appears necessary to confirm or falsify this perception.

Progress toward full recovery continues at a slow pace from the patient's perspective, ***but the prior progress has been spectacular***, compared to loss of essentially all vision in the left eye.

The acuity of the left eye, using a standard eye chart remain unsatisfactory, achieving 20/70 or poorer (uncorrected) using a hunt and peck approach to character identification. It involves moving the point of fixation around the character on the screen until it can be identified. Attempting to identify several characters in a row simultaneously is not possible.

In summary, the left eye at one year post surgery is totally functional but lacks acuity in the foveola and a scale problem in the perceived image within three degrees and to the left of the point of fixation . The spatial geometry of the imaging system has improved has improved at greater eccentricity than three degrees. The recent improvement appears to be due to the progress in returning of the wall of the foveal pit to its more symmetrical slope relative to the opposite wall. While leaving a scale problem within the three degree

eccentricity, the scale problem has diminished significantly in the three to five degree eccentricity to the left of the point of fixation, essentially matching the performance of the right eye. The point of fixation of the left eye, prior to fine convergence, remains displaced about one degree along the –45 degree radial in the perceived field.

The acuity of the foveola will remain unsatisfactory until the photoreceptors regain their nominal pointing and the scale factor returns to normal, by the field lens formed by the foveal pit returns to a symmetrical form. These two changes appear to be possible with time.

F.1.5.3 The *normal* foveal pit of the ILM as a Field lens

Section 2.4, and specifically **Section 2.4.3** of this work defines and describes the foveal pit as a field lens in accordance with the laws of physical optics. While previously controversial among the vision community, there is no doubt the curvature of the ILM forming the foveal pit constitutes a lens. ***The definition of a lens is a curved surface with different indices of refraction on its opposite sides.*** If the surface is not curved but flat, the optical name for the combination is defined as a prism.

Frame C & D of [Figure 2.4.5-1] suggested a spreading of the optical rays emanating from the field lens. **Figure F.1.5-3** expands on that representation based on the detailed form of the ILM indentation. In this figure, it is assumed the sloping portion of the ILM acts as a prismatic surface with a curvature. As a result, the rays reaching the entrance apertures of the photoreceptors, the focal plane, exhibit a varying degree of bending as shown. The result is the magnification in the presented image varies with distance from the center of the pit. This configuration is described in less detail in figure 3b of the review by Bringmann et al. (2018). That figure is a caricature that fails to conform to the laws of optics at the detail level. It omits the more common case of a finite radius rounded bottom to the pit. It does cite Hendrickson (2005).

From a morphogenesis perspective, **Section 2.4.4** describes a conformal mapping function that would form the foveola pit, curved outer segment array and the BM from a single "director" parameter. This function is a common one used in electronics and waveguides.

The scales are relative in the absence of an actual ray tracing. The ILM is shown as straight beyond ±2.5 degrees because of the scale. It is actually curved at a radius appropriate for the Gullstrand Schematic Eye. The system magnification scale is also shown without a detailed scale in the absence of a ray tracing and detailed nature of the curvature of the ILM. The maximum is known to be greater than 1.4:1 and may be as high as 7:1 in human eyes based on acuity versus eccentricity measurements.

This variation in magnification across the field of the retina contributes to the reason for the signals generated in the foveola to be processed within the pulvinar of the thalamus rather than in the visual cortex of the occipital lobe of the brain. It also suggests there is a degree of distortion, related to the image produced by the real eye on the retina that is not predicted by the Gullstrand or LeGrand models of the eye. These distortion surrounding the foveola may need to be removed by a spatial transform performed by anatomical computation. Anatomical computation involves the spatial rearrangement of projection neurons in a bundle (fasciculus or nerve) during their travel between stage 2 and stage 4, or between two stage 4, signal processing engines). Henschem

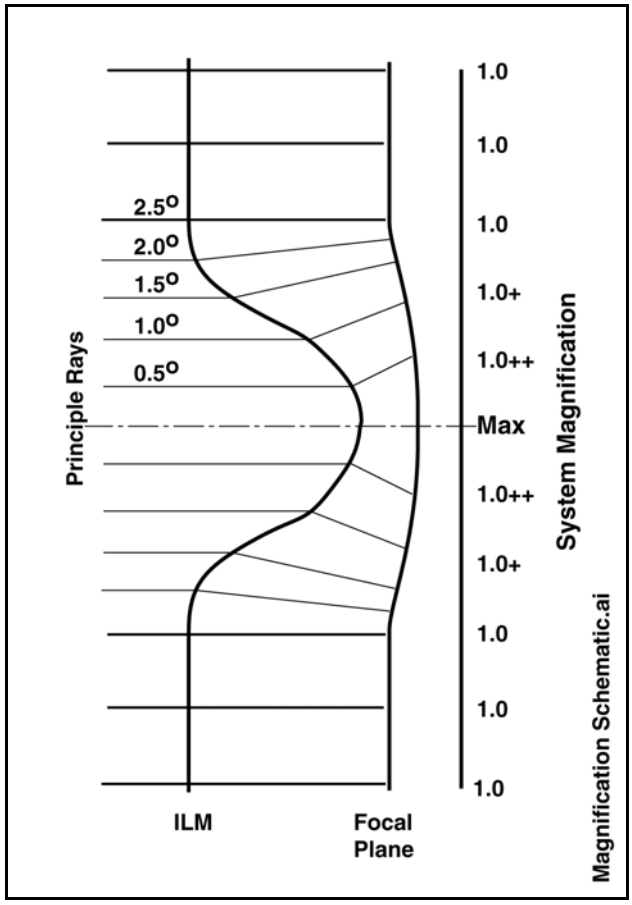

Figure F.1.5-3 The variation in magnification as a function of angle of the petzval image of the telescope presented at the focal plane of the retina.

describes this process in some detail in 1926[21].

Yiu et al[22]. provide very recent histological evidence supporting the field lens defined here. Frames A and C of their figure 1 are reproduced here as **Figure F.1.5-4**. The outer segments, OS, in frame C are not pointing toward the pupil of the optical system of the eye! They are instead, pointing toward the surface of the ILM where it is most highly curved. This pointing assures maximum effectivity in light capture at the OS aperture. Yiu et al. did not show or suggest a flat bottom to the foveal pit in *Macaque*, as some figures in the literature suggest. In fact, their figure 3L shows an even more refined thickness for the pit based on SDOCT than histologically; in both cases, a well rounded bottom for the pit is displayed.

[21]Traquair, H. (1938) An Introduction to Clinical Perimetry. St. Louis, MO: Mosby pg 74.

[22]Yiu, G. Wang, Z. Munevar, C. et al. (2018) Comparison of chorioretinal layers in rhesus macaques using spectral-domain optical coherence tomography and high-resolution histological sections *Exper Eye Res* vol 168, pp 69-76

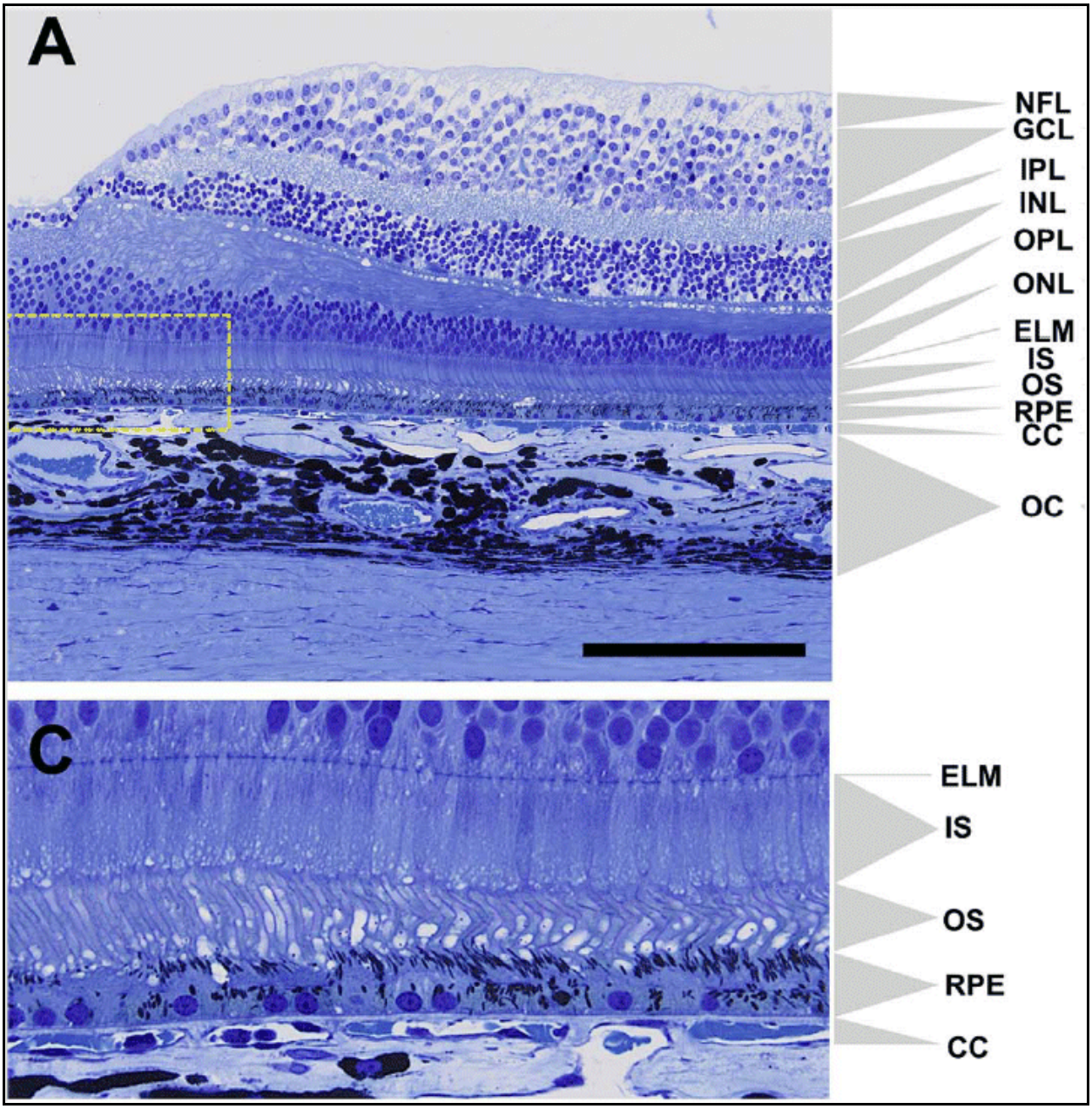

Figure F.1.5-4 Physical evidence of a field lens in primate eyes. C; Higher magnification of the area outlined in panel A (yellow dashed box) shows greater detail of the OS in the area adjacent to the axial rays of the optical system of Rhesus Macaque. The OS are pointed as much as 45 degrees from the visual axis of the optical system. This pointing would only be useful if the illumination arriving at these OS had been redirected by the curvature of the ILM acting as a lens. From Yiu et al., 2018.

The peripheral retina has recovered quite substantially from the stitching performed during retinal re-attachment.

The distortions still being experienced in the foveal region of the left eye can be associated, at least partially, with the defined field lens. The dominant geometrical symptoms are,

• A significant reduction in total foveal image size compared to the right eye (**Section 2.4.1.2**).

- A significant reduction in the nasal half of the foveal image perceived by the visual modality.
- A dislocation in the nasal half of the foveal image perceived by the visual modality.

These distortions appear to be directly related to the deformation of the field lens defined above. The full field reduction in image size can be associated with a reduction in focal length of the field lens. Since this is a field lens, a change in the curvature of only a portion of the lens can also be responsible for a change in focal length for a zone of the field presented to the photoreceptors. A change in the local slope of the lens surface can also result in a prism-like action displacing the presented image in any direction relative to the rest of the image presented to the photoreceptors.

Since the lens is formed entirely from the Inner Limiting Membrane, ILM, the lens is very susceptible to minimal pressure from the column of material between the ILM and the choroid caricaturized in the above figure. A cyst or excessive fluid in the choroid/RPE area can easily cause both the prismatic and curvature distortion.

F.1.5.4 Potential and realized asymmetry of the Author's foveal pit

The medical challenge after re-attachment surgery is to restore the foveal pit from its inverted character shown in **Figure F.1.2-5** to a usable form. The retina was surely stretched asymmetrically due to the forces applied to it by the large cyst between the choroid and the BM. This asymmetrical stretching is compatible with the early on displacement of the foveola and the ripples shown on the temporal portion of the BM.

As indicated above, the human foveal pit is normally described as circularly symmetrical (**Section 2.4.4.1.2**). **Figure F.1.5-5** shows the imagery obtained by a March 6, 2019 OCT volume scan of the Author's eye with radials collected at 30 degree intervals. In this presentation, the color within the 1 mm diameter inner circle shows a shift to more green in the lower right quadrant. The size of the spots used to average the colors presented in this scan was not noted. The color shift would suggest a variation in performance of the eye in this quadrant.

> *The circles presented in the Heidelberg OCT reports are not shown to scale in their data display. The outer circle representing a 6 millimeter diameter is only about 3.5 times the size of the 1 millimeter diameter circle.* The circle apparently represent the projection of the spherical eye onto a flat surface as used frequently in perimetry (the tangent board). Thus the circles appear to represent the tangent of the angle measured by the machine.

The small dotted arc of 0.3 degrees diameter, shown to the side of the point of fixation, represents the damaged portion of the foveola that is currently unresponsive to light. It qualifies as a semicircular central scotoma. This scotoma is too small to be evaluated under clinical conditions but can be evaluated using research grade AO-OCT equipment capable of resolving individual photoreceptors. The AO-OCT equipment must be able to cancel out the retinal tremor, RT, of the eye (See **Section F.2.1**).

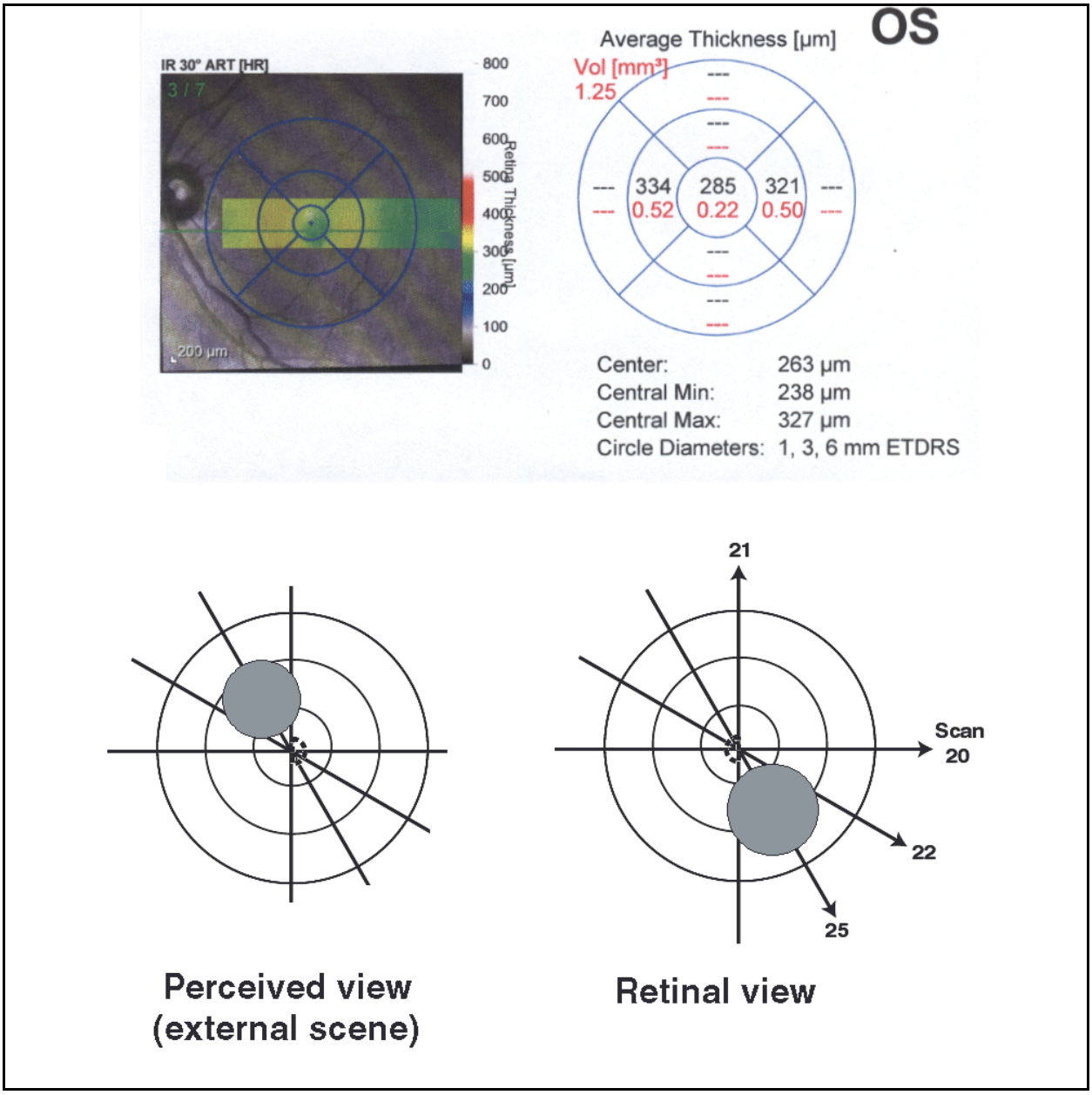

Figure F.1.5-5 Left eye OCT volume scan with retinal thickness overlay in color. The variation in color within the inner circle on the left is of significance. Bottom; Left frame shows the perceived area of maximum distortion while watching a flat screen television. The right frame would relate the position of the distortion on the retina. The shading is not meant to indicate a scotoma. The dotted arc of 0.3 degrees diameter represents the damaged portion of the foveola that is currently unresponsive to light. See text.

As a follow-up, the technician was asked to provide scans of this quadrant at 30 degree intervals

Figure F.1.5-6 shows a composite of the OCT scans associated with the fourth quarter of the fundascope of the left eye. The OCT scans for –30, -60 & –90 degrees all show extraneous material just above the brightest feature and to the right of the vertical reference line.

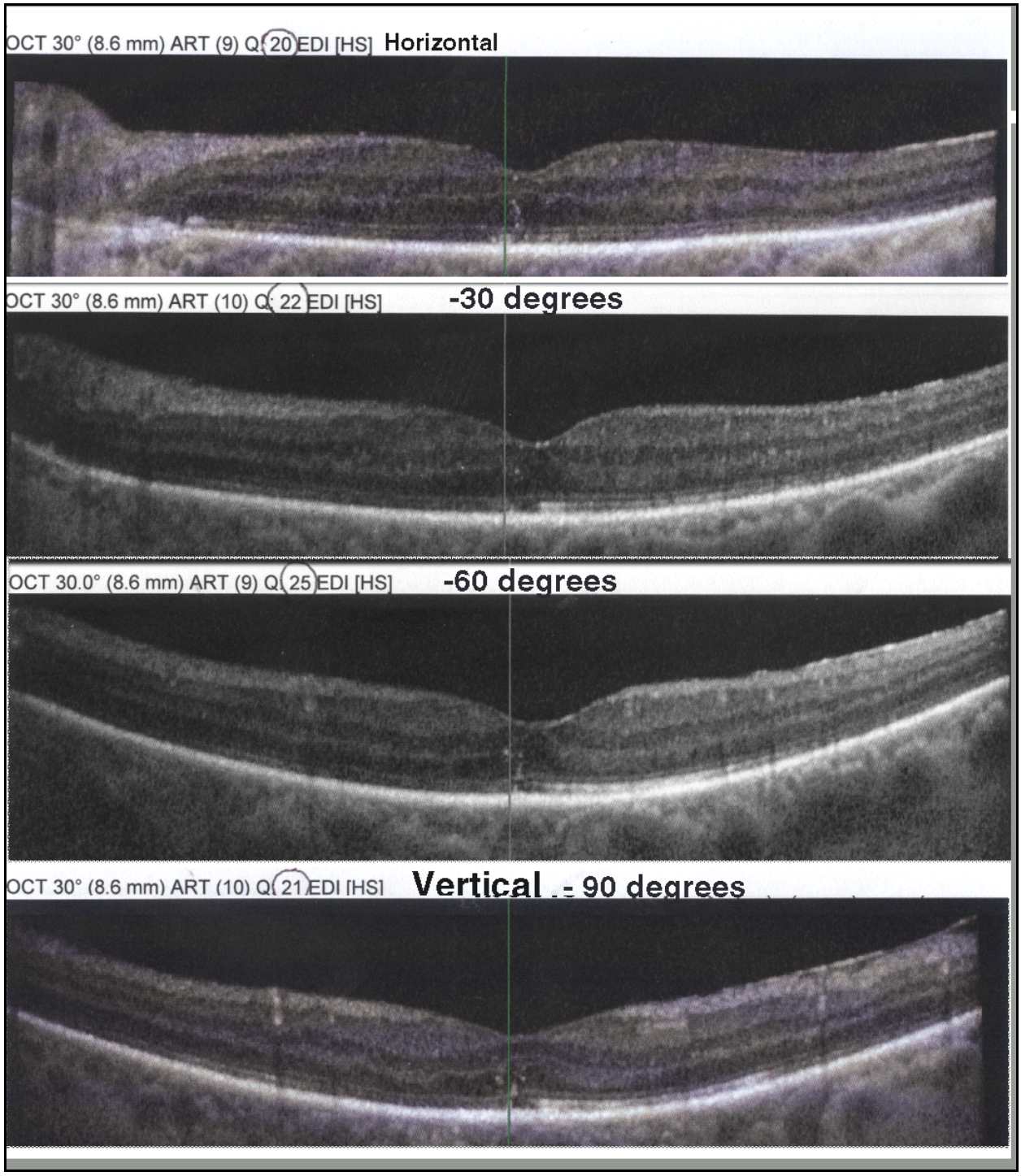

Figure F.1.5-6 Composite OCT scans of left eye of Fulton. Note the widths and depths of each foveola pit. Note also the asymmetry of the pits, particularly the bottom frame for the –90 degree radial. Note the extraneous material to the right of the vertical reference line and just above the bright feature. See text.

The brightest feature appears to vary depending on the OCT device used. In this case, it appears to

represent the RPE and choroid combined. In some cases, it is describes as combining the choroid and both RPE1 and RPE2.

The presence of this extraneous material appears to impact the shape of the ILM in the pit area. Note the depth and width of each pit illustrated. The horizontal, 0 degree, scan shows the narrowest and most symmetrical ILM shape. The – 60 and –90 degree scans clearly show the most asymmetrical ILM pits. The –90 scan shows the shallowest of the ILM pits. These conditions would suggest a reduction in magnification and relative position distortion within the grey area of the above figure in accordance with the earlier figure describing the nominal normal magnification and position distortion.

The composite OCT scan presentation appears to confirm the presence of distortion in the upper left external field of view and provides support for this distortion arising in the lower right quadrant of the retina.

The distortion is apparently generated by the extraneous material above the brightest surface in the OCT scans. The effect of this material is to push up the ILM (and all intermediate neural material) and reduce the curvature of the field lens formed by the ILM in the fourth quadrant of the retina. The result is both a reduction in the magnification and a spatial distortion in the perceived image in this region.

Genead et al. have noted, Six patients (50.0%) showed a shallow and broad foveal depression (possibly reflecting a degree of foveal hypoplasia or mal-development). They cited McAllister et al[23]. for more information based on the mal-development assumption. The McAllister et al. paper is well worth further review but it is the result of clinical investigations with too many uncontrolled (uncontrollable) parameters. The paper focuses on using SDOCT equipment for best results, compared to other OCT equipment. They show two drastically different pit shapes associated with "normals" but no supporting information about their visual acuity. No comments from the subjects were provided. It does mention the potential for loss in optical magnification within zones of the field of view in several contexts. Their figure 1 is particularly useful in comparing the SDOCT a– and b–scan views with the thickness of the retinas.

A followup to the above OCT figure was obtained on April 17, 2019 (42 days later). However, the differences require a skilled analyst to review them for significant changes.

Also on April 17, 2019, a "follow-up series of OCT scans" were provided to the author, comparing horizontal scans on 5/14/2018, 6/25/2018, 9/22/2018, 3/6/20**19** and 4/17/20**19**. Here also, a professional is needed to interpret the differences.

F.1.5.6 The clinical evaluation following the surgical solution at one year

As noted by Wilkinson in a 2009 review focused on RRD[24], the clinical situation related to the surgery appears entirely satisfactory using clinical OCT technology. However it does not necessarily correlate with the visual acuity condition. The scale problem combined with the confused perception by the right side of the field of view of the foveola suggests physical optics and/or structural problems remain at the histological level.

Wilkinson cited a paper comparing RRD and CSR results by Maruko et al[25]. Maruko et al. performed an extensive statistical investigation and interpreted their results using an undetailed model. The term model was used in the histologist's sense, of an animal model. In their case, they were citing Cook et al[26]. No physiological model of the retinal was cited. It appears the model only considered RRD that involves a tear allowing vitreous humor into the inter-photoreceptor matrix, ILM, exposing the outer segments of the photoreceptors to the oxygenated fluid. Using this model, they anticipated and sought areas of damaged photoreceptors, missing their outer segments (as expected

---

[23]McAllister, J. Dubis, A. Tait, D. et al. (2010) Arrested development: high-resolution imaging of foveal morphology in albinism. *Vision Res* Vol 50, pp 810–817

[24]Wilkinson, C. (2009) Mysteries regarding the surgically reattached retina. Trans Am Ophthalmology Soc. vol 107, page 55 *In my file as Wilkinson09pg55.pdf*

[25]Maruko, I. Iida, T. Sekiryu, T. et al. (2009) Morphologic Changes in the Outer Layer of the Detached Retina in Rhegmatogenous Retinal Detachment and Central Serous Chorioretinopathy *Am J Ophthalmol* vol 147(3), 489-494 *In my file as Maruko09pg489.pdf*

[26]Cook, B. Lewis, G. Fisher, S. & Adler, R. (1995) Apoptic Phtoreceptor Degeneration in Experimental Retinal Detachment *IOVS*, vol 36(6), pp 990-996

based on this work). Their conclusions suffer from the use of only one model and incorporate conjectures found in the literature. Maruko et al. provide useful statistical values for many parameters.

My surgeon indicated he was satisfied with the surgical results but did not offer any information concerning the scale problem or the "blind spot" associated with the foveola. His information concerning these extant problems followed the clinical literature. He dismissed the idea of a field lens formed by the foveal pit since it was not confirmed by his dated reference material. ***There is no other explanation for the dysmetropia, scale change, and/or metamorphopsias, locallized distortion, in the current literature except for an asymmetrical field lens***. Asymmetrical distortion of the field lens is also the only explanation for the short-term distortion described in **Figure F.1.5-4**. This effect would be due to the contours of the ILM outside the nominal one millimeter diameter of the foveola.

The Heidelberg Engineering OCT in common clinical use is normally set to examine the depth profile of the retina rather than the transverse spatial properties.

1. The topography of the "pit" of the retina can be causing several problems. The shape of the pit may be asymmetrical, resulting in the surface forming a lens in the immersed optical system of the eye. This could cause both a defocusing problem and a magnification problem. The temporal side of the pit might also be tilting the light rays arriving at the retina from the pupil.
2. The distortion related to the "pickup-sticks" phenomenon affecting the temporal half of the foveola, suggests a continued misalignment of the outer and inner segments of the photoreceptors, resulting in a potential Stiles-Crawford Effect, resulting in a pointing error associated with the outer segments. The turnover rate of the discs of the outer segment would suggest the outer segments alone are not crooked. This problem could also be associated with a residual fluid condition between the RPE and the photoreceptor layer.
3. The potential fluid buildup within the RPE-photoreceptor space could not be readily seen using clinical OCT equipment.

The vision modality continues to favor the right eye in most critical operations. The left eye is typically closed while reading. It is used normally when walking outdoors and driving, etc.

F.1.5.7 Evaluation of the retina from a scientific perspective at one year

A paper has been prepared in PowerPoint format to describe the scientific analysis of the biological (including human) visual system[27]. It has demonstrated that the eye exhibits a significant field lens in animals with a fovea. The essence of the paper, extending the Gullstrand "Schematic Eye" of 1911 to include the physiology of the retina has been incorporated into **Section 2.4.5**.

**** The following two figures are probably obsolete if the conformal transform of **Section 2.4.4.1** proves to be correct.****

Figure F.1.5-7 shows the horizontal scan from an optical computer-aided tomograph, OCT, through the point of fixation of the right eye. The OCT was optimized for depth measurements at the expense of transverse resolution as indicated by the scale at the upper left.

[27] Fulton, J. (2019) Schematic Eye (2016) http://neuronresearch.net/vision/ppt/Schematic Eye (2016).ppt

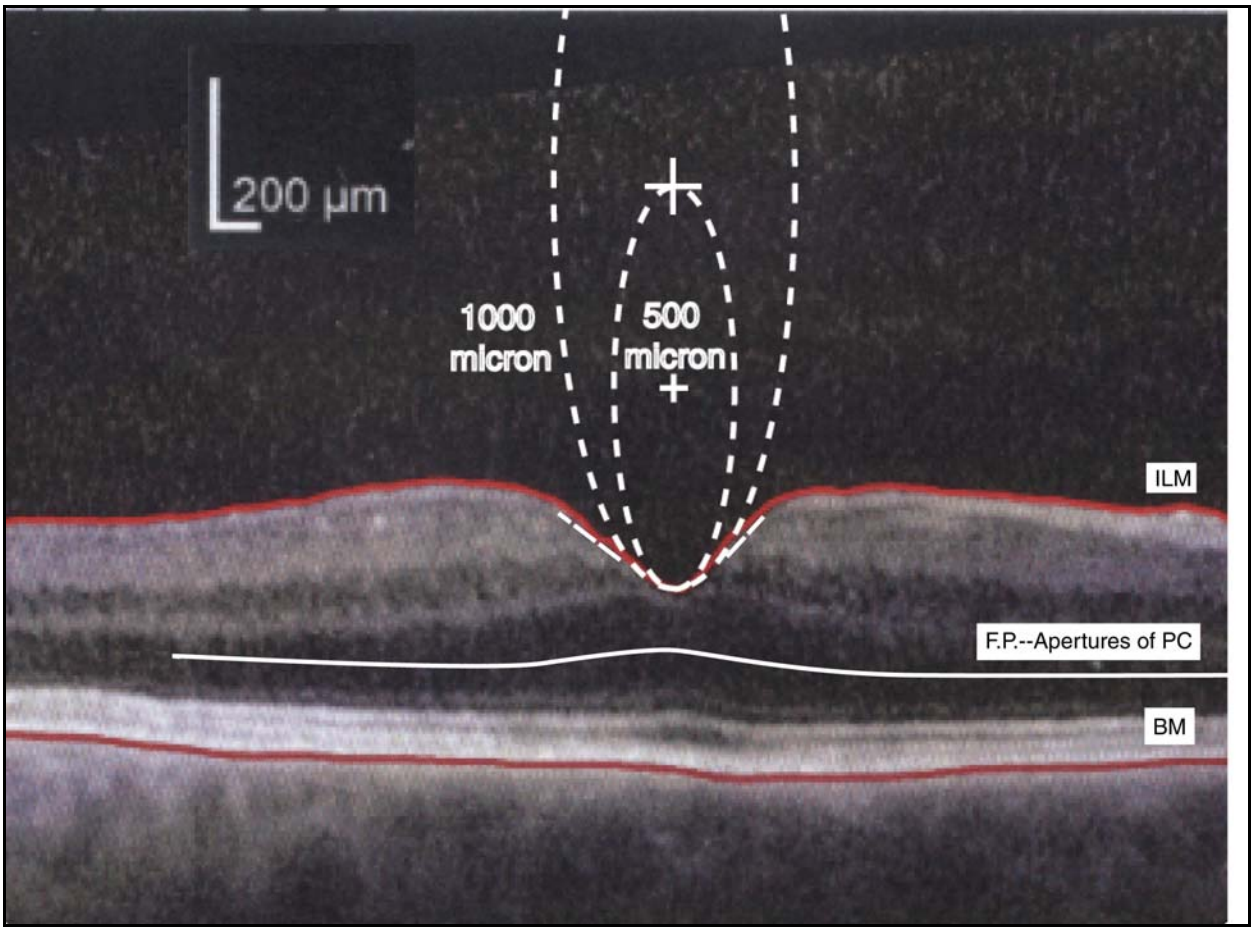

Figure F.1.5-7 Horizontal OCT scan of the author's normal right eye, 6 March, 2019 showing a 1000 micron and a 500 microns circle fitted to the curvature of the lower sector of the foveal pit. See text.

The OCT is not the ideal device for measuring the curvature of the ILM. However, estimates of the curvature of the lowest sector of the pit in the ILM can be made by curve-fitting. The 500 micron diameter circle would be a good match to the available data from a Rhesus monkey (Fine & Yanoff, 1972, figure 6-83). Their figure is reproduced in **Section 2.2.2.2.** It is also possible to estimate the slope of the prismatic portions of the ILM. From the figure, and using the scale at upper left, the slopes appear to be about 68 degrees from the optical axis.

Figure F.1.5-8 shows the vertical scan from an optical computer-aided tomograph, OCT, through the point of fixation of the left eye. The OCT was optimized for depth measurements at the expense of transverse resolution as indicated by the scale at the upper left.

A vertical scan is shown because it is a simpler case. The horizontal scan and the 30 & 60 degree scans, as a group, show a more complex situation suggesting the concave surface of the field lens was not spherical at the one year point.

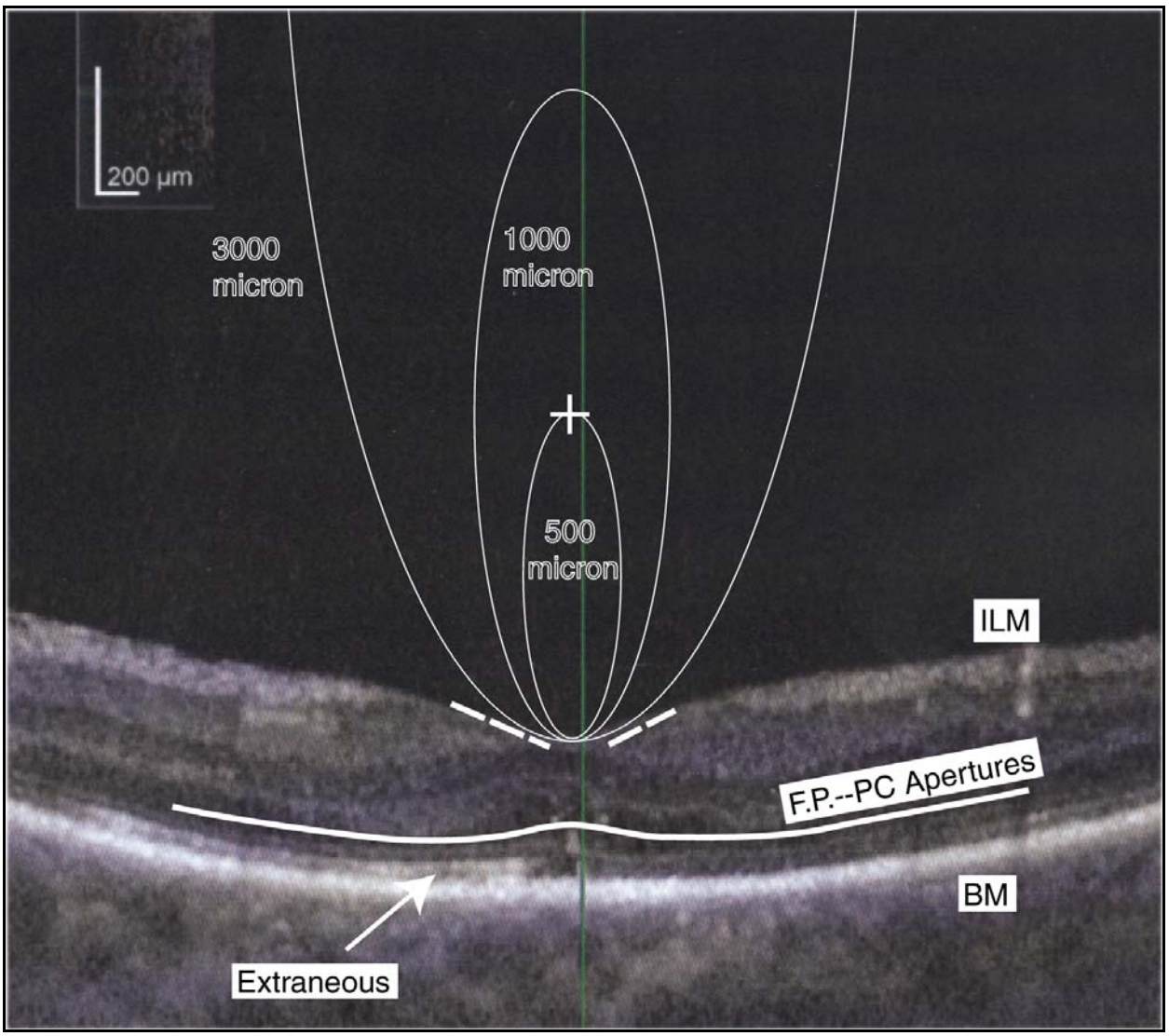

Figure F.1.5-8 Vertical OCT scan of the author's damaged left eye on 6 March, 2019 showing various diameter circles fitted to the curvature of the lower sector of the foveal pit. Also shown are dashed lines fitted to the higher slopes of the foveal pit. See text. ILM; inner limiting membrane, BM; Basilar membrane of retina, F.P.; focal plane of the retina. The photoreceptors are considerably shorter in length (vertically) than are those of the right eye.

The retina in this figure is substantially flatter in the foveola region. The diameter of the sphere most closely matching the curvature of the lower sector of the ILM is within the 1000 micron to 3000 micron diameter range. It is also possible to estimate the slope of the prismatic portions of the ILM. From the figure, and using the scale at upper left, the slopes appear to be about 75 degrees from the optical axis.

The photoreceptor region of the retina is, ‣ considerably thinner than in the right eye (suggesting either shorter outer segments and potentially lower sensitivity and lower range of adaptation) ‣ shorter inner segments (suggesting a poorer rate of disc formation and ultimately lower sensitivity and lower range of adaptation for the O. S.) or ‣ or photoreceptor neurons bent over and not pointing toward the incident stimulating light (suggesting poor sensitivity of the O. S. to light stimulation).

There remains a perception that the left eye is not exhibiting as high a signal output as the surrounding photoreceptors (resulting in a neutral gray perception for the foveola compared to surrounding regions).

The presumed shape of the retinal pit forms a field lens with a curvature that affects the magnification of the perceived image. Under this assumption, the curvature of the temporal side of the pit is less than desired and the curvature of the nasal side is considerably reduced.

My ophthalmologist examined my crystalline lens (under the conventional view that there is no field lens) and reported it was normal. It is not clear that the ophthalmological community is aware of, or has accepted, the field lens concept. Such a field lens would contribute considerably to the high acuity of the foveola (**Section 3.2.4.8.2**), even when all of the photoreceptors are of nominally equal diameter as is clearly the case.

One year after surgery for a detached retina, the OCT scan of the left eye shows a much shallower foveola pit, with the radius of curvature in the lower sector of the pit estimated at between 1000 and 3000 microns. The dashed lines also suggest less prismatic action than in the right eye. The result is a lower magnification of the image presented to the photoreceptor cells of the foveola and less movement of the part of the image outward when projected onto the F.P. adjacent to the foveola. These actions agree with what the author perceives; a significant reduction in the size of the image at the foveola (estimated at 30% of normal) and a reduction in the size of the immediately adjacent image to about 85% of normal. The thickness of the photoreceptor cell layer straddling the F.P. is less than half its normal thickness. The nature of the extraneous layer left of the foveola has not been investigated. This OCT scan was vertically through the point of fixation.

See **Section 2.4.5** for a more extensive discussion of the human eye where the foveola pit introduces a field lens contributing to a telephoto effect indicative of a telescope embedded in the overall retina.

As noted above, in **Section 2.4.5** and in conjunction with the happy face figure earlier, the telephoto effect introduces a system level magnification at the center of the foveola, m(0,0), equal to between 1.4:1 and as much as 7:1. An m(π,2.5), a horizontal measurement 2.5 degrees to the left of the point of fixation in the external view was estimated by the author as 1.4:1 in March of 2019. This was achieved by comparing the performance of the left eye following detachment and repair of the retina, with the normal right eye. The image of the right eye was 1.4:1 larger than in the left eye. More laboratory evaluation is needed to validate **Figure 2.4.8-4** in **Section 2.4.8.2**, the acuity as a function of eccentricity (especially within the foveola).

F.1.5.8 Clinical interpretations of damage from a detached retina

In 2006, Bringmann et al[28]. provided an extensive paper on the result of a detached retina on the elements of the foveola. It is more suggestive of what may have happened than informative of what did happen in a given case. It speaks of the impaired operation of the glutamate loop. Bringmann et al. focus on a detachment between the outer segments of the photoreceptor layer and the RPE layer. This allows oxygen to reach the outer segments and is much more destruction to the photoreceptors than a detachment between the choroid and the RPE layer.

In 2019, Burns et al[29]. presented an extended review of the state of the art in adaptive optics imaging. The progress in the research environment has been astonishing. **Figure F.1.5-9** illustrates a damaged foveola due to a serous detachment that appears similar to my current situation, except the void appears to be occupied by an extraneous material at the one year anniversary. The material may be similar to the white specs to the right of the red box. An interesting quote from Burns et al. is, “While reflectance based AO-OCT imaging has demonstrated RPE reliably (Liu et al., 2016), it has not been reliable with the AOSLO.” Frames **B** & **C** show the orderlines of the photoreceptors and at least the imprint of outer segments on the RPE.

---

[28]Bringmann, A. Pannicke, T. Grosche, J. et al. (2006) Mu¨ller cells in the healthy and diseased retina *Prog Retinal Eye Res* vol 25, pp 397–424

[29]Burns, S. Elsner, A. Sapoznik, K. et al. (2019) Adaptive optics imaging of the human retina *Prog Retinal Eye Res* vol 68, pp 1-306

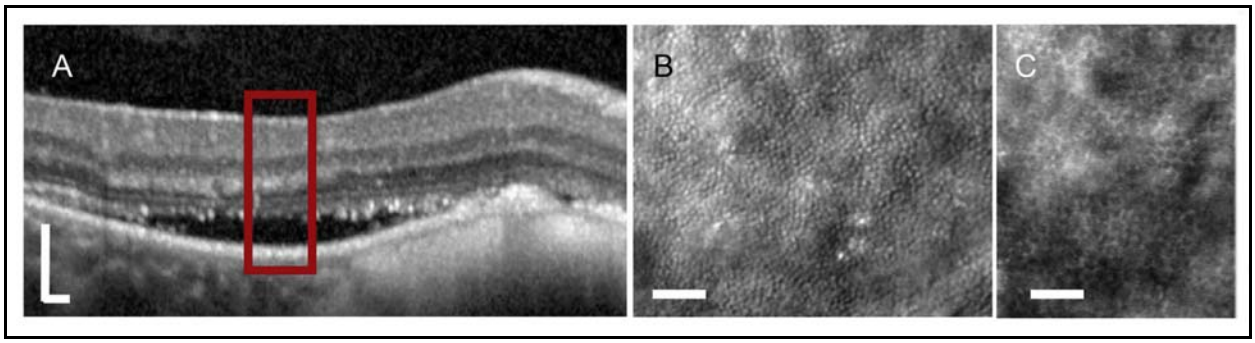

Figure F.1.5-9 Examples of changes in serous detachment via deep retinal images of the retina. A: OCT b-scan of a patient with a serous detachment secondary to a nevus. The red box indicates the approximate locations of panels B and C. B: Off set aperture images focused on the cones, showing regularly arranged mosaic of inner segments. C: Off set aperture images focused on the RPE, showing an array of RPE cells. Scale bars: A, 200 μm, B and C, 50 μm. From Burns et al., 2019.

- - - -

F.1.6 Dysmetropia & foveola acuity a year after the author's surgery

After one year from the author's April 2018 retinal surgery, a poorly understood feature of the human eye has been highlighted; the presence of a field lens and the incorporation of that field lens into a telescope of significant magnification (about seven to one) within the optical system of the of the human eye (**Section 2.4.8.2).**

Lee et al. as well as Ugarte & Williamson[30], reported only reduced image size when discussing dysmetropsia. Ugarte & Williamson used the term micropsia in their title to emphasize this fact. No macropsia was identified by either group. This fact is significant in demonstrating the presence of a field lens associated with the pit in the ILM. Ugarte & Williamson noted, "The reason for the disturbance in size perception is not well understood."

There is no reason that the micropsia should occur equally in orthogonal directions or over the entire visual field. In the author's case, micropsia occurred in two phases. The complete field within a 1.5 degree eccentricity experienced a 15% reduction in size (micropsia). In addition, the left temporal field experienced an additional 15% (net 22%) reduction within the left hemisphere. The degree of the micropsia was independent of direction in these cases. The remainder of the field encountered no micropsia.

The distortion of the shape of the ILM pit on the right (temporal field) side of the above series of OCT scans can be illustrated conceptually (in the absence of a formal ray trace) using **Figure F.1.6-1**.

The figure results from taking an OCT scan of each eye with the left field views arranged at the top of the figure and the right field views arranged at the bottom of the figure.

The assumption is made that the extraneous material to the right of the centerline in the bottom frames of the series is the cause of the shallower slope of the ILM on the right side of the these frames (which correspond to the upper left quadrant of the external visual field. This frame attempts to account for the distortions in the visual field by relating the shape of the ILM to the scale changes (magnification) and spatial distortions perceived. It can also be expected to influence the focus quality in these local areas. The longer radius of curvature of the ILM near the centerline for the left reduces the magnification to a lower level than in the right eye (under the telephoto assumption). %Max is estimated as 85% of Max in the figure and the magnifications are proportionally reduced above the centerline. Similarly, the geometric location of the principle optical rays arriving from the crystalline lens are redirected inappropriately as indicated by the sloping lines in the center of the figure (note the difference in redirection of the 2.5° principal rays in the two eyes).

Without the telephoto assumption due to the field lens, there is no theoretical way to account for the variation in size and the image distortion over a five degree radius in the upper left quadrant of the visual field being experienced by the author.

The bundle of rays associated with each principle ray will come to a focus at a different position than normal, causing a local defocus related to that bundle.

- - - -

One month since the above series of OCT scans, the extent of the distortion in the region of five to four degrees eccentricity in the upper left quadrant of the visual field appears to be returning to normal (based on little to no pin cushion distortion, see **Section F.1.4.1**, along the borders of a large screen TV). This would suggest some reduction in the amount of extraneous material on the right above the bright line in the series of OCT frames. The amount of material present will be research again in the coming week. The quality of focus also seems improved (with the ability to recognize familiar buildings at a distance of six miles).

[30]Ugarte, M. Williamson, T. (2006) Horizontal and vertical micropsia following macula-off rhegmatogenous retinal-detachment surgical repair *Graefe's Arch Clin Exp Ophthalmol* vol 244, pp 1545-1548

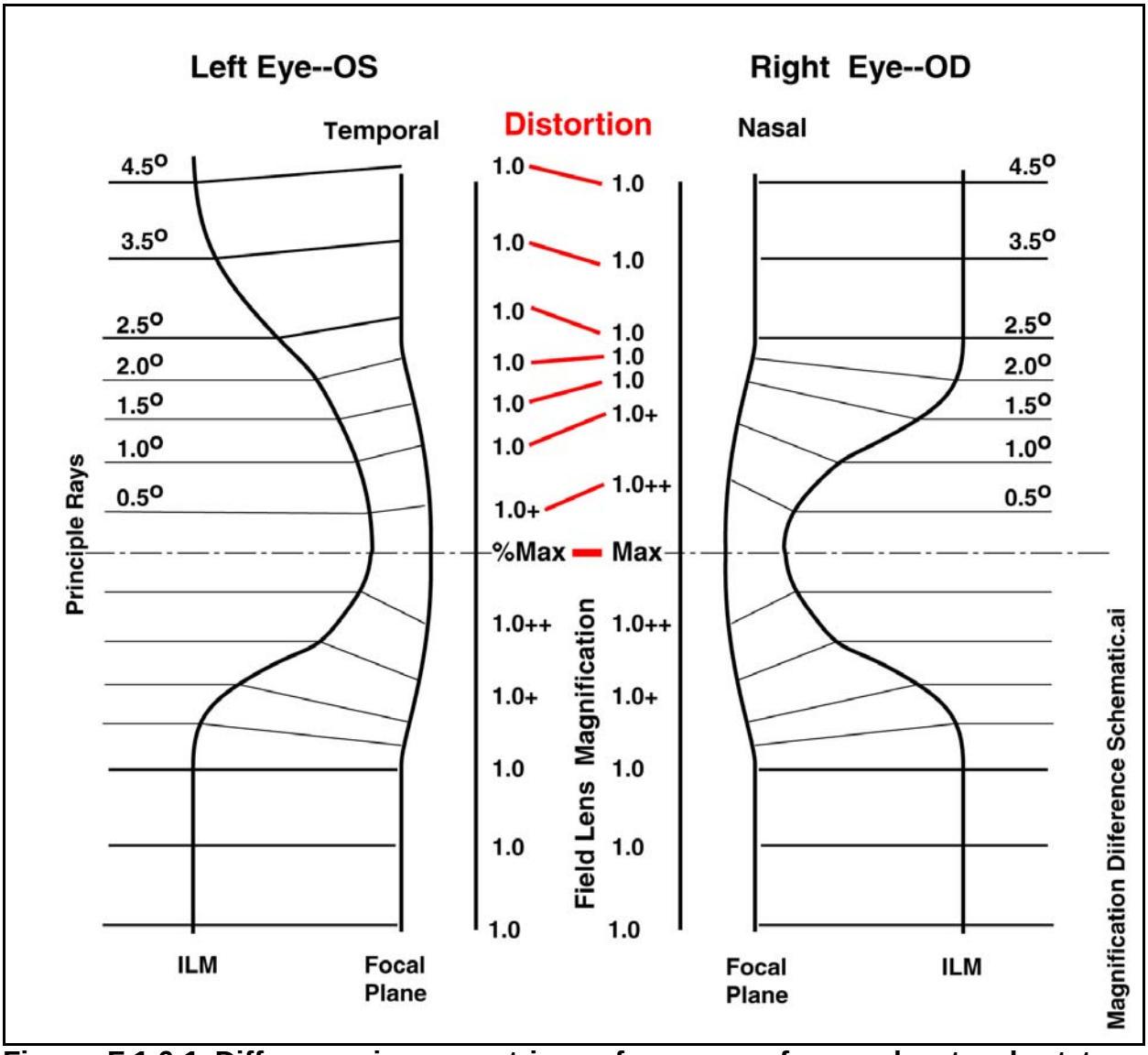

Figure F.1.6-1 Difference in geometric performance of eyes due to short term differences in pit shape. This performance was observed by the author one year after detached retinal surgery. The %Max magnification of the left eye was about 75% of Max and the magnifications were proportionally reduced and the principle rays were displaced as indicated by the slopping (red) lines between the two scales. See text.

- - -

The current displacement of the foveola is 1 degree nasal and 0.3 degrees inferior. This is smaller than the nominal foveola. Fine convergence is occurring spontaneously. The result is no binocular diplopia unless I seek to cause it.

The pin cushion distortion, previously prominent in the torus between 4 degrees and 5 degrees eccentricity has now disappeared. There may still be pin cushion distortion in the torus between 3 degrees and 4 degrees but it is difficult to quantify because of the continual distortion in scale within the 3-4 degree eccentricity in the left hemi-field.

The distortion in the left hemi-field within 3 degrees eccentricity has improved in the last two months to the point faces are now much more nearly horizontally and vertically symmetrical, but not at the same time because of the remaining scale difference. I attribute the scale difference to the reduced slope of the ILM pit in the lower left

quadrant of the retina of the left eye (reduced curvature of the field lens in this sector). Hopefully, the extraneous material between the outer segments and the choroid recorded in **Figure F.1-21** will be found reduced in the scans of 17 April 2019.

The foveola remains unusable for reading and the scotoma remains to its right in **Figure F.1-15**. The ability to perceive cars at 100 meters has improved but they still appear to be at 120-150 meters because of the scale error outlined earlier in **Figure F.1-14**.

F.1.6.1 Micropsia measurements in macula-off and macula-on conditions

Figure F.1.6-2 provides a comparison of data provided by Ugarte & Williamson in 2006 and the author's estimates of his micropsia. The comparison begs for more analyses. The Ugarte & Williamson protocol was clearly exploratory. It called for measuring the dysmetropsia at 7.5 degrees eccentricity in patients without foveola involvement, known as the macula-off condition. This author's protocol reported foveola involvement, known as macula-on within the ophthalmology community. The author reports negligible distortion at 7.5 degrees eccentricity after reporting pincushion distortion in the 4 to 5 degree eccentricity torus until 10 months post–surgery.

The macula–on condition did not vary significantly between the horizontal and vertical meridians; however, the situation was more complicated. The nasal hemifield from zero degree to 3 degree eccentricity showed micropsia of nominally 15% compared to the companion right eye. The temporal field from zero to 3 degrees eccentricity showed a much larger total micropsia of about 27% (roughly 1– (0.85)•(0.85)). The distortion as a whole is illustrated in [**Figures F.1.5-1 and F.1.5-2**].

Statistically, neither their macula–on or macula-off condition, qualifies as statistically relevant because of the number of cases cited. Wong has taken the approach that, "Macular fold is not a new phenomenon, as 2.8% of scleral buckling procedures with intravitreal injection of air/gas and cryotherapy have produced folds. Macular translocation has also been found to cause retinal folds."

The Ugarte & Williamson paper would suggest the author's codition was caused by a fold passing through the foveal pit. However, an alternate explanation appears more likely. It appears there may have been a seismic shift, a differential movement among the neurons on each side of the temporal side of the horizontal meridian. This is a weak point in the retina because only a very few neuron axons cross this meridian on their way to the optical nerve head. See **Section F.1.4.3**. It is probable that the scotoma in **Figure F.1.5-2** is a result of PC outer segments being bent out of plane by forces related to the juncture of the seismic shift along the horizontal meridian and the lip of the foveal pit.

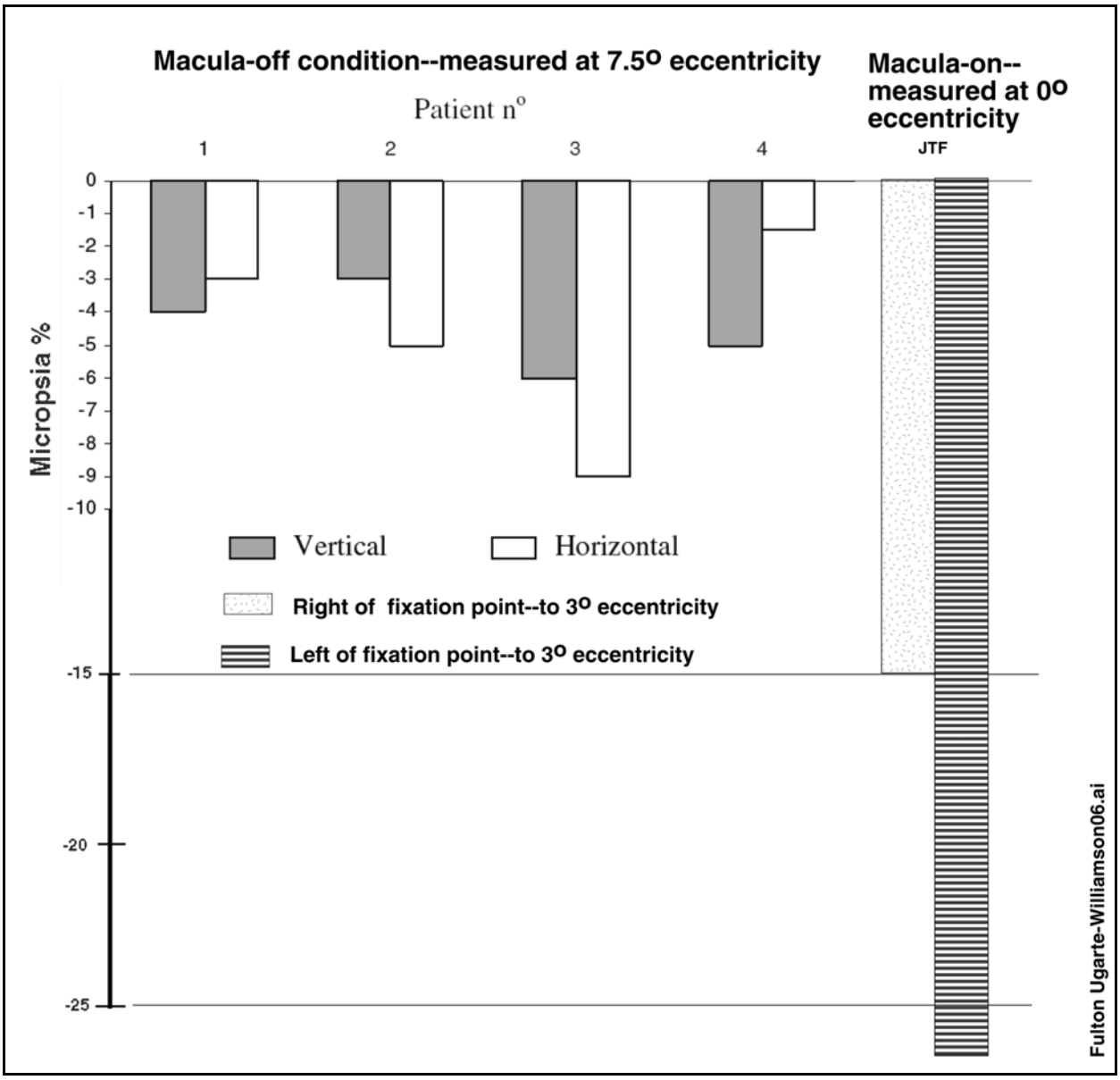

Figure F.1.6-2 "Horizontal and vertical dysmetropsia measurements (negative sign indicates micropsia) in four patients who had undergone pars plana vitrectomy and gas treatment (octafluoropropane, C3F8 or sulfur hexafluoride, SF6) for macula-off rhegmatogenous retinal detachment 6–7 months earlier." It is compared to the macula-on situation of the author at 6 months through 13 months post surgery. The macula-on condition was measued within a 3 degree radius of the point of fixation. See text. Modified from Ugarte & Williamson, 2006.

Ugarte & Williamson focused on macula-off situations. They described their test protocol in detail. "In summary, the test consisted of matched pairs of red/green semicircles with a central, white round (3 cm in diameter) fixation target shown on a black background monitor. The diameter of the red semicircle was 15 cm in each pair. The diameter of the green semicircle varied in 1% steps. Two series were used, one with semicircles matched horizontally and the second one vertically. The individuals viewed the monitor from a distance of 66 cm wearing the appropriate correction and red/green goggles. The eye with the red filter could see the red semicircle and the fellow eye the green one. The red semicircle projected an image 7.5˚ around fixation and with a fixation target 1.5˚. One percent variation in diameter corresponds with increases/decreases in retinal

image size of 0.15˚ (9 min of arc). Threshold dysmetropsia was measured by a bracketing process."

It is not clear what Ugarte & Williamson meant when they noted in their conclusion, "The effect on image size is heterogenous across the retinal area affected." Did they mean the dysmetropsia varied significantly with retinal position or did they mean the ratio between their vertical and horizontal values varied in some way. They did not give values for the heterogenous condition.

F.1.7 Summary of Encounter & Prognosis in April 2019

F.1.7.1 Summary of the Encounter as of April 2019

The summary status of the left eye after a temporal serous retinal detachment in the left eye can be described by summing the partial determinations in **Sections F.1.3.3, F.1.4.3 & F.1.5.7**.

As of this time, everything points to a complete functional recovery from the serous retinal detachment, except potentially reading, for the left eye. However, rehabilitation of the foveal pit, the indentation of the ILM, appears to be continuing. If the pressure on the ILM, and necessarily on the OS of the retina, continues to decrease it is likely that the asymmetry of the foveal pit will also decrease. This will reduce the metamorphosia within the foveola. This will also tend to reduce the displacement of the foveola from its current 1 degree eccentricity along a temporal/inferior diagonal, to near zero eccentricity. If the pressure on the OS is reduced, the PC's may be allowed to regain their normal angle with regard to the incoming illumination. This would tend to restore the spatial geometry of the current nasal scotoma within the foveola. The spatial geometry is key to achieving realistic reading in the left eye.

F.1.7.2 Other summaries of retinal detachments

Ojima et al[31]. has provided an expansive paper with many citations describing various recovery paths from (primarily central) serous detachments as examined with the OCT of the time. Table 1 and figure 3 of that paper is particularly interesting. Table 1 describes many outcomes for a large group of detached retina patients. Figure 3E appears to show extraneous material to the left and right of the foveal pit, or the absence of expected reflection in this layer immediately below the pit. Figure 3F does not show the same situation with three continuous bright reflections below the outer segments.

F.1.7.3 Prognosis in April 2019

As the symmetry of the foveal pit improves, the dysmetropia (scale difference between the two eye) will also be reduced. This scale change will also be reflected in a potential improvement in acuity. When presently observing a standard eye chart, the characters are necessarily 15% smaller than for the right eye.

The general conclusion seems to be let Nature take her coarse. If progress continues apace, reading at better than 20/70 using the left eye should be possible within the next six months.

The progress in photoreceptor spatial geometry within the foveola can now be tracked by high performance SDOCT, as described in **Section F.2**. However, influencing any needed changes at the cellular or at the IS/OS junction level appears to be beyond the current level of medicine.

F.1.8 State of the art–Surgery in the clinic and in the research facility

As of 2019, the Surgeons in the clinic are using OCT equipment, but generally not SDOCT equipment. They are also generally relying upon text and pedagogical material that predates the introduction of OCT. A problem of terminology continues, with one author using the term fovea and another using foveola to describe the same area related to the pit formed in the ILM. In the following discussion, the fovea is a large area of the retina defined as a disc with a diameter of 8.68 degrees. The foveola, on the other hand describes a small area of the retina defined as a disc with a diameter of 1.18 (or 1.2) degrees centered on the point of fixation. The foveola contains a nominal 23,000 photoreceptors. The center of the foveola is five degrees plus, from the center of the optical nerve head.

Many practitioners and researchers associate the term *rhegmatogenous*– (from the Greek for tear) with a tear allowing viscous humor access to the IPM between the RPE and the outer segments of the photoreceptors. They discount a tear separating the RPE from the Choroid. Unfortunately, there is no exclusive connection of the word

---

[31]Ojima, Y. Tsujikawa, A. Yamashiro, K. et al. (2010) Restoration of outer segments of foveal photoreceptors after resolution of central serous chorioretinopathy Japanese J Ophthalmology vol 54(1), pp 55-60

tear with either of these conditions. Del'Omo et al. have noted that most of the nomenclature has arisen from induced detachments in animal models[32] and very scant histological examinations of human eyes. The induced detachments involved separating the PC outer segments from the RPE. No induced serous detachments have been found in the literature.

Lewis et al. provided a report that apparently has been relied upon by many Surgeons. "a balanced salt solution (Alcon, Fort Worth, TX) was infused between the neural retina and the RPE with a glass micropipette. At either 1 hour (n = 3) or 1 day (n = 3) after the detachment, the retina was reattached. First a fluid–gas exchange was performed, with care taken to drain the fluid from under the retina. After the retina was flat, 20% sulfur hexafluoride (Alcon) in filtered room air was flushed through the eye. The use of a "balanced salt solution" rather than vitreous humor may cause difficulty in evaluating their results. The Alcon product "is preservative-free pH-balanced saline solution." The primary question here is, what was the dissolved oxygen level within the solution? Oxygen is a detriment to the chromophores present on the discs of the outer segments of the photoreceptors exposed during the above procedure. The Lewis team did not address the serous type of detached retina.

A tear between the RPE and the outer segment allowing oxygen rich vitreous humor to reach the outer segment via the IPM is a serious condition endangering the outer segment directly and inducing necrosis of these elements.

A tear between the RPE and either Bruch's membrane or the choroid is much less dangerous short term. It does not endanger the outer segments and leads primarily to distorted and defocused vision prior to complete loss of imaging involving large areas of the visual field. These detachments are generally described as serous. When they are near the posterior pole of the ocular, they are often described as central serous detachments.

Both of these conditions are arbitrarily labeled *rhegmatogenous* in the current surgical lexicon.
Recommendation: The noun for peel in Greek is floúda, The verb form is xefloúdizo, pronounced as sefloudiza. For serous detachments, it is suggested the term floúda (pronounced feelda by Google) replace the term rhegmatogenous previously used to cover virtually all retinal detachments.

F.1.8.1 Data base related to damage to the photoreceptors

Lewis et al. proceeded with their investigations by asserting, "Retinal reattachment studies in the cat (Erickson et al., 1983) and primate[33] have shown that the morphology of the OS/RPE interface does not return to normal, even after recovery periods of up to 6 months." They were not explicit in what they considered normal. The author had no loss of functional photoreceptors after 12 months from date of surgery. The surgery occurred at 46 days after initial detachment. In this paper, the author deduced that the detachment was of the serous type, the separation occurred at the RPE/BM interface, and no damage to the photoreceptors should be expected over the above interval. Color, sensitivity and adaptation performance appeared to be normal throughout this period. Only the acuity of the eye was hampered, probably due to a skewing of photoreceptors on each side of the horizontal meridian passing through the foveola.

Guerin, Lewis et al. provided evidence for, the believed to be more common situation, OS/RPE interface failure can have seriously different results. They summarized their investigations clearly in their Abstract,

"METHODS: To investigate the effects that retinal detachment and reattachment may have on this process, the neural retina from 12 adult rhesus monkeys (Macaca mulatta) was detached from the overlying retinal pigment epithelium (RPE) by subretinal injection of a balanced salt solution. After a standardized detachment period of 7 days, the two tissue layers were reapposed. Animals were labeled with 3H-fucose and killed at times ranging from 3-150 days after reattachment. RESULTS: During the 7 day detachment period, the majority of rod outer segments (ROS) and cone outer segments (COS) degenerated, but inner segments remained intact. During the first week after reattachment, a rapid increase in rod and cone outer segment length occurred in the absence of disc shedding. This was accompanied by re-establishment of a modified morphologic relationship between the apical processes of the RPE and the regenerating outer segments. ROS and COS regained approximately 40% of their control lengths after a 2 wk reattachment period. By 30 days of reattachment, ROS had regained 72% of their normal length and COS had regained approximately 48%. After 150 days of reattachment, photoreceptor outer segment mean length was not statistically different from

[32]Lewis, G. Charteris, D. Sethi, C. et al. (2002) The Ability of Rapid Retinal Reattachment to Stop or Reverse the Cellular and Molecular Events Initiated by Detachment *IOVS* vol 43(7), pp 2412-2420

[33]Guerin, C. Lewis, G. Fisher, S. et al. (1993) Recovery of photoreceptor outer segment length and analysis of membrane assembly rates in regenerating primate photoreceptor outer segments *IOVS* vol 34(1), pp 175-183

control areas."

Their CONCLUSIONS were less clear.

They clearly induced an OS/RPE interface detachment using a "balanced saline solution." They provide excellent statistical data on their clearly exploratory investigations. No information relating to a serous detachment was cited.

F.1.8.2 Displacement of the foveola during detachment and surgical repair

During the 2000-2019 period,it has not been common for surgeons to rigorously examine the eye with the detachment prior to surgery, even after the introduction of first generation OCT equipment, . As a result, the community has presented numerous papers on the "unintentional displacement" of the foveola during surgery[34], or "unintentional retinal displacement after vitrectomy[35]." Liazos et al. questioned a different fundamental premise of the Shiragami et al. paper. Lee et al[36]. noted the presence of "macula displacement" in 72% of 32 consecutive fovea-involving detachments treated with vitrectomy and gas. They did not discuss whether any or all of these displacements were present prior to surgery.

In [**Figure F.1-3**]of this paper (with a date stamp at lower right), a documented case of the displacement being present prior to any surgery is shown. A careful interview of the patient before surgery would likely identify this condition prior to surgery. It is associated with diplopia if the displacement exceeds 2 degrees eccentricity. The cause of the displacement appears to be due to stretching of the retina due to the buildup of the cyst shown. Review of [**Figure F.1-6**] shows the OCT image of the pit of the ILM indicative of the foveola totally inverted. The foveola is significantly displaced transversely as well as axially. Note the wrinkles on the right in the membrane closest to the choroid. The wrinkles suggest the fluid has caused a stretching of the membrane on the left and compression forces are present in the membrane on the right. Lee et al. did provide a set of specific terms,

- Dysmetropsia– a distortion of image size in the affected eye relative to the fellow eye.
- Metamorphopsia– a distortion of image form in the affected eye relative to the fellow eye.
- Binocular diplopia– diplopia in the convergence of the eyes rather than a psychotic condition.
- Asthenopia– retinal rivalry as a result of poor convergence.

Lee et al. as well as Ugarte & Williamson[37], reported only reduced image size when discussing dysmetropsia. Ugarte & Williamson used the term micropsia in their title to emphasize this fact. No macropsia was identified by either group. This fact is significant in demonstrating the presence of a field lens associated with the pit in the ILM. Ugarte & Williamson noted, "The reason for the disturbance in size perception is not well understood." They then suggested, in the absence of any other proposal, that their patients suffered a uniform expansion of photoreceptor spacing across the entire retina, which appears highly problematical. Making measurements across the entire angular field is extremely difficult. In the author's case, the micropsia was limited to within a six degree diameter field centered on the point of fixation. Outside of this area, at least in the horizontal plane dysmetropsia was not observed. The micropsia they reported did not exceed a 9% reduction in size. None of their four subjects exceeded a 3% difference between the vertical and horizontal planes. The author exhibited a 15% reduction in the full field out to about 3% eccentricity with a further reduction of 15% (net reduction of 28% for the left hemifield within the 3% eccentricity (**Section F.1.5.1**). This condition remained until the 12 month anniversary of surgery. Beyond 3 degrees, the visual field was normal in all four quadrants.

The Lee et al. paper, citing Shiragami et al., suggest the vast majority of macular displacements are downward, with gravity contributing to this effect. However, they note the statistics are inadequate to confirm this assumption. In the authors case, the displacement is clearly at a temporal-inferior angle of 45 degrees as noted earlier. Gravity should have a negligible impact on the retina when in a liquid environment and zero impact when in a liquid-crystalline environment. Figure 3 of Lee et al. is an interesting way to present their summary. However, the

---

[34]Shiragami, C. Shiraga, F. Yamaji, H. et al. (2010) Unintentional Displacement of the Retina after Standard Vitrectomy for Rhegmatogenous Retinal Detachment *Ophthalmology* vol 117, pp 86–92

[35]Codenotti, M Fogliato, G. luliano, L et al. (2013) Influence of Intraocular Tamponade on Unintentional Retinal Displacement after Vitrectomy for Rhegmatogenous Retinal Detachment *Retina* vol 33, pp 349–355

[36]Lee, E. Williamson, T. Hysi, P. et al. (2013) Macular displacement following rhegmatogenous retinal detachment repair *Br J Ophthal* vol 97, pp1297-1302 doi:10.1136/bjophthalmol-2013-303637

[37]Ugarte, M. Williamson, T. (2006) Horizontal and vertical micropsia following macula-off rhegmatogenous retinal-detachment surgical repair *Graefe's Arch Clin Exp Ophthalmol* vol 244, pp 1545-1548

accompanying text is clearer. "These results indicate that the retina has not been purely rotated around the disc, or shifted downwards, but instead there is a more complex movement with some regions within the macula being displaced more than others."

F.1.8.3 Folds in the retina identified mostly after surgery

Folds in the retina have been identified post-surgery in most cases, although looking at earlier OCT images frequently allow definition of the pre-surgery condition.

Del'Omo et al[38]. have reported on folds related to the outer retinal layers. "The aim of the present study was to analyze prospectively the evolution of outer retinal folds, ORFs, through a follow-up period of six months and to discuss their pathogenesis." They note, "The advent of spectral domain-optical coherence tomography (SDOCT) has permitted, without invasive intervention, to acquire pathologic data *in vivo* showing that persistent foveal detachment, distortion, and disruption of outer retinal layers (ORLs) and macular folds are common findings following successful surgery for retinal detachment (RD)."

They go on, "On the basis of previous OCT reports and our observations, we believe that hypothesis 3 is the most likely; 3. hyperreflective lesions at the level of the ORLs might be due to partial-thickness folds involving the outer layers of the retina. For such reason, in a previous paper we deemed appropriate to refer to these abnormalities as "outer retinal folds" (ORFs). ORFs must be differentiated from full-thickness retinal folds, which involve all retinal layers and may also occur after successful repair of RD.

Del'Omo et al. made an observation that may be relevant to the author's recovery process.

> "During the follow-up, flattening of the ORFs left behind areas of abnormal reflectivity of the IS/OS band, that we previously named IS/OS skip RAs. It is possible that IS/OS skip RAs reflect morphologic changes and/or very subtle misalignment affecting the distal end of photoreceptors. As such, IS/OS skip RAs might be not necessarily related to resolved ORFs but could be observed in association to other abnormalities causing misalignment of the ORLs. Indeed, we also found changes reminiscent of IS/OS skip RAs in areas previously occupied by pockets of subretinal fluid (Fig. 3). At the end of follow-up, IS/OS skip RAs were still visible in almost 50% of the examined eyes, indicating they tend to persist longer than ORFs after operation. Further studies that include more patients are needed to elucidate if these subtle changes can influence visual acuity or be responsible for metamorphopsia in the long term."

"In conclusion, we report on the evolution of ORFs, a common finding occurring after vitrectomy and injection of gas for RD repair. The pathogenesis of ORFs is probably multi-factorial with several variables concurring to their formation."

Not one of the described papers considered the structural stresses imposed on the retina, particularly important in so-called macula-on types of detached retina, by the buildup of fluids within the retina.

F.2 Review of the adaptive optical OCT devices & techniques in 2019

Because of the progress in various extensions to basic OCT, it has been noted by many that comparing the imagery between machines or with the broader histological base remains difficult at this time. Ko et al[39]. (2004) have provided a comparison between a conventional OCT at a nominal 10 micron axial resolution and 20 micron transverse resolution, with an ultra high resolution, UHR-OCT, at a nominal 3 micron axial resolution and 15-20 micron transverse resolution. Neither system resolved the IS or OS of individual photoreceptors. Consequently, most recent activity with simple, even so-called UHR-OCT, has focused on location individual layers rather than the cells forming those layers.

---

[38]Del'Omo, R. Tan, H. Schlingemann, R. et al. (2012) Evolution of Outer Retinal Folds Occurring after Vitrectomy for Retinal Detachment Repair *IOVS* vol.53, pp 7928-7935. doi:10.1167/iovs.12-10322

[39]Ko, T. Fujimoto, J. Duker, J. et al. (2004) Comparison of Ultrahigh- and Standard-Resolution Optical Coherence Tomography for Imaging Macular Hole Pathology and Repair Ophthalmology vol 111, pp 2033-2043

Ojima[40] define a more advanced system in 2007, They describe their early FDOCT, "This system uses a superluminescent diode with a center wavelength of 830 nm and a bandwidth of 50 nm as a light source, resulting in an axial resolution of 6.1 microns and 4.3 microns in air and tissue, respectively." "Using the current system, the image acquisition time for each 3-D data set is approximately 3.5 seconds. A simple and fast correlation-based algorithm was used to cancel axial eye motion artifacts." "Horizontal cross-sectional images clearly showed 2 distinct lines corresponding to strong backreflection from the IS/OS and ELM in a normal retina. The ELM, the external limiting membrane, is also known as the OLM, the outer limiting membrane. Neither of these very old names are functionally precise.

The introduction of adaptive optics to these machines, and various types of Fourier Domain operations, during the 2007–2019 period, have provided astonishing improvements in performance, including higher operating speeds commensurate with clinical operations.

Del'Omo et al. described their machine in 2012, "Images were acquired with HRA+OCT (Spectralis; Heidelberg Engineering, Heidelberg, Germany), which combines a SDOCT with a confocal scanning laser ophthalmoscope that provides a reference fundus image. The SDOCT records up to 40,000 A-scans per second with an axial digital resolution of approximately 4 μm and a transversal digital resolution of approximately 15 μm in the high-resolution mode. The "Automatic Real-Time" function incorporated in the software permits performing of multiple frames at the same scanning location, which reduces noise and increases image quality. Using an active eye-tracking technology, the system automatically follows eye movements relating OCT B-scan to the selected fundus image."

In 2017, Marcos[41] and virtually every researcher in the field authored an extensive paper. It provided a broad review of the hardware configurations used in adaptive optical OCT, some images collected by a variety of investigators using these configurations, and an extensive section discussing the future trends in the field.

Figure F.2.1-1 reproduces figure 10 from that review. It indicates the astonishing performance of these machines at the *research level*. The figure is credited to Jonnal et al[42]. The Jonnal et al. paper discusses the latest research-based combination of adaptive optics, AO, optical coherent tomography, OCT, and active retinal tracking, RT, to insure minimal perturbations due to spatial distortions introduced by the subject. Their configuration actually used a spectral domain, SD, type of OCT. Thus, an appropriate label for the configuration could be, AO–SDOCT–RT.

The AO–SDOCT portion of their system achieved "nominal axial resolution in retinal tissue (n = 1.38) was 2.6 microns." In the absence of RT, their system achieved "Its high lateral resolution (~2.5 μm compared to ~15 μm for SLO and OCT). The system recognized several reflections from surfaces of individual photoreceptors, primarily from the OS. The Jonnas et al. paper (2016) defines COST as the cone outer segment tip. It appears to be the same as the OS/RPE interface within the inter photoreceptor matrix, IPM, environment. The title COST is a misnomer and does not suggest the actual complexity of the OS/RPE interface (**Section F.1.3.1.1** and **Section 7.1**).

---

[40]Ojima, Y. Hangai, M. Sasahara, M. et al. (2007) Three-dimensional Imaging of the Foveal Photoreceptor Layer in Central Serous Chorioretinopathy Using High-speed Optical Coherence Tomography *Opthalmol* vol 114, pp 2197-2207

[41]Marcos, S. Werner, J. Burns, S. et al. (2017) Vision science and adaptive optics, the state of the field *Vision Res* vol 132, pp 3–33

[42]Jonnal, R. Kocaoglu, O. Zawadzki, R. et al. (2016) A review of adaptive optics optical coherence tomography: Technical advances, scientific applications, and the future *Invest Ophthal Vis Sci* vol 57(9), pp 51–68. http://dx.doi.org/10.1167/iovs.16-19103. Also published simultaneously in *Biomedical Optics Express*

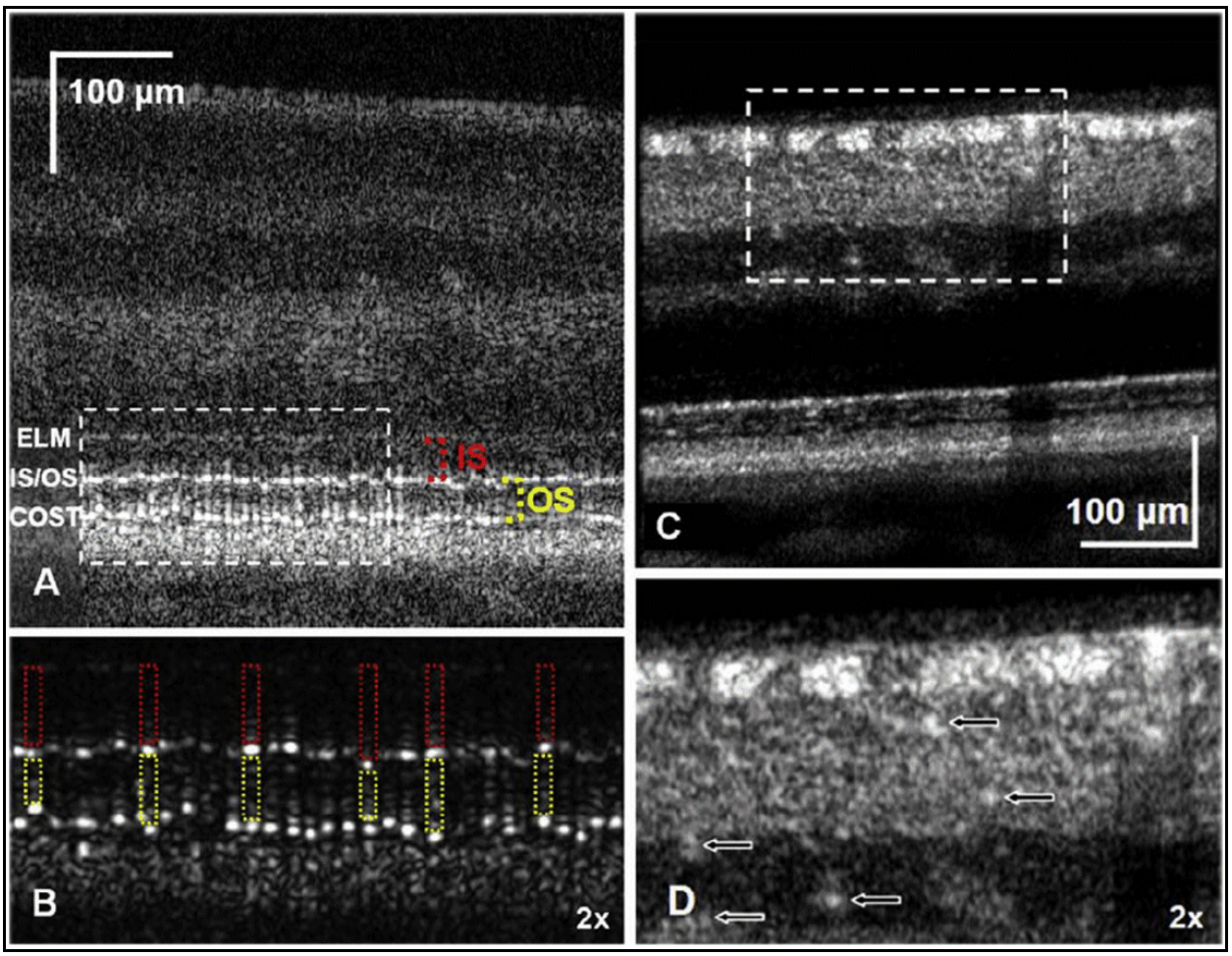

Figure F.2.1-1 Images acquired with AO ultrahigh-resolution OCT. In a log-scale B-scan focused on the outer retina (A), the ELM, IS/OS, and COST bands are clearly visible, demarcating the IS and OS of the cones. In a linear-scale, magnified view (B), the IS/OS and COST reflections from individual cones are clearly visible, with red and yellow boxes outlining the relatively transparent individual inner and outer segments. The width of the bright reflections is consistent with known inner segment widths, while their height is comparable to the axial PSF height, which suggests origination at thin reflectors. Axial displacement of neighboring reflectors is apparent in both layers. When focus is shifted to the inner retina (C), individual nerve fiber bundles, up to 50 microns in diameter but separated as little as 5 microns, become visible. A magnified view of the latter (D) reveals capillaries (arrows) laying in multiple plexuses. These individual structures of the inner and outer retina appear as uniform bands in clinical OCT images from Jonnal et al., 2016.

Figure F.2.1-2, also from the Marcos et al. review, shows a single frame typifying the available image quality of AOSLO devices from Harmening et al. in 2014. That paper provides much more information.

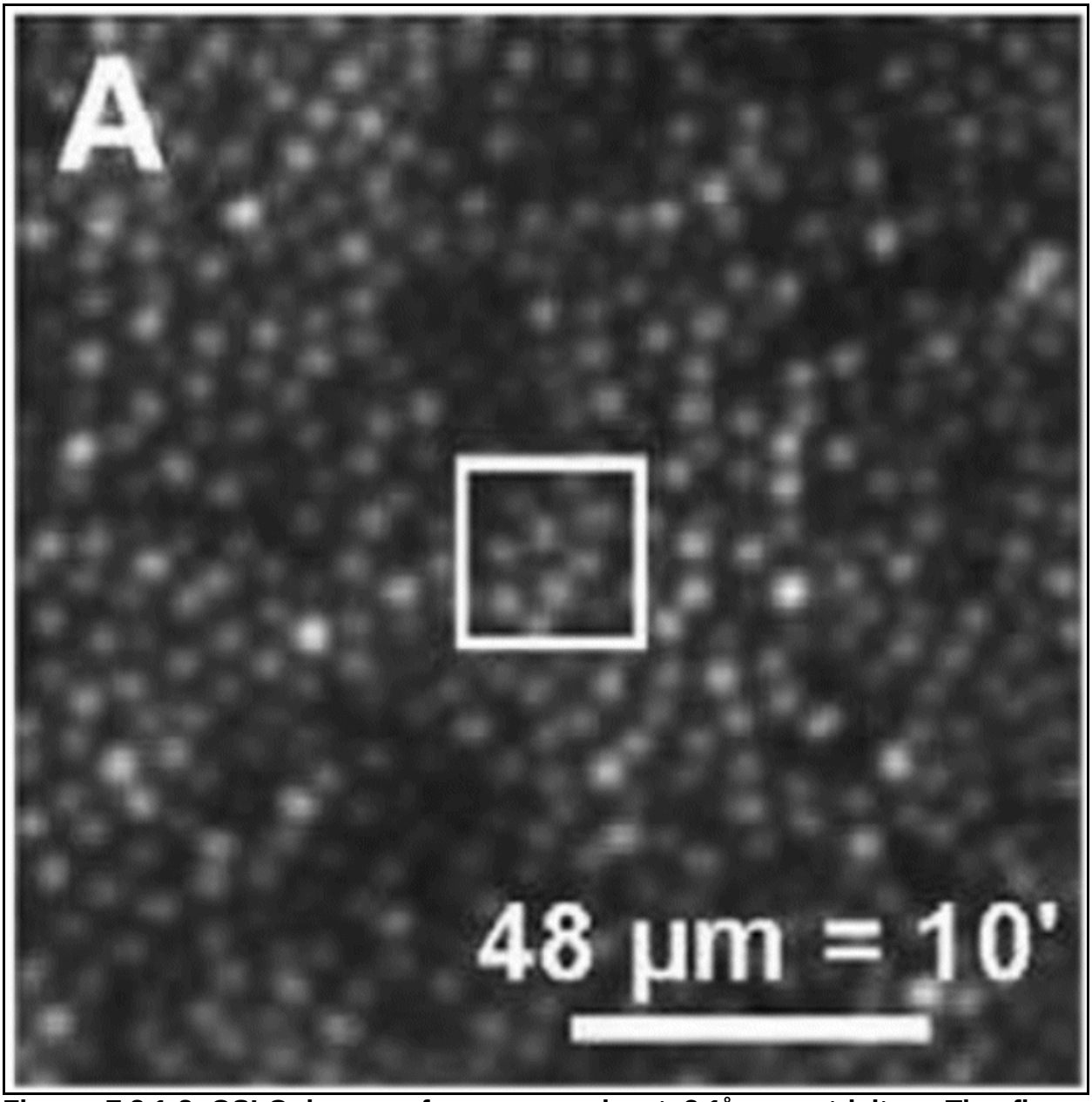

Figure F.2.1-2 OSLO image of cone mosaic at 3.1˚ eccentricity. The figure demonstrates the state of the art in imaging with AOSLO technology in 2014. See the original article for details. From Harmening et al., 2014.

In 2018, Bringmann et al[43]. presented a very large scale review of the visual system with a focus on structural features of the primate fovea at the histological level and comparing images of similar area of the *Macaque* and human eyes. The paper was prepared by a large committee and suffers from a lack of continuity of thought. It cherry picks facts from many unrelated papers in order to describe numerous cameo (stand-alone) situations. There are many (countless without a computer) uses of the expression, "may."

Their figure 11D, the caption and the related text describe the Müller cells as a controlling function "in determining

[43]Bringmann, A. Syrbe, S. Görner, K. ... Reichenbach, A. (2018) The primate fovea: Structure, function and development *Prog Retinal Eye Res* vol 66, pp 49-84

the slope of the OLM in the foveola according to the angle of the light path." It is unusual to hear of the Müller cells described as exerting tension forces along their length. "A further role of the central-most Müller cells may be the vertical mechanical stabilization of the fovea externa, i.e., the pyramid-like arrangement of the elongated cone segments in the center of the foveola (Fig. 11D)." It does provide a detailed discussion of the surface of the ILM in the region of the foveal pit, but does not provide an explanation of the potential image magnification satisfying to an optician. The use of the term smooth without describing the relationship relative to the wavelength of light leaves it essentially meaningless.

The paper contains many interesting details, if an investigator had the opportunity to place them all in proper relationship and perspective.

Also in 2014, IN•OCT[44], an international panel proposed what is rare in a biological field, a set of standard Nomenclature for SDOCT technology. They noted,

> Definitions for various layers changed frequently in the literature and were often inconsistent with retinal anatomy and histology. The panel introduced the term "zone" for OCT features that seem to localize to a particular anatomic region that lacks definitely proven evidence for a specific reflective structure. Such zones include the myoid, ellipsoid, and the interdigitation zones.
>
> A nomenclature system for normal anatomic landmarks seen on SD-OCT outputs has been proposed and adopted by the IN•OCT Panel. The panel recommends this standardized nomenclature for use in future publications. The proposed harmonizing of terminology serves as a basis for future OCT research studies.

The Staurenghi et al. material is addressed in greater detail in **Section F.2.4**.

The IN•OCT activity was followed by another group, Xie et al[45]. in 2018, attempting to correlate histological and electron microscope records with the OCT imagery. The experiments centered on the optic nerve head rather than the foveal pit, and employed pigs.

F.2.1 Details from SDOCT of the RPE/Choroid interface–Yiu et al

Yiu et al[46]. have provided detailed measurement of the RPE/choroid interface of the Rhesus monkey. They also provided equivalent information gained histologically *in-vitro* and the information gained *in-vivo* using SDOCT technology as of 2018. The superiority of the SDOCT data for most purposes is obvious from their figures 2 and 3, although in measuring the thickness of certain layers, the histological material is easier to define edges. On the other hand, the effects of shrinkage are more difficult to define precisely.

A comparison of their figure 3 and their Table 2 accentuates the old adage, a figure is worth a thousand words. Their caption to the table does not indicate the width they assign to their measurements of each feature. None of the statistical values in their table reflect the near zero values approached within the depth of the foveola illustrated in figure 3. They do not define the diameters or other features they used to bound the values in their "foveal" or their "parafoveal" columns of Table 2 (although it can be assumed from the upper right column of page 71 that they averaged the thickness values over the 1 mm diameter of the fovea their foveal measurements and over the area of the the 1mm parafoveal ring surrounding the fovea.

> The graphs of figure 3 are invaluable. The numerical values in Table 2 assume the underlying forms are well behaved and symmetrical, and not like those in figure 3A and 3C. Performing the integrations on the left and right halves of the areas involved separately would give different numbers.

In their figure 1, they compare the imagery from a histological cross section of the retina with an SDOCT cross section. They note specifically the difference due to the SDOCT depending on reflected light from changes in the

---

[44]Staurenghi, G. Sadda, S. Chakravarthy, U. & Spaide, R. (2014) Proposed Lexicon for Anatomic Landmarks in Normal Posterior Segment Spectral-Domain Optical Coherence Tomography: The IN•OCT Consensus Ophthalmology vol 122(7), pp 1572-1578 https://doi.org/10.1016/j.ophtha.2014.02.023

[45]Xie, W. Zhao, M. Tsai, S-H. et al. (2018) Correlation of spectral domain optical coherence tomography with histology and electron microscopy in the porcine retina *Exp Eye Res* vol 177, pp 181-190

[46]Yiu, G. Wang, Z. Munevar, C. et al. (2018) Comparison of chorioretinal layers in rhesus macaques using spectral-domain optical coherence tomography and high-resolution histological sections *Exper Eye Res* vol 168, pp 69-76

index of refraction between volumes of the retina. The SDOCT only sees edges of a material, not its bulk interior. As per discussions in Section F.1.1 of this report, the ILM is not identified as a physical membrane in either the histological or SDOCT images of Yiu et al. It is becoming rare to find an ILM defined specifically in recent SDOCT images.

F.2.2 Details from SDOCT of the Field Lens of the eye–Patel et al.

Patel et al[47]. have provided a great deal of statistically precise data concerning the shape of the field lens generated by the curvature of the inner limiting membrane forming the foveal pit in the eyes of *Macaca mulatta*. The material appears directly applicable to the human eye. Their OCT scan of figure 4B is particularly clear and well labeled. Other figures are incorporated into **Section 2.4.4.1**.

F.2.3 Potential folds in macula-off and macula-on conditions

A search of the literature was made concerning folds associated with the surgery for retinal detachment. No such folds were encountered in the author's case. The following material is not pertinent to the main paper.

Wong has been more specific based on his SDOCT imagery. He defines three patterns of folds; ripple, taco, and displacement. "Ripple and taco folds were found to resolve spontaneously." "Displacement folds also resolved, but left the macula translocated inferiorly, causing binocular diplopia." In patient 10, the long term binocular diplopia was only overcome by the use of prisms.

His figure 6 is particularly interesting, showing a "Taco" fold of the displacement type "with inferior displacement of the fovea." His imagery and discussion indicate an investigator very close to his work. The OCT cuts cited in the caption and associated with the fundus image are omitted. Without these indicators, the directions of the SDOCT scans are ambiguous. The ILM is shown with ripples resulting from the displacement of the ILM pit.

Wong also notes the "clumping of photoreceptors outer segment within the apex of the fold. Wang and associates also showed evidence of sequestration of these outer segments by macrophage." It is not clear whether these are the macrophage normally part of the RPE and normally in juxtaposition with these same outer segments. Wang and associates did not discuss the normal structure of the retina in their mice or in humans sufficiently to answer this question.

The clumping identified by Wong is probably the cause of the remaining distortion within the right half of the foveola illustrated in **Section F.1.5.1** if the clumping is associated with the seismic shift described in this work. If the seismic shift continues to resolve, the apex will disappear and it is possible the clumping will also be favorably resolved.

Lee, Wong et al[48]. have provided a follow up longitudinal study of displacements after vitrectomy. "Macula displacement was evident postoperatively in 72% of 32 consecutive fovea-involving detachments treated with vitrectomy and gas." "There was a significant correlation between the presence of macula displacement and symptoms of distortion in the early postoperative period (p=0.013). Symptomatic patients described bending of lines with or without objects appearing smaller or narrower in the operated eye. Quantifying the displacement demonstrated that the extent of displacement was associated with distance from the optic disc (p=0.005) and the extent of retinal detachment." Presumably, the last sentence refers to the distance of the fold from the optic disc.

F.2.4 Standardized nomenclature of the IN•OCT panel

As noted earlier in a paper by Staurenghi et al., a small, due to logistic considerations, panel of experts was convened to attempt to arrive at a consensus on features consistently recognized using *spectral domain* OCT, i.e., SDOCT. Only a small number of scans from healthy eyes were circulated among the panel prior to their gathering for an attempt to reach a consensus. They considered their report preliminary and subject to review within the next ten years. They also defined certain features that can not be recognized regularly, either due to equipment limitations, or inconsistent reflectivity. These features were named zones, rather than layers, for the short term. Their Table 2 identified 18 layers, where some of the features could not be specifically identified reliably. These layers were given names ending in zone following an educated guess as to what tissue was within the zone.

---

[47]Patel, N. Hung, L-F. & Harwerth, R. (2017) Postnatal maturation of the fovea in *Macaca mulatta* using optical coherence tomography *Exper Eye Res* vol 164, pp 8-21 https://doi.org/10.1016/j.exer.2017.07.018

[48]Lee, E. Williamson, T. Hysi, P. Wong, R. et al. (2013) Macular displacement following rhegmatogenous retinal detachment repair Brit J Ophthalm vol 97(10), pp 1297-1302

Even with this new nomenclature, some features are not clearly identified in many SDOCT images. They used two terms that are unusual in other technologies, hyper-reflectivity and hyporeflectivity. No calibration has apparently appeared as to what hyporeflectivity means, other than less reflective than a hyper-reflective feature. **Figure F.2.4-1** reproduces the first of two annotated images from the panel.

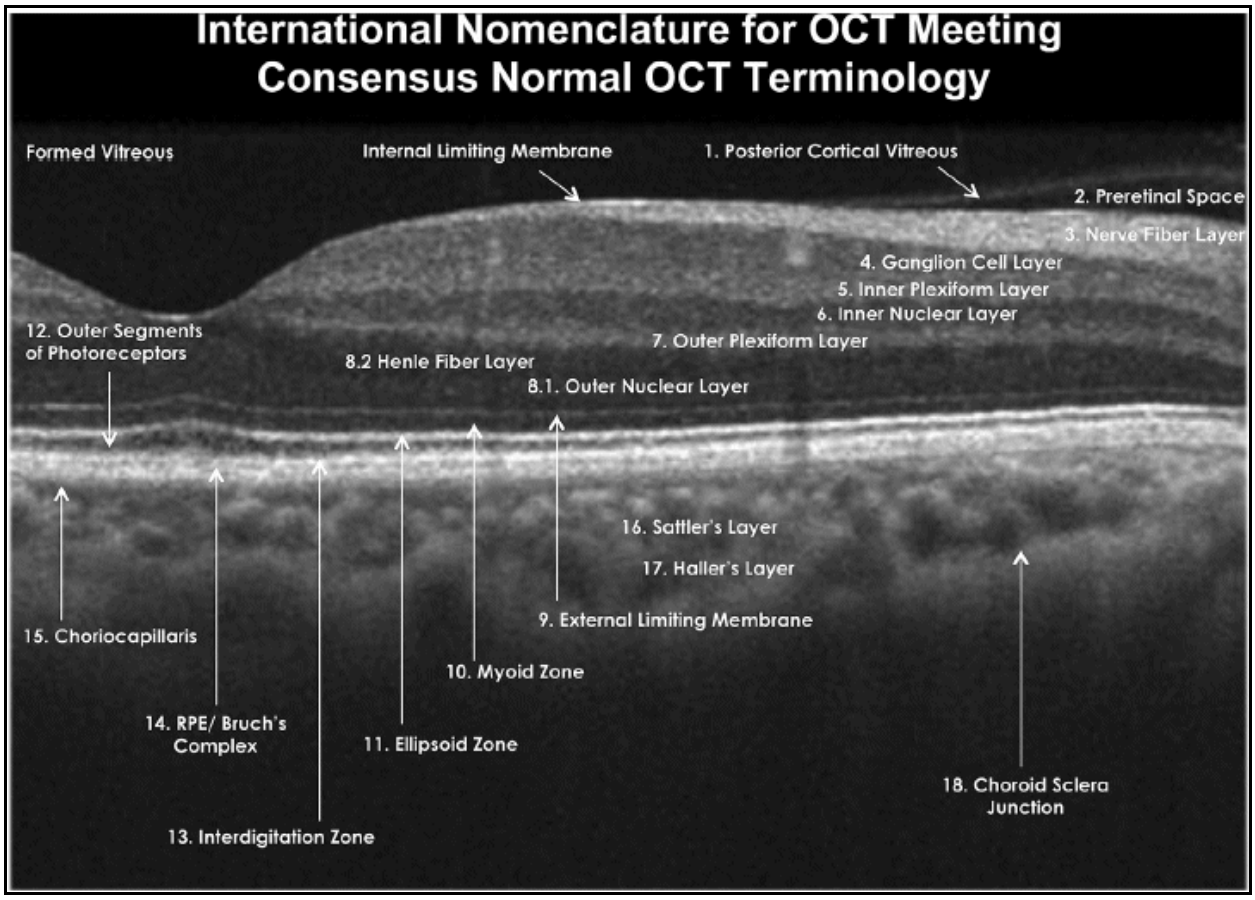

Figure F.2.4-1 Nomenclature for normal anatomic landmarks seen on spectral domain optical coherence tomography (OCT) images proposed and adopted by the International Nomenclature for Optical Coherence Tomography Panel. Healthy retina imaged using Heidelberg Spectralis. RPE = retinal pigment epithelium. From Staureghi et al., 2014.

It appears the ellipsoid zone (#11) may be the pocket between the inner and outer segments where opsin is secreted from the inner segment, is formed into individual discs and then coated with the chromophores of vision.

Zone #12 is labeled hyporeflective outer segments of the photoreceptors. However, as illustrated in Section F.2.1 (from Jonnal et al., 2016), the end caps of the outer segments are generally hyper-reflective.

Zone #13 may be further defined as the storage area of the RPE, near the disc phage junction beteeen the outer segments and the RPE interdigitate. The storage area contains a large amount of proto-chromophore material that may lead to high reflectivity in this zone.

The panel notes that their layer #14, the RPE/Bruch's membrane, can frequently be resolved into more than one band.

Figure F.2.4-2 is the second of two from the panel,

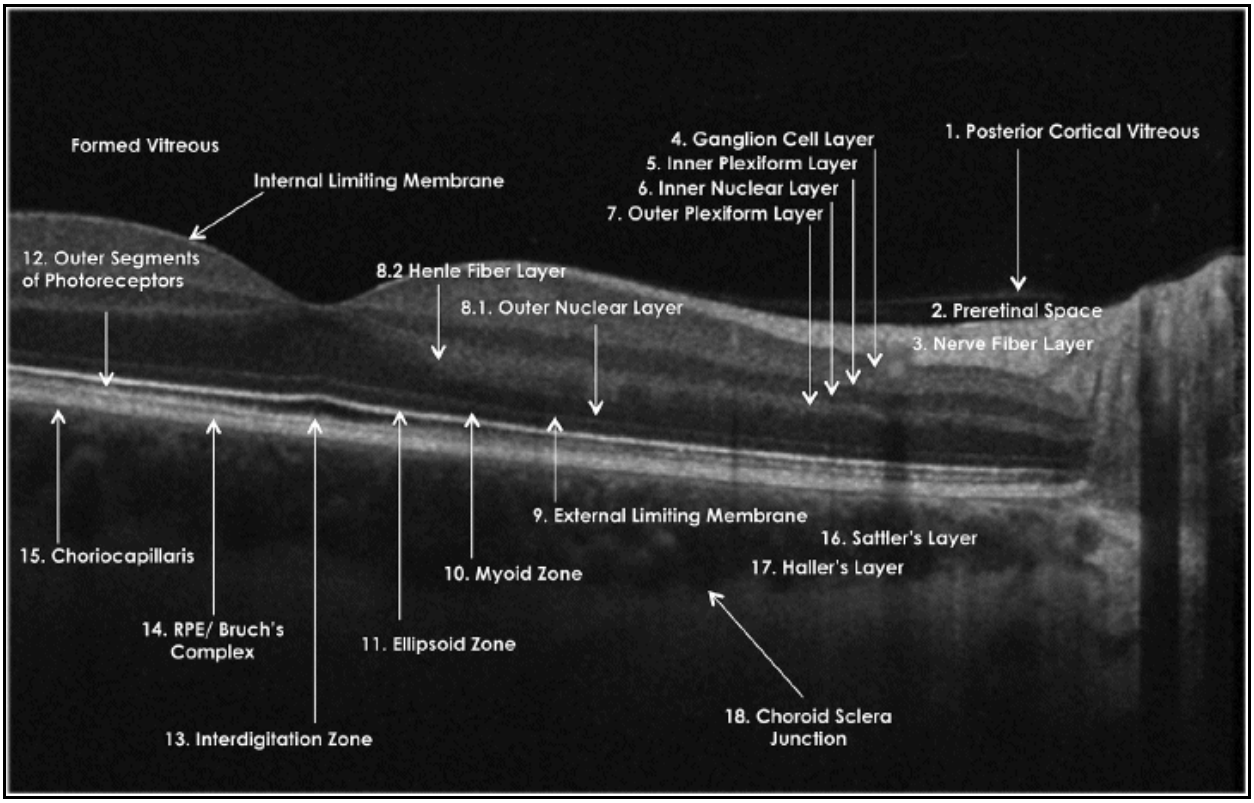

Figure F.2.4-2 Nomenclature for normal anatomic landmarks seen on spectral-domain optical coherence tomography (OCT) images proposed and adopted by the International Nomenclature for Optical Coherence Tomography Panel. Healthy retina imaged using Zeiss Cirrus. RPE = retinal pigment epithelium. From Staureghi et al., 2014

F.2.4.1 Resolving the debate over comparing OCT and histology data

Spaide & Curcio[49] made an excellent effort prior to 2011 to define the features of the retina associated with the photoreceptor neurons. In the process, they developed some carefully scaled drawings of such neurons associated with both the fovea and perifoveal. They apparently did not distinguish between the photoreceptors of the foveola and the fovea. They did not indicate the statistical aspects of their measurements. However, their Table 1 provides their estimates for many features and lists of citations they reviewed for each feature. Their figure 1 indicates their inability to resolve the multiple bright lines related to the two sides of the RPE layer of the retina; this is done routinely in more recent material as noted by lines #13 & #14 of the IN•OCT panel, above. The figure did note the variable length of the outer segments frequently found between the fovea and the perifovea. **Figure F.2.4-3** illustrates their concept of a cone within the fovea.

[49]Spaide, R. & Curcio, C. (2011)anatomical Correlates to the Bands Seen in the Outer Retina by Optical Coherence Tomography: Literature Review and Model *Retina* vol 31(8), pp: 1609–1619. doi:10.1097/IAE.0b013e3182247535.

The drawing remains not scaled as indicated in the caption as well as no supracone space is shown for the second cone. The space between the top of the contact cylinder and the bottom of the supracone space is the region of

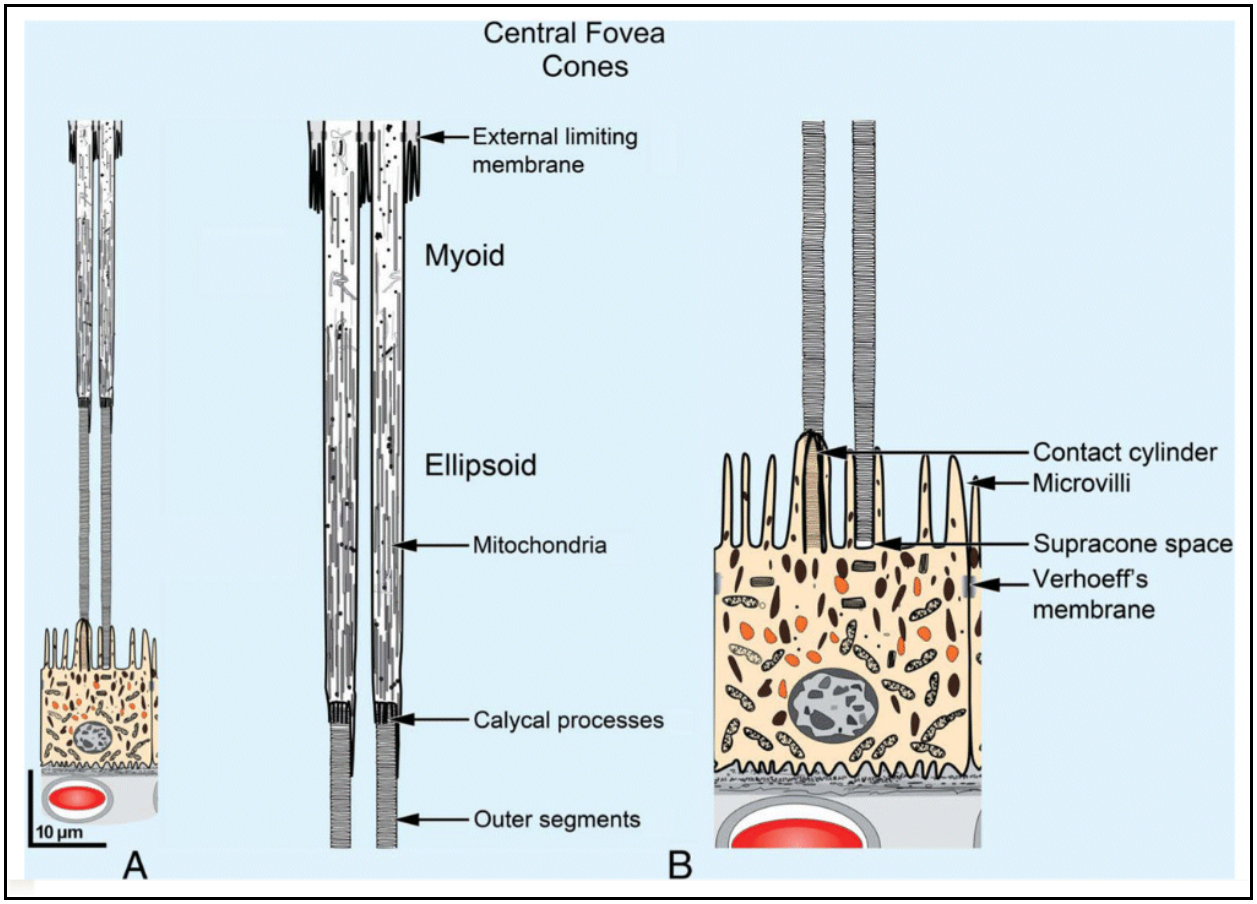

Figure F.2.4-3 Scale drawing of a central fovea photoreceptor neuron. "A; Lower magnification and (B) high magnification in two parts. A scale drawing of the outer retina showing cones in the central fovea (A, low magnification). In (B) (higher magnification) the Muller cells form junctional complexes with the photoreceptors that when viewed in aggregate are called the ELM. In reality, *it is not a membrane*, limiting or otherwise. The foveal cones are narrow and cylindrical, like rods. The inner portion of the IS is called the myoid and the outermost division is the ellipsoid, which contain numerous thin mitochondria. Extending over the proximal OS are fine cytoplasmic extensions called the calycal processes. The RPE has small apical extensions called microvilli. The OS continue to the RPE and are enveloped in specialized apical processes forming a contact cylinder (left cone). A small gap (the supracone space) is present between the outermost part of the OS and the RPE, seen in the cross-sectional view (right). Retinal pigment epithelial cells have junctional complexes (drawn larger than scale for clarity) formed with neighboring RPE cells. The confluence of these complexes as seen by light microscopy is called, in a manner analogous to the ELM, Verhoeff membrane." See text for interpretation. From Spaide & Curcio, 2011.

digestion of the discs by the RPE, phagodiscosis. As noted elswere, the label supracone is inappropriate. All photoreceptor outer segments, OS, undergo phagocytosis in this volume. The space below the RPE in this figure is not identified by the investigators. It is the region where retinoid material is delivered to the RPE by the SRBP + TTR "bottles" via the blood stream. This area involves large numbers of unstructured chromogens similar to the

material within the contact cylinders. Both of these areas appear to form bright lines, the interdigitation zone (#13) and the RPE/Bruch's membrane (#14) layer, in high resolution OCT. Optically, the myoid is a distinct feature of the photoreceptor neurons with a high index of refraction (similar to that of the OS. However, the ellipsoid identified in this figure is not a distinct feature. It is essentially the volume of the neuron not identified as to purpose. In fact, it is an area devoted to preparing the protein opsin for extrusion into the cup formed by the IS/OS junction. The index of refraction in this area is not notable. It should be noted that Spaide & Curcio do not show the discs encased within the lemma of the IS. They are not so encased. They do show the calycal processes (neural dendrites) extending a finite distance along the OS. The arrangement of these neural dendrites actually form a crucible surrounding the disc stack. The arrangement is hinted at in **Figure F.1.1-2** of this appendix and shown in greater detail in **Section 4.3.5.1**.

Spaide & Curcio provide other scaled drawings of rods and cones at two different locations in the retina. They portray all of the OS identically, and discriminate between their rods and cones based on the diameter of the IS, while simultaneously noting that the rods and cones of the fovea both exhibit cylindrical IS. Quoting, "The foveal cones are narrow and cylindrical, like rod." ***Any association between their analyses and any functional analyses relating to spectral performance is entirely specious***.

Spaide & Curcio note, "The RPE has small apical extensions called microvilli." without discussing these elements further. These are the actual location of the secretion of chromophores into the inter-photoreceptor matrix, IPM, between the RPE, and the body of the photoreceptor neurons known as the IS. Within the RPE, the chromophores are stored as granules isolated between each other, and therefore do not form an organized reflection apparent in OCT images.

Figure F.2.4-4 is reproduced here because of a feature not addressed in their text. The caption is quoted verbatum. The figure does label the External limiting membrane. "The ELM designates junctional complexes named for their appearance by light microscopy." As noted earlier in this Appendix and by quoting Spaide & Curcio, the ELM is not a membrane but a complex region at the inner end of the IS near where the axon of the neuron exits the IS.

Immediately below the label, "External limiting membrane," is a feature shown on both sides of the IS. This feature is actually an electrolytic terminal of the Activa inside each and every photoreceptor neuron. This terminal, known as the podite terminal, is critically important to the operation of this structure as a neuron. (**Section 4.3.3**).

They note the contact cylinder is located farther from the RPE in the earlier figure. They associate that elongation of the contact cylinder with a shorter OS.

Spaide & Curcio note in their caption, "These ensheathing apical processes have cellular machinery not ordinarily found in microvilli such as ribosomes and mitochondria. Shed OS are moved back to the RPE cell body for phagocytosis through the supracone space. The RPE apical junctional processes are labeled according to their appearance on light microscopy." The problem, these identified "microvilli" are not conventional microvilli. They are part of the production machinery employed in the preparation and secretion of the chromophores into the IPM space. The content of the RPE is not addressed by Spaide & Curcio. However, the RPE stores four types of chromophores as separate granule types within the RPE. This is illustrated in **Section 4.6.2** from Wolken (1966).

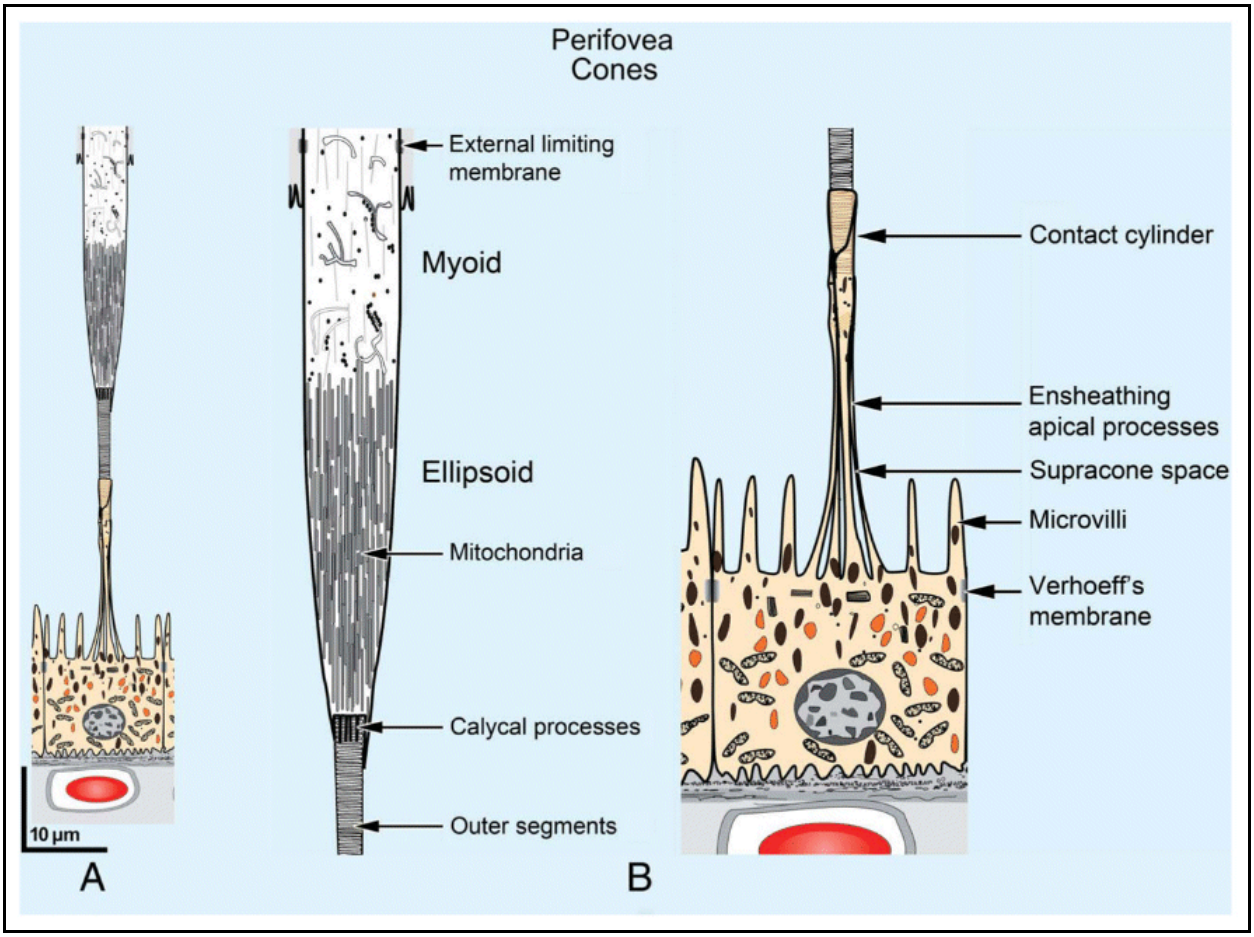

Figure F.2.4-4 Scale drawing of a perifoveal phtoreceptor neuron. "A. Lower magnification and (B) high magnification in two parts. IS, perifoveal cone. Cone IS widen with greater eccentricity from the foveal center. Mitochondria fill approximately 75% of the ellipsoid volume and account for the enormous oxygen use by photoreceptors. Like foveal cones, perifoveal cones have small cytoplasmic extensions called the calycal processes that extend over the innermost OSs. The ELM designates junctional complexes named for their appearance by light microscopy. Outer segments of cones outside of the central macula stop well short of the underlying RPE cells. Specialized apical extensions arise from the RPE to encase the outer one third of OS length, recognized here by the faint obscuration of the OS disks. These ensheathing apical processes have cellular machinery not ordinarily found in microvilli such as ribosomes and mitochondria. Shed OS are moved back to the RPE cell body for phagocytosis through the supracone space. The RPE apical junctional processes are labeled according to their appearance on light microscopy, Verhoeff membrane.

F.2.4.2 The debate of 2015–Spaide vs Jonnel et al.

Jonnal et al[50]. and Spaide[51] were in a significant debate over terminology in the rapidly advancing ability to identify and measure the length of axial features in the retina using AO-SDOCT techniques. There is a significant problem in their debate; they have not identified the materials within the IS/OS interface they are observing by reflection. The material consists of the bulk chromophore, one of the four Rhodonines of human vision (**Chapter 5**), that is being used to coat the discs of the OS with a uniform monomolecular liquid crystalline coating. Their debate even involved the archaic question of rods versus cones, without providing any evidence of the spectral performance of any of their outer segments. *Their discussion was based only on OCT evidence versus histological evidence*. No physiological or spectral (chromatic) information was used. Additionally, there was confusion regarding the myoid and the ellipsoid as the define them compared to previous optically obtained information. In Table 1 of the Spaide & Curcio (2011) they describe the indices of refraction of the myoid and ellisoid as 1.3605 and 1.394 respectively for a "cone." they provide no similar values for a "rod." They rely upon very old data from the 1950's by Sidman[52]. As noted in the title, liquid crystalline material was not recognized as a state of matter in 1957. Sidman asserted,

> "Several uncertainties persist concerning the cytology of rods and cones. A variety of fibrillar structures on the surface or within the substance of the outer and inner segments has been reported but few of these have been closely studied or their actual existence verified. The nature of the junction between the outer and inner segments is uncertain, as are also the relations of several subdivision of the inner sement to one another." Several of these fibrillar were probably associated with the neurites and axons of the neural portion of the photoreceptor.

While there were other dimensions to the debate, neither party is offering any primary data collected by their team with regard to the importance of the myoid versus the ellipsoid. Sidman offered primary data he collected and stated that the ellipsoid was surrounded by the myoid! He tabulated the refractive index of the myoid in monkeys as 1.3605

In addition, Sidman draws the outer segment as conical in cones, rather than cylindrical as in Spaide & Curcio. See **Chapter 4** for more recent data in this area.

Their debate of 2015 was largely archaic by April, 2019.

F.2.5 Reading OCT images

ODwire.org[53] (optometric advice & education) has provided two excellent webinars on reading and understanding OCT images,

• Macular OCT Interpretation: A Practical Discussion with David E. Lederer, MD • Mastering OCT Interpretation with Dr. Mark Friedberg

The webinars are available for Continuing Education credit.

---

[50]Jonnal, R. Kocaoglu, O. Zawadzki, R. et al. (2015) Author's Reply: Outer Retinal Bands; Letters to the Editor *IOVS* vol56, pp 2507-2510 doi:10.1167/iovs.15-16756

[51]Spaide, R. (2015) Critique: Outer retinal bands. *IOVS* vol 56, pp 2505–2506

[52]Sidman, R. (1957) the Structure and Concentration of Solids in Photoreceptor Cells Studied by Refractometry and Interference Microscopy *J Biophysic & Biochem Cytology* vol 3(1), pp 15-24 http://doi.org/10.1083/jcb.3.1.15

[53]https://www.odwire.org/

Table of Contents

Detached Retina: A Unique Diary & its Repair 1
F.1 Macular dystrophy involving mechanical failures of the posterior ocular 1
F.1.1 Mechanical failure (traction) at the vitreous/neural tissue interface 5
F.1.2 Scotoma resulting from detached retina at the periphery encountered by the author 6
F.1.3 Lab work detailing the Detachment of the author's retina & repair surgery 13
F.1.3.1 Sudden detachment in an 82 year old without trauma 13
F.1.3.1.1 Interpreting the BM representation in OCT of 3/12/2018 15
F.1.3.2 The repair surgery 18
F.1.3.3 Determination of the type of retinal detachment 19
F.1.3.4 Followup on the retinal detachment surgery–diary for 1st 6 months 20
F.1.3.4.1 The dimensions of the gas bubble 29
F.1.3.5 Patient's partial evaluation of the surgical solution to detached retina 30
F.1.4 Spatial distortion (metamorphosia) of the perceived scene after surgical repair 31
F.1.4.1 Biological description of pincushion distortion 32
F.1.4.2 Astable spatial distortion outside of the fovea and beyond the retina 33
F.1.4.3 Explaining the astable aspect of the merging along the horizontal meridian . . . 35
F.1.4.4 Potential re-mapping of Petzval surface on to retina ADD 38
F.1.5 Evaluation of the detached retina experience at 1 year point 38
F.1.5.1 Perception at the one-year point–patient's evaluation of the surgical solution to detached retina 38
F.1.5.3 The *normal* foveal pit of the ILM as a Field lens 43
F.1.5.4 Potential and realized asymmetry of the Author's foveal pit 46
F.1.5.6 The clinical evaluation following the surgical solution at one year . . 49
F.1.5.7 Evaluation of the retina from a scientific perspective at one year 50
F.1.5.8 Clinical interpretations of damage from a detached retina 53
F.1.6 Dysmetropia & foveola acuity a year after the author's surgery 55
F.1.6.1 Micropsia measurements in macula-off and macula-on conditions . . 57
F.1.7 Summary of Encounter & Prognosis in April 2019 59
F.1.7.1 Summary of the Encounter as of April 2019 59
F.1.7.2 Other summaries of retinal detachments 59
F.1.7.3 Prognosis in April 2019 59
F.1.8 State of the art–Surgery in the clinic and in the research facility 59
F.1.8.1 Data base related to damage to the photoreceptors 60
F.1.8.2 Displacement of the foveola during detachment and surgical repair . 61
F.1.8.3 Folds in the retina identified mostly after surgery 62
F.2 Review of the adaptive optical OCT devices & techniques in 2019 62
F.2.1 Details from SDOCT of the RPE/Choroid interface–Yiu et 66
F.2.2 Details from SDOCT of the Field Lens of the eye–Patel et al. 67
F.2.3 Potential folds in macula-off and macula-on conditions 67
F.2.4 Standardized nomenclature of the IN•OCT panel 67
F.2.4.1 Resolving the debate over comparing OCT and histology data 69
F.2.4.2 The debate of 2015–Spaide vs Jonnel et al. 72
F.2.5 Reading OCT images 73

List of Figures

Figure F.1.1-1 Macular dystrophy tree 2
Figure F.1.1-2 The photoreceptor cell-IPM-RPE interface 3
Figure F.1.1-3 Ultrahigh-resolution spectral OCT image of living human macula 4
Figure F.1.2-1 Perimetry of an *acute onset*, short lifetime *unilateral hemianopic scotoma* 7
Figure F.1.2-2 Fulton scotoma beginning 25 Feb 2018 9
Figure F.1.2-3 Fulton scotoma, 2 March 2018 10
Figure F.1.2-4 Vitreous fluid flows through a retinal tear 12
Figure F.1.3-1 OCT scan of authors detached retina after forty days 15
Figure F.1.3-2 Composite of functions occurring within the PC & RPE/Bruch's complexes 17
Figure F.1.3-3 Retinal map caricature showing multiple tears/peelings and stitch locations following surgery . . . 19
Figure F.1.3-4 Pincushion distortion 23
Figure F.1.3-5 Aniseikonia from Shaw Lens Co 24
Figure F.1.3-6 Volume and linear transverse OCT scans of 14 May 2018 for Fulton 25
Figure F.1.3-7 Gas bubble dimensions with time as observed looking straight down. 29
Figure F.1.4-1 Principle spatial distortions following surgical repair 31
Figure F.1.4-2 Pincushion parameters for rotational symmetric and asymmetric cases 32
Figure F.1.4-3 Amsler Grid at day 86 after surgery 34
Figure F.1.4-4 The observed field against an Amsler Grid, Oct. 2018 35
Figure F.1.4-5 Visual field processing within the neural circuitry of the visual modality 36
Figure F.1.4-6 Visual modality signal flow diagram, annotated 37
Figure F.1.5-1 Perceived spatial performance of foveola at one year point 40
Figure F.1.5-2 Perceived distortion in a rotating pattern of dots by foveola 42
Figure F.1.5-3 The variation in magnification as a function of angle 43
Figure F.1.5-4 Physical evidence of a field lens in primate eyes 45
Figure F.1.5-5 Left eye OCT volume scan with retinal thickness overlay in color 47
Figure F.1.5-6 Composite OCT scans of left eye of Fulton 48
Figure F.1.5-7 Horizontal OCT scan of the author's normal right eye, 6 March, 2019 51
Figure F.1.5-8 Vertical OCT scan of the author's damaged left eye on 6 March, 2019 52
Figure F.1.5-9 Examples of changes in serous detachment 54
Figure F.1.6-1 Difference in geometric performance of eyes due to short term differences in pit shape 56
Figure F.1.6-2 "Horizontal and vertical dysmetropsia measurements 58
Figure F.2.1-1 Images acquired with AO ultrahigh-resolution OCT 64
Figure F.2.1-2 OSLO image of cone mosaic at 3.1˚ eccentricity 65
Figure F.2.4-1 Nomenclature for normal anatomic landmarks seen on spectral domain optical coherence tomography 68
Figure F.2.4-2 Nomenclature for normal anatomic landmarks seen on spectral-domain optical coherence tomography 69
Figure F.2.4-3 Scale drawing of a central fovea photoreceptor neuron 70
Figure F.2.4-4 Scale drawing of a perifoveal phtoreceptor neuron 72

SUBJECT INDEX

3D . . . 38
3-D . . . 63
50% . . . 7, 9, 12, 22, 23, 28, 62
action potential . . . 8, 9
Activa . . . 71
acuity . . . 1, 5, 7-11, 19, 20, 22, 24, 26-28, 30, 31, 41-43, 49, 53, 55, 59, 60, 62
adaptation . . . 52, 60
anatomical computation . . . 43
AO–SDOCT . . . 63
AO–SDOCT–RT . . . 63
association areas . . . 37
blob . . . 8, 9
calibration . . . 68
clock . . . 21, 28
compensation . . . 4
computation . . . 9, 43
cross section . . . 2, 3, 66
data base . . . 60
depth perception . . . 9, 21, 31
diode . . . 63
drusen . . . 4
evolution . . . 62
expanded . . . 9, 10, 13, 26
fasciculus . . . 43
FDOCT . . . 4, 63
field lens . . . 1, 30, 39, 43-46, 49-51, 53, 55, 57, 61, 67
glutamate . . . 53
hole . . . 6, 62
hypoplasia . . . 49
in vivo . . . 62
index of refraction . . . 18, 20, 29, 31, 67, 71
intelligence . . . 38
in-vitro . . . 18, 66
in-vivo . . . 2, 5, 18, 66
lips . . . 22
liquid-crystalline . . . 61
lookup table . . . 38
LOT . . . 9
mesotopic . . . 7
microvilli . . . 70-72
morphogenesis . . . 5, 43
navigation . . . 1
neurites . . . 17, 73
noise . . . 63
OCT . . . 2, 4, 6, 12, 13, 15-20, 22, 24-28, 30, 35, 39, 46-55, 59, 61-64, 66-69, 71, 73
off axis . . . 31
off-axis . . . 7
perimetry . . . 6, 7, 9, 44, 46
pgn/pulvinar . . . 37, 38
pin cushion . . . 21, 27, 41, 55, 56
precision optical servomechanism . . . 22, 38
protocol . . . 57, 58
pulvinar . . . 37, 38, 41, 43
reading . . . 1, 22, 27, 28, 30, 50, 57, 59, 73
residue . . . 2, 41
rhegmatogenous . . . 5, 13, 49, 55, 58, 60, 61, 67
saliency map . . . 21, 37
scotoma . . . 1, 6-11, 19, 38, 42, 46, 47, 57, 59
SDOCT . . . 4, 18, 30, 42, 44, 49, 59, 62, 63, 66-68, 73
servomechanism . . . 22, 23, 38
sleep . . . 13
sparkles . . . 7

SRBP 18, 70
stage 0 . . . . . 8, 27
stage 1 8
stage 2 . . . . . 8, 17, 43
stage 3 . . . . . 8, 9
stage 4 . . . . . 21, 38, 43
Stiles-Crawford 30, 41, 50
surface tension 24
syndrome 9
thalamus 37, 43
threshold 59
tomography 2, 4, 6, 8, 14, 21, 44, 62, 63, 66-69
topography 50
tremor 20, 22, 31, 46
TTR 18, 70
Verhoeff's 4, 14
visual acuity 5, 9, 19, 30, 31, 49, 62
visual cortex 36, 43
Wikipedia 10